Assessment of Thermally-Aged Conformally-Coated Printed Circuit Boards

by

Ehsan Zeynali

A thesis submitted to the Faculty of Graduate Studies of
The University of Manitoba
in partial fulfillment of the requirements of the degree of

Master of Science

Department of Electrical and Computer Engineering
University of Manitoba
Winnipeg, MB, Canada

Abstract

Printed circuit boards (PCBs) are key components of electrical and electronic systems. The electrical performance of PCBs under harsh operating conditions is a decisive factor to ensure the reliability of the system. As a result of increased demand for electric power, the operating voltage of many systems is increased. The increased operational voltage level, imposes a higher level of electrical stress on the insulation system and, therefore, discharges and failure are more likely to happen. To provide a better insulation level, PCBs are coated with a film of conformal coating polymer. The protective layer provides a barrier against environmental factors including moisture, contamination, temperature changes, and mechanical abrasion. However, in exposure to humidity and temperature, some levels of aging happen in the coated PCBs. Degradation of the conformal coating layer decreases the performance of the coated assembly.

In this thesis, a series of experiments were conducted to evaluate the electrical performance of conformally-coated PCBs under accelerated aging conditions. Test samples were designed and fabricated based on industry standards. Test boards were coated with silicone conformal coating using dipping application technique. Partial discharge tests were conducted on coated samples under pollution and conductive particles. The impact of conductive particles and location of the pollution on PD activity were observed. A group of test samples were aged using an automatic thermal and humidity chamber. Specimens were exposed to temperature and humidity. The level of degradation was evaluated by visual inspection. Capacitance and loss tangent of the test samples were measured using a dielectric spectrometer after cycles of aging. The level of change in the capacitance and loss tangent due to aging was investigated. Further, the breakdown voltage of both aged and new test samples was measured. Electrical performance of the different samples were discussed based on the partial discharge activity and breakdown voltage.

Acknowledgements

First and foremost, I would like to express my appreciation to my advisor, Dr. Behzad Kordi, for his great support and supervision during this research. I deeply appreciate all his valuable comments and guidance.

Many thanks to my thesis committee, Dr. Shaahin Filizadeh and Dr. Pooneh Maghoul for their comments and suggestions to enhance this thesis.

I am also grateful to Ryan Bridges who helped me during this research work. I would like to express many thanks to Daryl Hamelin, Cory Smit, Zoran Trajkoski, and the University of Manitoba Nano System Fabrication Lab (NFSL), particularly Dwayne Chrusch for all their practical consultations, cooperation, and guides for test setup design and preparation.

Many sincere thanks to my wife, Bita, for her kindness, patience, and support while I was pursuing my studies. Infinite thanks for her encouragements and for always being there for me and our daughter, Vanda.

Table of Contents

List of Figures

List of Tables

Nomenclature

PD Partial Discharge

PCB Printed Circuit Board

SIR Surface Insulation Resistance

PWB Printed Wiring Board

IPC Institute for Printed Circuits - Association Connecting Electronics Industries

HASL Hot Air Solder Leveling

FR Flame Retardant

TDS Technical Data Sheet

RH Relative Humidity

CTE Coefficient of Thermal Expansion

PDIV Partial Discharge Inception Voltage

ENIG Electroless Nickel Immersion Gold

LPI Liquid Photo Imageable

CAD Computer Aided Design

NSFL Nano System Fabrication Lab

RMS Root Mean Square

Chapter 1

Introduction

1.1 Motivation

The demand for more electric power is increasing due to more reliance on electrical systems. Many recent developments in aerospace and automotive industries for example, place emphasis on replacing the mechanical system with electrical substitutes in order to increase the efficiency, improve the reliability, lower the maintenance cost, and minimize the complexity of entire systems [1]. Providing a system with more electrical power at low voltages without any change in conductors diameter has the drawback of undesirable electrical power loss issues. On the other hand, using conductors with higher ampacity to carry more power without energy dissipation is also not the right solution, because it may not only increase the cost but also increase the weight of the entire system. Besides, larger conductors occupy more space and affect the size of other connected equipment. Therefore, increasing the level of operating voltage is considered as the solution of transmitting more electrical power throughout systems while using conductors of the same weight and ampacity [2] [3]. For example, in one of the most recent aircraft electrical system designs, Boeing 787 Dreamliner, the operational voltage has increased from 115 V to 230 V in the AC power system and from 28 V to 270 V in the DC system. This aircraft has four generators providing 250 kVA along with two auxiliary power units that generate 234 kVA [4]. It is predicted that even more power demand and consequently higher operational voltage levels will feasible in future industrial designs [3].

However, the increase of operational voltage level imposes an moderate electrical stress on the entire insulation system. Moderate levels of stress will increase the risk of partial discharges (PD), breakdown, or even insulation failure in power systems. Breakdown or disruptive electrical discharge occurs through insulation between two conductors energized by a significantly high voltage. In the instant of breakdown, a high current flows through the insulator and the conductors are momentarily short circuited. Disruptive discharge can happen between a pair of non-insulated pins or conductors [5] [6]. PD is a localized electrical discharge that occurs when a high electric field is present [7]. Since the electric field is reduced outside of the localized region, PD does not bridge the insulation between two conductors and full current flow is prevented. In the event of PD, most systems can perform their normal operation as the discharge current is very small. However, continued PDs in a power system are known as a severe source of damage to equipment in the long term [8].

Printed circuit boards (PCB) are one of the key components of electric or electronic system and basically designed to connect elements via conductive traces and hold components in place. While a few years ago the concept of a high voltage PCB was little-known, recent high voltage PCBs are able to handle up to 40kV [9]. The ability of PCBs to perform required function under operating conditions is an important factor to ensure the reliability of the entire power system. The narrow space between energized traces or the gap between connector pins, where a high electric field is present, are the most vulnerable points of discharge occurrence in PCBs [10]. Extra conductor clearance or additional insulation is required for PCBs and electrical components to cope with the increased voltage level. PCBs are usually coated with a protective polymer of a typical 50µm thickness insulation material to increase the reliability of the board. The coating layer conforms to the board for its operational condition. This coating barrier protects the PCB from harsh environmental conditions such as high humidity and temperature changes, component abrasion, exposed contamination or solvents, and increases the surface insulation resistance (SIR) to maximize the operation integrity of the electrical system [11]. As a result of increasing the dielectric strengths between conductive traces, smaller and more compact design of PCBs would be feasible.

In practice, coated PCBs experience different conditions. Circuit boards with conformal coating are expected to maintain their integrity at temperate gradient, humidity difference, various air pressure, and electrical stress. The qualification and performance requirement of coated PCBs are defined through a series of design guidelines, application standards, and test methods [12]. These standards ensure the reliability of freshly designed and coated boards. However, during the operational life time of coated PCBs, various factors can affect the quality of coating and, consequently the reliability of coated PCBs. Levels of degradation and material aging occur as a spontaneous natural trend. On the other hand, due to high operational voltages, the risk of PD between energized traces is increased, which is known as another source of coating degradation [8]. High levels of coating damage appear as surface degradation in terms of cracks and shrinks. Besides, the quality of coating adhesion suffers from mechanical stress caused by damages. Such aging collectively will noticeably change the dielectric properties of the coating material and will increase the risk of failure.

Under low air pressure conditions, higher levels of aging happen that result in lower discharge inception voltage [13]. Some experiments [14] have demonstrated that under a high temperature situation the degradation level is severe and the risk of failure is even higher. High operational voltage and levels of degradation in PCBs may result in PDs in early stages and might eventually lead to a disruptive discharge. Therefore, it is important to investigate and quantify the quality of insulation system for conformally-coated printed circuit boards especially under harsh environmental condition and under the impact of contamination in order to keep them away from failure and provide a safe operation.

1.2 Research Objectives and Outline

The objective of this research is to investigate the performance of conformally-coated PCBs under different operation conditions. The impact of pollution on coated PCBs was tested as well as the influence of thermal aging. Although qualification requirements and implementation standards are available for design, application, and testings, these guidelines and standards are unable to provide the reliability of coated PCBs after some levels of aging. A number of available qualification evaluation tests for PCBs provide only visual inspection which in many cases might not be a reliable method. In this research, PD measurements are employed as a non-destructive method for the evaluation of the quality of insulation material of a PCB [15]. The break-down voltage is also measured as a part of tests to examine the withstand voltage for coated boards.

In the first experiment of this research study, PD in PCBs with silicone coating was measured in the presence of pollutants. Drops of 5% sodium chloride solution and aluminum conductive particles were used as two different types of pollution on the top of coated PCBs.

For this purpose, test boards with a “Y” shape pattern consisting of two parallel conductive traces were designed and fabricated. Boards trace pattern layout was selected from the available test method (IPC-TM-650) for dielectric withstanding voltage test in coated PCBs [16]. Cleaning and coating process was performed according to industrial approved standards (IPC-CC-830B) for PCBs [17] and boards were coated with MG-Chemicals 422B silicone modified coating material. Three different zones were selected on test boards as sample locations for localized contamination. The impact of the pollution on the three different zones of an energized sample were tested and observations were reported.

The second task of this research study was to investigate the influence of environmental condition on coated PCBs. Heating and cooling cycles in the presence of humidity were the test condition to simulate the environmental condition [18]. Standard “D” comb pattern layout was chosen as test specimens according to the IPC-TM-650 standard [18] for moisture and insulation resistance qualification. The same process of cleaning and coating was applied to the new test samples. The same conformal coating material was used for these samples. Some samples were energized during the aging process and a group of test boards were aged without power. Environmental test was performed while samples were energized using a bias voltage source in order to provide an operational situation for boards under operational condition. Measurements of capacitance and loss tangent were performed using a dielectric spectrometer. The influence of thermal and humidity aging on coated PCBs were examined and observations are presented.

A series of PD and breakdown voltage tests were performed on different types of coated test samples. For this part of the study, thermally-aged samples with different conditions and different aging level were tested. Both energized and non-energized aged test boards were examined. Besides, samples with additional layers of coating were tested. The thickness of coating for the later group was measured as double the normally-coated ones. The breakdown voltage and momentary discharges were observed and the results were reported. The impact of various factors on PD and breakdown voltage were tested and observations were reported.

1.3 Contributions

The contributions of this thesis are as follows:

- The influence of pollution on PD activity in conformally-coated PCBs were investigated through a series of experiments. The presence of a 5% sodium chloride solution drop was tested on three different possible zones on a test sample.

- The impact of electrical discharge on degradation of PCB traces and the resulted corrosion were discussed. It is shown that the PD can result in severe damage even with protected coating film.

- The behaviour of PD and momentary disruptive discharges in the presence of distributed conductive particles on the top of coated boards were examined. Aluminum conductive particles were used as they are good examples for soldering residues in PCBs.

- The influence of thermal and humidity aging on coated PCBs under operational condition was tested. Classification of degradation of coating as a product of environmental condition was quantified after certain number of heating and cooling cycles. Coated samples with two different surface finish were aged and results were reported and compared with the control specimen.

- The reliability of conformal coating was reported as a function of aging level based on dielectric loss.

- The role of conformal coating on breakdown voltages in test boards with different conditions was studied. The impact of additional aging, different PCB surface plating, and additional coating layer were discussed.

1.3.1 Publications

The outcome of this study has been partially published in conference paper in IEEE Electrical Insulation Conference (EIC 2019). The main focus of this paper was on the influence of pollution on conformally-coated PCBs with application in aerospace industry [19].

1.4 Thesis outline

This thesis is classified into five chapters as defined below:

Chapter 1: Motivation, research objectives, and contributions are presented.

Chapter 2: Background about printed circuit boards including a brief history of PCB and requirements for design and fabrication process are discussed along with the PCB related standards for qualification and performance. Different choices of industrial-approved materials for conformal coating are introduced and a discussion on the advantages and disadvantages of each material is presented. Coating application techniques are compared and industrial approved test methods for inspection and evaluation of coated PCBs are presented.

Chapter 3: A series of different tests on conformally-coated PCBs are presented in this chapter. Partial discharge, breakdown voltage, surface insulation resistance, and dielectric measurements, that are the electrical ones and accelerated aging and degradation due to environmental conditions are discussed. Non-electrical visual inspections are also described in this chapter.

Chapter 4: Test sample preparation including test board selection and design procedures are provided. The process of cleaning and coating application are described. Measurements of cured coating layer for all prepared samples are provided. Visual inspection of test boards under UV light, prior to testings, is presented.

Chapter 5: Electrical tests of new coated specimens are performed in this chapter. Tests on PD under pollution and PD under conductive particles are presented and breakdown voltage test of 'Y' shape pattern samples are examined. Results and observation of tests has discussed.

Chapter 6: Assessment of thermally-aged coated PCBs are presented in this chapter. Properties of employed environmental condition test chamber and aging cycles are given. Visual inspections and measurements of capacitance and dielectric properties are performed. PD and breakdown voltage tests of aged samples under different conditions are presented and observations are described.

Chapter 7: Conclusions of this thesis project and potential future research work are discussed.

Chapter 2

Background

2.1 Printed Circuit Boards

2.1.1 History

A PCB is a complex platform made of a range of different materials, produced to provide the electrical interconnections between elements and mount components in place [20]. The invention of the PCB goes back to the early 1900s when Albert Hanson patented the ideas of "printed wire" in England to deal with the telephone exchange demand [21]. Since the regular flexible electrical wiring were initially replaced with a flat surface of conductive paths, the PCB was introduced as printed wiring board (PWB). Thin cuts of copper and brass were options of conductive conductors on a rigid substrate mostly made of Bakelite, Masonite, and thin wood cuts. Hanson also understood the advantage of miniaturized high density PWBs and included the idea of a double side PWB. His design described through holes on the substrate to provide jumper connections between selective paths. He also mentioned that conductors could be formed in an electro-deposition process or applied as conductive powder ink on the substrate. His ideas in 1903 pointed at a number of recent PCB design concepts [22]. In the 1950s, the types of material used for the substrates shifted towards resins, while conductors made of thin flat copper foil were adhered to one side and electrical components were mounted on the other side of the PCB.

Improvements have been added to circuit design and production until the demand for more robust PCBs were increased during World War II. The major achievements were the development in replacing the ceramic substrate and using a conductive printable ink instead of metal foils. After the war, the PCB technology moved forward into a commercial level lead by a symposium supported by US Aeronautical Board and the National Bureau of Standards [21]. In 1950, an Austrian inventor, Dr. Paul Eisler, patented a solution in England for mass production of PCBs using photo etching process. The process involved the photographing from the sketched wiring paths into a zinc plate which is used for further mass offset printing. From that time onward, photo-lithography method is remained as the common process for the recent PCB fabrication. The institution of printed circuits (IPC) was founded in 1957 and the first meeting on standards and regulations for PCB manufacturing was held in Chicago, IL [23]. This organization issues the industrial approved standards and qualification requirements for PCBs and provides applicable test methods related to PCB assemblies. During the 1970s to 1980s, surface finishing and solder mask treats were introduced and developed as additional processes to add a protective layer on the top of copper traces. A thin layer of tin, solder, silver, gold, or organic finishing were used to protect copper from oxidation and improve the solder-ability of PCBs. Hot air solder levelling (HASL) is an example of surface finishing which is still the most common finishing method [24]. The process of HASL finishing consists of immersing the PCB into a molten pot of tin and lead and removing the excessive solder using hot air to provide an even layer. Another surface plating which is also used in this research is electroless nickel immersion gold (ENIG). A layer of $0.05 - 0.1$ µm of gold is formed over a $3 - 3.5$ µm thick nickel layer on the top of copper traces to provide a barrier for copper traces and make the most possible flat surface with longest shelf life for PCBs. In addition, liquid photo imageable (LPI) solder masks were introduced by Japanese developers as an aqueous-based screen protection process. Solder masks are mainly used to prevent solder penetration or unwanted short connection between traces during the soldering process.

2.1.2 Design and Fabrication

The PCB design process is done to achieve all the requirements the circuit should meet for active operation as well as preventing excessive loss and manufacturing costs. Material tolerance, operational supply voltage, temperature changes, and components parameters are examples of a PCB requirements. Computer-aided software are used for engineering, design, and manufacturing steps. Engineering software such as PSPICE and SPICE are employed to analyze and evaluate the circuit design prior to production. Design software is used for layout sketching based on the PCB size and components in the circuit. The output of computer-aided design (CAD) software is usually a group of files which are used for PCB manufacturing. Upon the completion of the analysis and design steps, the main procedure for many common PCB production techniques involves image transfer, etching, drilling, and electroplating. For numerous current PCB fabrication, subtractive photo-lithography is the most productive and cost-efficient method of circuit board mass production. In this method, an image of designed circuit path layout is transferred from a file or a glass film onto the copper layer of the raw PCB. Then, the selected layer of copper foil is uniformly etched to create the sketched traces pattern. This method is known as “print-and-etch” technique

[20]. Another common PCB production technique is the additive process. First, the layout of traces is formed as a sensitized pattern on the substrate surface. Then, a layer of copper is formed on the selected locations of the substrate using the electroplating method for copper. This method does not involve any etching process.

PCBs are categorized based on several factors including but not limited to substrate thickness, thermal expansion, water absorption, dielectric constant, and glass-transition ratings. The IPC-4101 for "Specification for Base Materials for Rigid and Multi-layer Printed Boards" is the common standard that applies for base materials of PCBs. Different factors should be considered for a substrate depending on the requirements that the PCB should meet. Exposure to soldering temperature during the assembly process and components thermal expansion compatibility are two sources of stress on the PCB substrate. A range of materials are available for substrates according to the physical characteristics required for the PCB. Mainly, board's substrate material is categorized into two major types of organic and non-organic substrates. Organic substrates have layers of paper, epoxy resin, woven glass cloth, or polymers. Ceramic, glass, and metallic materials are examples of non-organic substrates [25]. For most commercial and industrial applications, glass-reinforced epoxy laminate called FR-4 is widely used as the PCB's substrate. In this material, a flame-resistant (FR) epoxy resin bonds the fibreglass cloth layers in FR-4 substrate. The conductive layer for PCBs have a variety of choices for material and thickness. Copper, Aluminum, and Nickel are the approved metal foils for PCB manufacturing [26]. The weight of conductive foil (in ounces) present in each square foot area of the raw PCB is the parameter that indicates the thickness of the foil layer [27]. The standard area weight and nominal thickness for PCB metal foil according to the IPC-4562A for "Metal Foil for Printed Board Applications" are provided in Table 2.1.

Table 2.1: Foil weight and thickness according to IPC-4562A [28]

Foil designator	Industry terminology	Area weight (g/m^2)	Nominal thickness (µm)	Area weight (oz/ft^2)	Area weight ($g/254in^2$)	Nominal thickness (mils)
E	5 µm	45.1	5.0	0.148	7.4	0.20
Q	9 µm	75.9	9.0	0.249	12.5	0.34
T	12 µm	106.8	12.0	0.350	17.5	0.47
H	1/2 oz	152.5	17.2	0.500	25.0	0.68
M	3/4 oz	228.8	25.7	0.750	37.5	1.01
1	1 oz	305.0	34.3	1	50.0	1.35
2	2 oz	610.0	68.6	2	100.0	2.70
3	3 oz	915.0	103.0	3	150.0	4.05
4	4 oz	1220.0	137.0	4	200.0	5.40
5	5 oz	1525.0	172.0	5	250.0	6.75
6	6 oz	1830.0	206.0	6	300.0	8.10
7	7 oz	2135.0	240.0	7	350.0	9.45
10	10 oz	3050.0	343.0	10	500.0	13.50
14	14 oz	4270.0	480.0	14	700.0	18.90

2.1.3 Acceptability and Standards

In PCB design standards, a balance between electrical, mechanical, and thermal properties should be maintained to meet both the reliability requirements and manufacturing cost. The acceptability of a PCB is defined based on the purpose that the assembly is manufactured for. Requirements are varied for military, telecommunication, and consumer products. Some acceptance criteria are only determined by the manufacturer based on product quality, life span, and company reputation [29]. Military specifications regulations for PCB design such as MIL-STD-2000 are applicable for certain circuit boards and rarely used in other industries. Detailed conductor size and separation, trace finish and condition, cleanliness, and solder connection requirements are provided with specific details in military standards. The recognized standards for PCBs in telecommunication and network industries are published by Bell Communication Research (Bellcore). Generic Physical Design Requirements for Telecommunications Products and Equipment, TR-NWT-000078, includes both design and manufacturing requirements [29]. The most recent industry approved standard for acceptability of electronic assemblies is the IPC-A-610. Specifications for PCB acceptability presented in this standard are widely recognized by many manufacturer of consumer and commercial products. The visual quality acceptability requirements for the manufacturer of electrical and electronic assemblies are provided in this standard as well as details regarding the handling and joint soldering. In this standard, the quality of acceptance is classified in four different levels of: target condition, acceptable condition, and either defect condition or process indicator condition [30]. Target condition is defined as the desirable condition close to perfectly described details in the standard. In many cases, the target condition is not achievable and may not necessarily be required for the reliability of the assembly. Acceptance condition characteristic of an assembly ensures the integrity and reliability of the PCB under service environment and is the most common applicable option. Any insufficient requirement to ensure the assembly work at working environment is known as defect condition. A rework, service, redesign, or repair may be required for items fit in defect condition. The quality of a defect PCB should be examined after any repair or rework. A condition that a minor damage is caused by a material, design, or operator failure, but the PCB still meets the acceptable condition is called process indicator condition. This situation requires monitoring of control system and production line to prevent any further cause in defect condition [30].

The generic physical requirements for the design information of organic PCBs is provided in IPC-2221 standard. Minimum conductor spacing and thickness for conductors are presented as well as minimum thickness requirements for each type of coating materials. Mechanical properties for material and mounting standards are described and thermal consideration for optimum condition is provided. The recommendations for PCBs with and without components are also available in this standard. Components might be through-hole, surface mount, fine pitch, or array mounting. Design information for different board types according to the end item use is classified into three different classes [27]:

- **General electronic products:** Consumer electronic products, computer boards, and some general military application PCBs are included in this class. The functionality of the circuit board is the main requirement for this group.

- **Dedicated service electronic products:** This class includes business equipment, communications facilities, and military equipment. Extended life-time and high performance under continues operation are the requirements of this class.

- **High reliability electronic products:** The highest level of quality and operation is essential for this class. Military and commercial PCBs that require continued performance with minimum downtime are fitted in this group. Critical weapons system and medical equipment are examples of products that the reliability is essential.

Supplementary fine details for IPC-2221 are presented for rigid or flexible PCBs design structure in IPC-2222 and IPC-2223 respectively.

Another industrial approved standard regarding the PCB is the IPC-CC-830B. This standard establishes the qualification and performance requirements for conformal coating insulation in PCBs. The scope of this standard is qualification and quality of conformal coating materials [12]. Details of PCBs related test methods are presented in Chapter 3. The conformance of conformally-coated assemblies is tested using a series of industrial approved test methods and test coupons. A range of different test vehicles are introduced in this standard. These standard test samples are used for the purpose of different inspections instead of using the real manufactured PCBs. Each test method indicates the standard test sample that should be used for the purpose of inspection test. The final goal of these standards is to assist designers and manufacturers of board assemblies in understanding the requirements and characteristics of various PCB applications. Also, standards provide users with the factors that might have influence on the quality of final product. Therefore, by check of these requirement qualifications and tests, a higher level of reliability and function for a PCB assembly could be achieved.

2.2 Coating

2.2.1 Conformal Coating

In general, PCB coatings are divided into two groups, solder mask and conformal coating. Solder mask is a tough surface finishing that applies on most consumer and high-technology PCBs. This protective layer is applied after the completion of all copper processes. The main role of the solder mask layer is to prevent the high possibility of short-circuit between electrical paths during the soldering process. It also works as a barrier to protect the PCB from corrosion. Solder mask layer can be formed as a dry film or a cured liquid film [31]. Conformal coating is a protective insulation layer that conforms the circuit board topology. According to the IPC-CC-830 standard, conformal coating is a thin, homogeneous, transparent polymer, and free of harmful substances. The purpose of this coating film is to protect the coated assembly from harsh environments and varying temperatures [11, 32]. High humidity, airborne contamination, and particles are examples of harsh environment for electrical boards. Depending on the PCB application, coating barrier mainly protects boards from the following failures due to operation in harsh environment [17]:

- Short circuit or current leakage between electrical paths or joints.
- Arcing, corona discharge, and partial discharge in high voltage assemblies.

- Corrosion and degradation of traces on the board.

- Solder joints fatigue failure.

Besides, conformal coating provides a mechanical support for tiny electronic parts in the moment of vibrations and movement shocks. These issues are more likely to happen as a result of small track spacing due to more compact design as well as increased voltage levels with higher frequencies in recent electrical assemblies.

It is important to mention that conformal coating is different from encapsulation of a PCB. Encapsulation is a process that the entire PCB unit is filled with a compound in order to increase the reliability and prevent others from discovering the properties of the assembly. This protection barrier provides a good electrical and mechanical protection for the encapsulated unit. However, the final product of encapsulation is not repairable and any thermal expansion might result in defects in the cured resin [31]. Additionally, this type of protection is an expensive option which takes more material and longer production time.

Originally, conformal coating was introduced to provide the insulation requirements for electrical equipment in the military section. Recently, the application of this coating includes aerospace, electrical and hybrid automotive, telecommunication, renewable energy, and home appliance industries. Requirements for coating method and curing processes are dependant on the type of application and material chemical properties. Right coating material should be selected based on the PCB application to protect the final assembly in the operational environment for the service period it has been designed for. Discussion about popular coating types as well as pros and cons of each material are presented in Section 2.2.2. Based on the application, the final thickness of protective film for different coating materials is varied. In the IPC-CC-830 standard, typical thickness of a cured coating is introduced in the range 12.5 µm (0.49 mil) to 200 µm (7.9 mil).

2.2.2 Coating Materials

Conformal coating materials are polymeric liquids that are employed to protect circuit assemblies from failure in unfavorable working condition [33]. These materials should provide a high level of insulation for the coated PCB and able to withstand against a range of solvents and contaminants. They also should be resistant to moisture and humidity in harsh environments. The IPC-HDBK-830, Guideline for Design of Conformal Coatings, categorizes conformal coating materials into two liquid groups of organic and silicone. The primary classification of popular coating types are acrylic (AR), urethane (UR), epoxy (ER), and parylene (XY) as organic types and silicone (SR). Depending on the basic resin that these materials are made from, two families of solvent base and solvent free are available for each type. Further subcategories in each family of coating materials exist based on the coating cure mechanism. A complete classification of coating material including all subcategories is illustrated in Fig. 2.1.

For some coating applications, a combination of each material are mixed to achieve the desired cured and uncured chemical properties. The combination of conformal coating material might be varied to provide the maximum adhesion to the board, increase insulation level, improve cure process, or make the coating repair work possible [17]. Some choices of silicone coatings are initially soft so that the repair work is easier. Silicone has a high dielectric strength and easily cures at room temperature. On the other hand, acrylic coatings are easy to dissolve in a range of different organic solvent since no polymerization take place during the curing of this material. Therefore, a combination of silicone and acrylic, which is used in this research, benefits from higher insulation level, faster cure time, and easier application. The final cured film properties and application method should be considered for selecting the suitable conformal coating for each assembly.

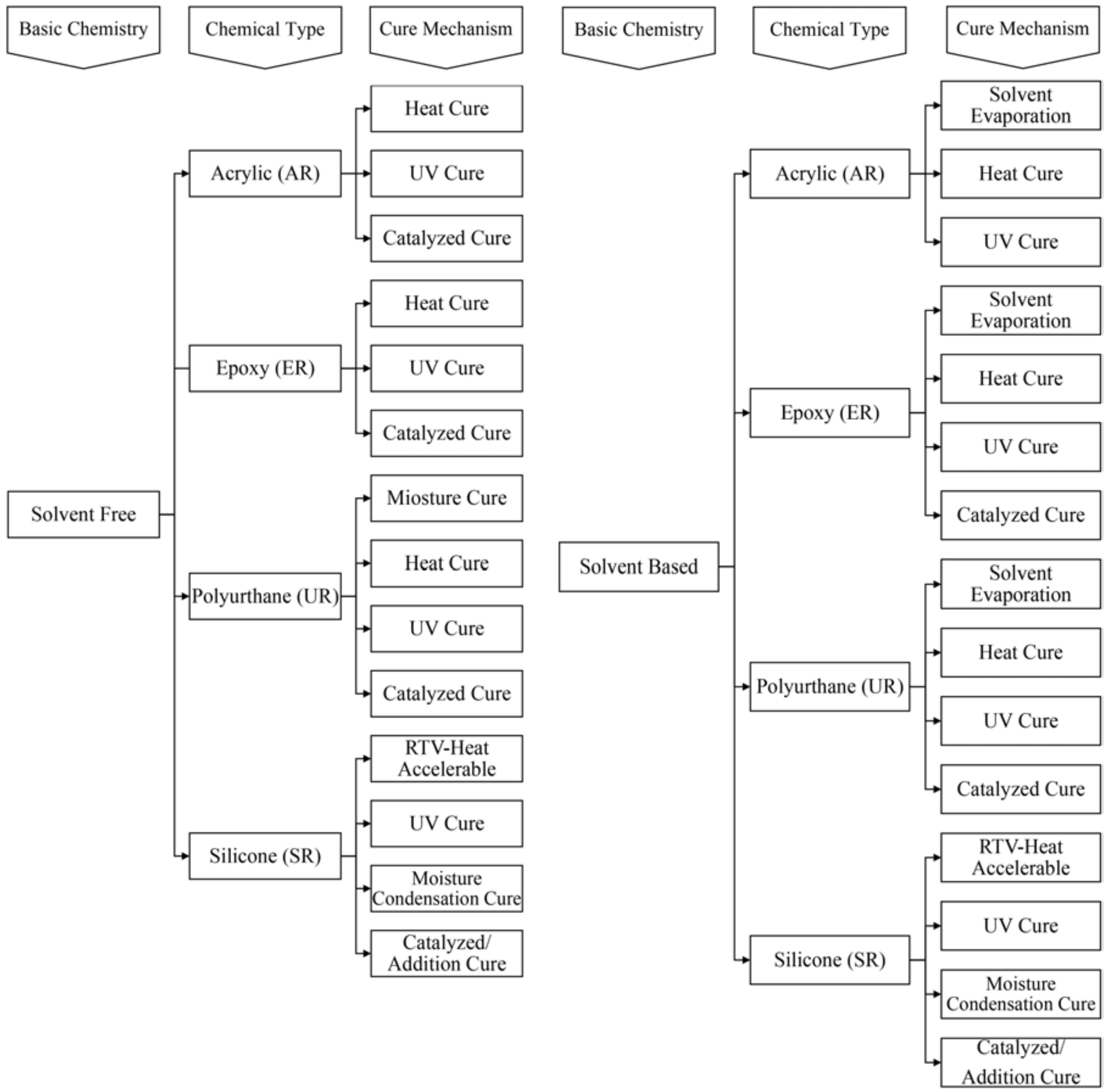

Fig. 2.1: Conformal coating materials family tree based on IPC-HDBK-830 [17].

The chemistry of each conformal coating material have some unique specifications that makes them different from each other. Acrylic (AR) coating has an easy application method as it is one part polymer with tack free and fast cure time. Easy rework and localized removal are some advantages of acrylic that makes the repair of the final coated board accessible. It is also fungus resistant and provides a good protection against humidity. During the cure time, acrylic generates little to no heat which makes it a proper choice for PCBs with heat-sensitive electronic components. Once the solvents evaporate from the acrylic coating, no shrinkage occurs on this material. It has a relatively good dielectric strength and provides a fairly general protection for circuit boards.

Silicone (SR) is another popular one part coating material mostly used for assemblies with an extreme temperature working environment. This material can typically withstand -45 ℃ to $+200$ ℃ which makes it a suitable choice for automotive industries. High humidity and chemical resistance, and good adhesion to almost all surfaces are other advantages of this coating material. Handling, application, and curing the silicone are straight forward and it can be cured faster in the presence of heat or UV light. Due to the rubbery nature of the cured silicone, it is not abrasion resistant. The final cured coating thickness for silicone can be larger than other conformal coatings depending on the viscosity of the raw material. Removal of this coating for repair purposes could be challenging and might need special solvents.

Urethane (UR) coatings have high dielectric properties and provide a good level of humidity and chemical resistance. This coating material is easy to apply and available as a one part or two part polymer. Single part urethane requires a couple of days for optimum curing while the two part polymer cures in hours. Once this coating has cured, it is difficult to do any rework or replace a component from the coated PCB. Polyurethane coated boards might

suffer from instability or peeling of the film in high humidity and temperature conditions.
Epoxy (ER) coatings are available as two part materials. Good humidity, chemical, and abrasive resistance are the key features of this coatings. One of the best advantages of this coating material is the long pot life because the epoxy starts the polymerization only after two parts are mixed together. This feature allows for easy coating application. It takes 3 to 7 hours for the mixed compound to reach optimum curing. After the complete cure, coating removal is almost impossible. Reworks can be done only by cutting the coating using a burning knife or a soldering iron.
Parylene (XY) is the trade mark of paraxylylene coating materials. The main difference in this group of materials is the method of application that is called chemical vapor deposition. In this process, the polymer becomes a gas when it is heated. The gas forms a thin film on the surface of the PCB when it is put into a cool vacuum chamber. The product of this application process is a uniform thickness and bubble free conformal coating. Parylene has good dielectric properties, abrasion resistance, and excellent chemical resistance. Heat softening, plasma etching, and excimer laser are the methods that are used for rework and board repair for PCBs with this coating. The cost of this coating with this material is higher than other options due to the special coating application. Circuit assemblies in medical and biomedical systems are usually coated with this material [17, 34].

When choosing a conformal coating material for a PCB or other electronic assemblies, it is essential to consider the application technique, protection properties, required functionality, board repairs, and environmental conditions. A brief conclusion of advantages and disadvantages of conformal coating material is presented in Table 2.2 [17, 35, 36].

Table 2.2: Conformal coating comparison table.

Conformal Coatin	Advantages	Disadvantages
Acrylic (AR)	Easily applied and removed	Low solvent resistance
	Good for rework or repair	Low abrasion resistance
	No shrinkage and fast curing process	Not suitable for harsh environments
	Good moisture resistance	Not ideal for high-temperature application
Silicone (SR)	Stable performance in extreme temperatures	Difficult to remove
	Excellent humidity resistance	Repair and rework is not easy
	Good chemical resistance	Removal requires strong chemicals
	Excellent adhesion to most PCB components	Short pot life
Urethane (UR)	Good chemical resistance	Difficult to remove
	Good humidity resistance	Risk of peeling in extreme condition
	Good dielectric properties	Long complete cure time
	Available in one and two part compound	Repair and rework is not easy
Epoxy (ER)	Excellent abrasion resistance	Difficult to remove
	Good chemical resistance	Shrinkage during curing process
	Good humidity resistance	Repair and rework is difficult
	Good performance in extreme environments	Difficult to maintain viscosity
Parylene (XY)	Great performance in extreme temperatures	Difficult to remove
	High dielectric strength	Application needs special equipment
	Excellent chemical resistance	Repair and rework is not easy
	Uniform coating film	Not ideal for extreme condition

2.2.3 Cleaning

Since surface cleanliness is the most important factor for the conformal coating adhesion [37, 17], cleaning of the PCB prior to coating application is essential. Values of dielectric withstand voltage and insulation resistance will decrease in an unclean test coupon [12]. Contamination on a PCB could occur due to a variety of different sources. Soldering paste residues is the most common surface contamination in PCBs with mounted components. Improving the soldering process and monitoring the flux usage could minimize this type of contamination. However, for the purpose of conformal coating, proper cleaning is essential even if no-clean or low-residue flux have been used during the soldering process [25]. Particles in the air, ionic residues, and oily materials might cause poor coating adhesion, corrosion, and degradation and will consequently cause failure in the circuit assembly. Proper cleaning and complete drying is recommended prior to coating application process [17]. Depending on the type of employed flux, a range of cleaning materials and associated cleaning process is used. Also, the compatibility of components with the cleaning material should be considered. A typical cleaning process consist of three steps [31]:

- Degreasing the surface using a compatible solvent fluid.
- Removing inorganic salts by rinsing the assembly with deionized water or isopropyl alcohol.
- Baking in an oven for 2 hours in a temperature of 65 ℃ to 70 ℃ for complete driness.

In order to avoid any moisture or contamination exposure, PCBs should be handled using clean rubber or latex gloves and should be kept in sealed bags if the coating application would be applied at a later time.

2.2.4 Masking

During the conformal coating application, some parts and components of the PCB should remain uncoated due to the insulating nature of the coating. Examples of these locations are sockets, connection pins, and adjustable components. Masking process is usually performed manually by an operator and could be in form of plastic covers, pads, masking tape, or peelable wet masks [38]. It is essential to provide a proper masking depending on the coating application method. Simple coverage with an adhesive tape is often sufficient for masking against manual spraying. If dipping coating method is employed, fully encapsulated coverage is necessary to prevent any penetration of the coating material under the masked area. Due to the nature of vacuum coating chamber, a totally airtight masking is needed when vacuum deposition is the coating application. Besides, chemical properties of the masking material should be considered to prevent any unwanted chemical reaction with the coating or leaving any adhesive residues on the surface. Once the coating application is performed and the coating is cured, de-masking should be done with caution to avoid any peeling, cracks, or damage to the coating. [38]. Since standard test boards without any components were used in this research, no masking process is performed prior to coating.

2.2.5 Application Techniques

After the proper conformal coating material is selected, the coating application method should be picked from a variety of different options. According to the IPC-HDBK-830, spraying, dipping, brushing, selective coating, and vacuum deposition, are the five most popular types of application method. The decision about the right application method is dependent on the coating and curing processing time, board complexity and design limitation, equipment requirements, pre-coating process, and final coating requirements [39]. For each type of coating material, the preparation time, speed of coating, and the time that it takes before the board can be safely handled is different. This information is available for each conformal coating technical data sheet (TDS) provided by the manufacturer. Board design limitation and complexity factors should be considered for solvent sensitive components and mechanical properties of the coating material. Shrinkage or thermal expansion might result in component removal. Board assemblies with connector pins or sockets require proper masking before the coating process is started. Any required cleaning or other preparation, such as oven heat, should complete prior to the masking step. Required equipment and possible methods of application for each type of coating are provided in the material TDS. Finally, the cured coating thickness, uniformity, and coverage are decisive factors to choose the application technique [32, 12].

Spraying is a method in which a low solid content coating material is spayed onto the board and could be in either forms of manual or automatic spraying. Manual spraying is usually utilized when low volumes of coated production is required for a reasonable cost. Aerosol containers or handheld gun spray are used in a manual coating process. Since areas that do not need coating should be masked to prevent any unwanted flow, this method can be time-consuming. Also, operator spraying technique has a great influence on the quality of coating, coverage, and uniformity of the coating [17]. Manual spraying method is not suggested for mass PCB coating application because a large amount of material may spray on unwanted parts and the quality of coating is operator dependent. Automated spraying is performed using a programmed spray system that moves in different directions. This method provides a more controllable coating quality and it is not dependent on the operator technique. Automated spray coating yields the ability of localized coating using a small nozzle for a PCB assembly. Both manual and automatic spraying methods require suitable exhaust to remove chemical fumes. The specification of exhausting is specified by coating manufacturers in the product TDS.

Dipping is an efficient conformal coating application method especially for high volume PCB coating processing. In this method, the circuit board is immersed vertically into a tank of conformal coating material and withdrawn after a short dwell time. The immersion and withdrawal speeds and the viscosity of the coating material are the factors that determine the coating thickness and quality [40]. These speeds are varied for different coatings in a range of 150 mm/min to 300 mm/min. The optimum immersion and withdrawal speed is provided in each coating material TDS by the manufacturer. Boards with mounted components should remain in the dipping tank for a while to let air bubbles remove from around the components.

Due to the cascade effect of the coating, slower withdrawal rate results in a thinner coating on the assembly. A fast withdrawal speed from a low viscosity coating material might result in a non-uniform coating [17]. As the whole PCB is immersed into the tank, proper masking is essential for connection pins or areas that should not be coated. However, the masking process and cost can be eliminated or minimized if the components that should not be coated are placed to one side of the PCB during the board design process. As such, boards would be immersed into the coating tank up to a certain point to prevent any unwanted coating. Dipping coating technique is a practical choice when high volume production coating is required on both side of a PCB [39]. The coating process is repeatable, and the coating thickness is controllable. As shown in Figure 2.2, most dipping coating machines, including the one built for this research study, are able to coat multiple PCBs at a same time. Due to the short pot life for some materials, choices of coating might be limited for this method.

The most simple and low cost method for application of coating for a limited number of PCBs is the brushing technique. This method does not require any special equipment and is usually applied manually by hand, similar to a brush painting process. The advantage of brushing technique is that no special masking is required because the operator only applies the coating to specific areas of the assembly. Although it seems not to be an expensive option for coating, it is labour intensive. Besides, it is difficult to obtain a uniform coating surface and there is a high chance of bubble formation while employing this method. Brushing is a suitable choice for reworks and repairs of conformal coatings.

Selective coating is introduced as a new growing technique for conformal coating. The coating application fundamental in this method is similar to the automated spraying technique. Two major advantages of this method are eliminating the costly and time consuming masking operations, and reducing the required labour during the coating process. A three

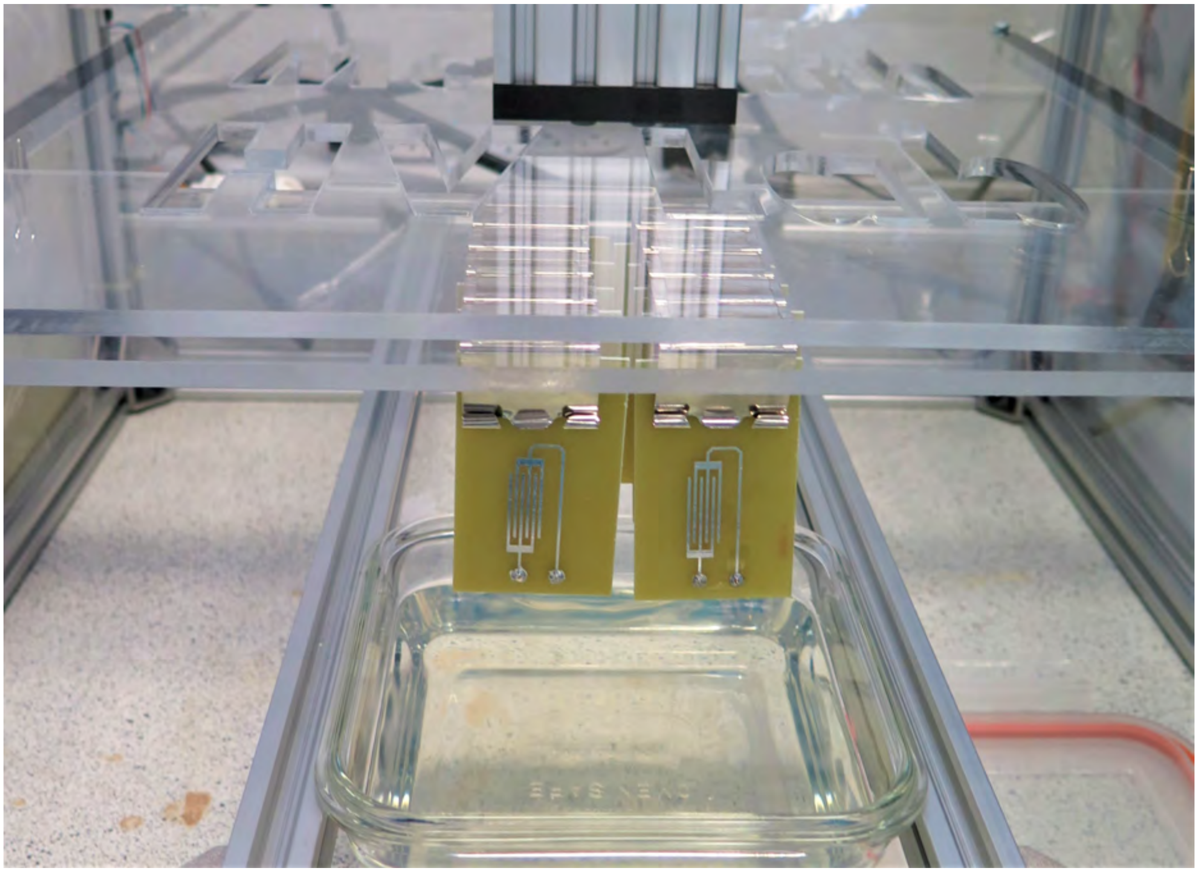

Fig. 2.2: PCBs mounted on the tray of conformal coating dipping machine designed and built in this research.

axis programmable robot is worked in conjunction with an adjustable moving surface to provide the maximum flexibility for the movement [41]. Therefore, the nozzle can easily move over the assembly under coating. In this method, almost any PCB configuration can be locally coated without any masking needed. Different applicator nozzles are employed providing an atomized mist or a curtain flow of coating material. Nozzles are fed from a pressurized tank of conformal coating material. The required pressure is created by completely dry air or nitrogen gas pressure to minimize any polymerization of the material in the tank. Although the capital cost for initial equipment is higher than manual operation, in mass production, it saves more expense by reducing the labour cost and maximizing the coating material usage.

Vacuum deposition application method is only employed for parylene (XY) conformal coating material. A thin, uniform, full coverage of parylene is deposited on the target assembly through a vapor deposition polymerization in a vacuum chamber. In this method, an even layer of conformal coating is formed all over the PCB and proper masking might be required for areas that should not be covered. As the coating application is a gaseous process and performed in a vacuum chamber, masking should be airtight and properly sealed. The deposition process is repeatable when higher thickness of coating is desired. Since a special vacuum chamber and sophisticated operator are required for this process, the final cost of coating application is high. However, the product of vacuum deposition parylene conformal coating provides a perfect coating coverage with excellent dielectric strength, moisture resistance, and stability in long term [17].

2.2.6 Curing

Once the coating material and its application method for an assembly are selected, curing is the last step for conformal coating. Depending on the chemistry of the coating material, one or a combination of room temperature cure, heat cure, UV light cure, moisture cure, and catalytic curing processes could be employed [17]. Optimum cure techniques are suggested by the supplier in the TDS of each coating material. In room temperature curing, the liquid solvent evaporates naturally, therefore, coating resin is simply formed on the assembly's surface. Sufficient ventilation and exhausting are required for coating with flammable solvents [12]. Heat and UV cure mechanisms are relatively faster than room temperature curing. For some coatings like silicone, evaporation of the solvents in the coating is accelerated in the presence of heat. Heat curing can be recruited as a secondary mechanism for UV, moisture, or room temperature cure. While higher levels of heat might increase the curing speed, thermal sensitivity of PCB's component must be considered [39]. In moisture cure coatings, silicone and some urethane for example, the material uses the ambient humidity for the polymerization process. UV cure mechanism absorbs UV light energy for polymerization process and the coating forms quickly. Based on the chemistry of the coating material, suppliers provide the duration, wave-length, and intensity of the UV source that is required for curing. A secondary cure method is available for most UV curable conformal coatings to cure the coating materials that are placed in shadowed areas. Catalytic cure materials are solvent-free, organic conformal coatings that start the polymerization process by a chemical reaction between two parts once they are in contact. This method is employed for shadowed parts of UV curable materials. The area between the bottom of a component and the PCB assembly it is attached to is an example of when this method would be utilized.

In conclusion, selecting the right coating material based on the required properties and working conditions of the final assembly is an essential factor. The compatibility of coating material with components from chemical and electrical view points and the final cost of the coated board should also be considered. A proper coating application method is picked according to the coating material, number of the final coated assemblies, available equipment, and cost of the coating operation. Pre-coating steps, including cleaning and masking are important to provide the functionality and reliability of the coated board. Finally, a wet coated board should be completely cured according to the supplier recommendations and the assembly limitations to ensure the quality of the coated board. The uncured conformal coating should be free of debris, bubbles, dark or white spots, wrinkles, cracks, and peeling.

The cured coating should be smooth, transparent, homogeneous, and tack free. Inappropriate coating material, improper preparation and application method, or incorrect cure mechanism might cause a defect in the conformal coating leading to a failure in the assembly.

2.2.7 Approved Inspections

The quality of a conformally coated PCB is assessed based on a series of electrical, physical, and basic environmental inspection tests. These assessments are employed for both qualification requirements and qualification retention of a coated circuit assembly [42, 12]. Examinations are performed to ensure that the final circuit assembly has the required qualifications to perform reliably. The reliability of a PCB is defined as the ability of a board to perform the required operation under specific working conditions for a given period of time [17]. Depending on the target industry that the PCB is designed for, long-time reliability of the circuit assembly is defined through several ways. A number of approved test methods and techniques are available to examine the requirements of the international industrial standards as discussed in Section 2.1.3. For some specific circuit assemblies with special applications, additional military, environmental, safety, or local standards might be applied to ensure the performance of the coated PCB. In this research, a series of test methods for qualification and reliability of conformally coated PCBs are presented, and some electrical examinations and measurements are performed and evaluated.

A set of test methods from various organizations and companies are available for the reliability of coated PCBs. A list of suggested test conditions based on the IPC organization standards, as the industrial and military approved provider, for assemblies with conformal coatings is presented below.

- **Thickness:** Similar to any other insulation, a minimum thickness of the cured con-

Table 2.3: Thickness requirements for test boards according to IPC standards [12].

Coating Material	Required Thickness (μm)
Acrylic	25 - 75
Polyurethane	25 - 75
Silicone	25 - 75
Epoxy	50 - 200
Paraxylylene	12.5 - 50

formal coating is required to be able to provide the protection for the PCB assembly. Depending on the coating material and the application method, the thickness varied from 0.01 mm to 0.2 mm [17]. The optimum coating thickness of each material is provided in TDS by the manufacturer according to the chemistry of the coating material. For the purpose of quality inspection, a range of cured coating thickness is presented in [12]. Table 2.3 shows the thickness requirements for test vehicles based on the IPC standards. While the advantages of additional coating has presented in [8, 14], no proof is available that coating with double thickness could provide as twice protection as a single coating layer.

Several methods can be employed for the measurement of the thickness of a cured conformal coating. The most applicable and easy way to perform measurement is using a micrometer. The thickness of the uncoated board needs to be measured prior to the coating application. Other thickness measurement equipment such as eddy current probe, ultra sonic gauges, or optical devices can be used depending on the size and the number of samples.

- **Flexibility:** This test method is designed to evaluate the physical resistance of the conformal coating film against bending. Four coated electroplated tin panels are used as test coupons. The sample is bent by 180° while a mandrel of 0.3 cm holds the center of the panel. Bending should be done over the mandrel. Results of the test are expressed by inspection using visual magnification for possible cracks and crazing [43].

- **Abrasion:** The resistance of the coating surface against abrasion is assessed in this test method. A square shape coated test board with 10.8 cm side is tested using an abrasion machine with 1000 grams load wheels [44]. In this evaluation, changes in coating thickness and level of physical damage is assessed and results are compared with new samples.

- **Dielectric withstanding voltage - polymeric conformal coating:** This test method is used to ensure the safe electrical operation of a coated circuit assembly at its designed rated voltage and momentary over voltages. It determines whether the insulating coating material and PCB tracks spacing could provide the reliability necessary under the designed voltage. Five standard "Y" shape patterns (Labeled as 'C') of IPC-B-25A multi-purpose test boards are required as shown in Figure 2.3. Boards should be cleaned and coated by conformal coating material based on the PCB requirements and coating material provided in the TDS. An adjustable voltage source capable of supplying up to 1.5 kV AC at 50-60 Hz is required to energize the test boards. It is recommended to clean the uncoated samples with isopropyl alcohol for 30 seconds prior to the test and completely dry the cleaned sample in an oven of 50 ℃ for a duration of $3-5$ hours. Test samples are energized and voltage is increased from zero to 1500 V AC at $50-60$ Hz at a 100 V per second rate. The leakage current is tested for samples up to maximum 10 micro-amperes. During this test, sample boards should not experience any flash-over, spark-over, or breakdown [16].

- **Fungus resistance:** The resistance of the conformal coating material to fungi and the

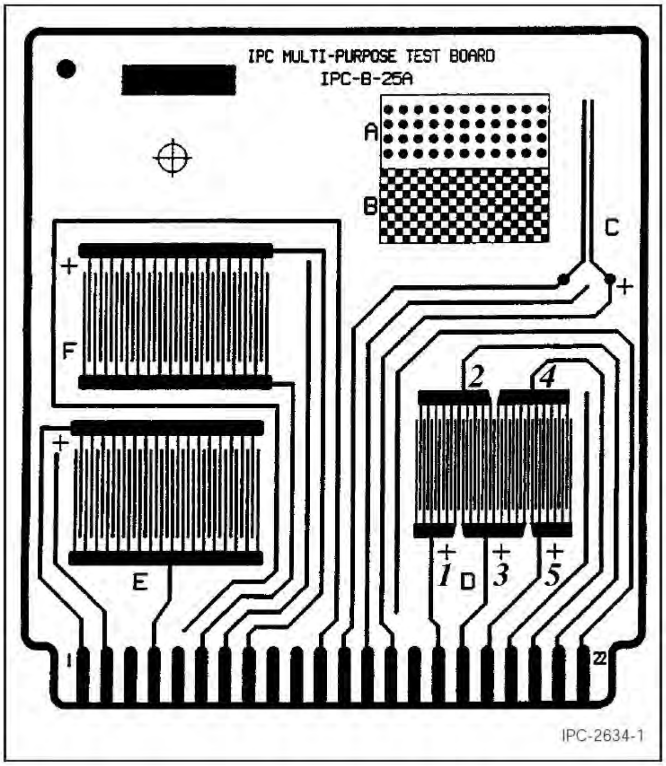

Fig. 2.3: IPC multi-purpose test board IPC-B-25A. Including "Y" shape, "D", "E", and "F" comb patterns [12].

impact of fungi presence on the coating material is evaluated. This test is performed in high humidity, warm environment, and in the presence of inorganic salts as desired conditions for fungus growth. Five different types of spores are examined on conformal coating. Corrosion from the fungus test should be reported. The conformal coating should not cause and develop any growth of biological attack [45, 12].

- **Moisture and insulation resistance:** Insulation resistance of coated samples exposed to high humidity and heat condition is examined. This test method is approved and applicable for both acceptability of PCBs (IPC-A-600) and, qualification testing of coated PCBs (IPC-CC-830). Five standard “D” comb patterns of IPC-B-25A multi purpose test boards are required. Four coated samples as specimens and one un-coated sample as a control object should be prepared. A controlled chamber capable of programming and recording environmental condition is required for this test. The test is performed in a temperature range of 25 ℃ to 65 ℃ , and 90 % relative humidity (RH) for a duration of 20 cycles. Insulation resistance of the specimens is measured after the first, second, third, forth, seventh, and tenth cycle. Test boards should be energized in the chamber using a DC power source. Once samples are stable, insulation resistance, visual appearance of the test board, and dielectric withstanding voltage should be evaluated as the target of this test [18].

- **Thermal shock:** This test method determines the physical ability of the conformal coating to withstand sudden temperature changes. Extreme thermal shock of fast cooling and heating cycles from −65 ℃ to 125 ℃ is designed as the test condition. Samples are exposed for 15 minutes in each cycle with 2 minutes intervals for one hundred cycles. After 100 cycles, visual appearance and dielectric withstanding voltage requirements should be based on IPC-CC-8310 standard [46].

- **Hydrolitic stability - conformal coating:** The quality of conformally-coated PCBs under storage condition is the target of this examination. The resistance of the applied conformal coating to return to a liquid condition in exposure to specific heat and high humidity is determined in this test method. Five conformally coated “Y” shape patterns of multi purpose test board is employed. Four samples are exposed to 85 ℃ and 95 % RH for 120 days. One coated sample is kept as control. Specimens should be examined for evidences of reversion, crack, tackiness, loss of adhesion, or

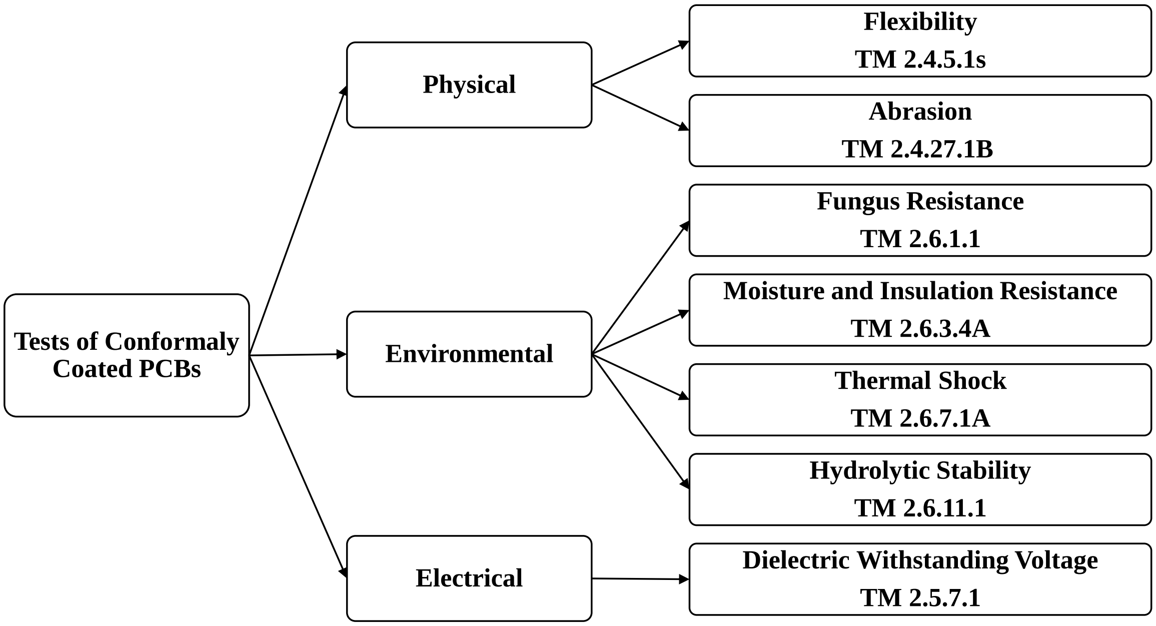

Fig. 2.4: Test methods for qualification of PCBs with conformal coating based on IPC TM-650 approved test methods [48].

liquefaction at 28th, 56th, and 84th days of test [47].

Figure 2.4 illustrates the categorized approved test methods for circuit assemblies with conformal coatings according to the IPC organization. All of these tests are not required or even applicable for all assemblies due to the design and application of the PCB. Standard test methods including test vehicles and required evaluations are presented for inspection in each test condition. No evidence of bubbles, wrinkle, pinholes, corrosion, peeling, cracking, and reversion is accepted for test coupons in visual inspections before and after of all the test methods.

In addition to qualification tests, it is important to evaluate the success of coating process. Simple visual inspection and automated systems are employed to control the coating coverage, thickness and uniformity, voids, bridging, and workmanship faults in coated PCBs [17].

Some reworks might be done before or after the curing if any issue is detected. Magnification is the simplest method of visual control for loss of coating or unexpected damages. Enlargement of 2X or 4X is recommended in [17] as the sufficient magnification level. Inspection with UV light is another mean of conformal coating visual evaluation for coating materials that fluoresces under UV light. A low intensity UV light (fluorescent or LED) is used as a non-expensive and effective technique for inspection. Most cracks, dirt, bubbles, and delamination can be observed clearly under UV light. Besides, automated inspection systems are available for some inspections, especially when a large volume of boards should be tested. Automatic camera-based systems and laser-based tests are two common automated inspection technologies that respectively use image processing and reflection detection techniques for inspection.

2.3 Summary

In this chapter, a brief history of PCB was presented and different types of PCBs with various conductor and substrate properties were introduced. Methods of design and process of fabrication for a PCB were described. A series of standards and guidelines for design and fabrication were presented and application of the standards based on the PCB application discussed.

This chapter also provided information regarding the conformal coating in PCBs. The reason for conformal coating layer application and advantages of coating were presented. Different types of coating material, conformal coating selection, methods of application, and curing process were described. Required preparation prior the conformal coating was presented and a number of inspections and test methods that can be performed to evaluate the quality of the coated assembly have been described.

The next chapter involves electrical and non-electrical testings of PCBs. Destructive and non-destructive test methods are provided and the method of measurement for each test is presented according to the standard test methods.

Chapter 3

Literature Review

3.1 Partial Discharge

Electrical discharges between two conductors with high voltage difference could be either disruptive or partial. In the moment of disruptive discharge, conductors are joined unintentionally and a significant discharge current flows between them. Such disruptive electrical discharge is also called breakdown. An electrical protective device, fuse or breaker for instance, is needed to control the fault and disconnect the current. Breakdown discharge usually happens between two insulated conductors with a high voltage difference. A partial discharge (PD) also happens between two conductors with high electric potential difference. According to IEC60270 standard, partial discharge is a "partially localized electrical discharge that does not bridge the insulation between conductors". In the moment of partial discharge, a very small fault current flows between conductors and consequently, the electric field is reduced below the breakdown point in the high electric field region. Therefore, risk of full discharge current flow is reduced and system can operate normally. Partial discharges usually occur in the insulation structure between two electric conductors through surface, voids or particles [49, 7]. Partial discharge is detected in the form of a pulse with a duration of less than 1 µs and might happen in a void within the insulation material, on the surface of the insulation, or externally as corona discharge. The magnitude of the voltage in which the partial discharge pulse is detected, is called the partial discharge inception voltage (PDIV).

In power systems, partial discharge activity can result in physical or chemical degradation of the insulation material. Degradation could be in the form of damages, cavities, chemical change, or failure of the insulation in the long term. A series of factors including impurities in the insulation, contamination, and operating condition such as vibrations, air pressure, temperature, and humidity have great impact on the existence and continuity of PD activity whether inside or on the surface of the insulation system [50].

Printed circuit boards are the infrastructures for almost any power electronic systems. As a result of increased operational voltages in PCBs, the risk of discharge failure within the narrow clearance space between energized traces has increased [10]. As described in Section 2.1.3, the minimum conductor spacing and thickness for an individual layer of a PCB is determined in [27] based on the PCB operating voltage. In addition to clearance, PCBs are usually coated with conformal coating material to improve the dielectric strength level and increase the reliability of PCB assembly. However, in the moment of discharge, the coating insulation material suffers from degradation and the quality of insulating material is downgraded [5]. The degraded insulation may result in more PDs in early stages and might eventually cause a breakdown in the assembly.

Partial discharge detection is used to evaluate the quality of the solid insulation material in high voltage assemblies. This technique is employed as an effective method for testing the integrity of the insulation material on coated PCB [51, 7]. Several research work have been performed on PD activity in PCBs with or without coatings. Koch *et al.* [52] tested six different PCBs with various coating materials including solder masks and silk screens lacquers with different curing mechanisms. Prior to testing, some levels of thermal and humidity aging preconditions were applied on test samples. PD was introduced as non-destructive tool for coating quality inspection in PCBs. They found that the applied preconditions did not have negative impact on PD inception and extinction voltages. They also reported that a series of other aging mechanisms such as fast temperature cycles, heat and humidity aging, or extreme temperature might be needed for the purpose of accelerated aging in the coating of a PCB. No evidence of void, defects, and de-lamination was reported. Another study on the influence of PD aging on polymer coated boards are reported in [53]. The authors employed test boards with various conductors separation but the coating material for samples was not reported. They found that the coated conductors with smaller distance may increase the PD strength and degradation of polymer coating was observed. In [54], surface degradation of silicone rubber material under corona discharge was tested. They reported that the silicone exposed to corona discharge was damaged physically and chemically. Cracks and damages was observed on the surface of the silicone and hydrophilic by-products was formed on the surface which is undesirable for insulation material working in wet conditions. Emersic *et al.* [55] tested the impact of PD sourced from high voltage in traces on degradation of silicone coating. Test samples with arbitrary layout of a curved shape design were used in their study and the coating thickness was in range of $60 - 200$ µm. They observed severe level of silicone degradation in samples with coating thickness less than 70 µm. Inconsistent PDIV was reported as a result of degradation and accumulation of some unknown dark substance on the coating surface. The influence of surface pollution layer on discharge location in PCBs with conformal coating was tested in [56]. Three different conductive pollution was tested on boards with silicone conformal coating. It was reported that the breakdown discharge occurs through the applied conductive pollution on the surface of coating.

In this study, PD in PCBs with silicone conformal coating were examined in the presence of two different types of pollution on the coating surface. Boards were designed, fabricated, cleaned, and coated according to IPC standards as discussed in Sections 2.1.3 and 2.2.1. In the experiments, a high voltage was applied to the board traces rather than corona discharge to provide operational conditions. Complete experiment process and observation is described in Chapter 4.

3.2 Breakdown Voltage

According to [57], dielectric breakdown voltage is the electric potential difference that the failure is occurred in the insulating material between two electrodes. This test is a technique for determining the electrical breakdown resistance of the insulating material subjected to $50-60$ Hz high voltages and might be applied at different levels of humidity, temperature, or air pressure. The dielectric strength of conformal coating material is a property of interest for selection and application of the coating material. Results of a breakdown voltage test does not provide the behavior of the insulation and in many cases should be used in parallel with results from other functional tests. In this thesis, breakdown voltage test was performed on coated and uncoated test boards in atmospheric and low air pressure to compare the impact of air pressure on the performance of the conformal coating from the breakdown point of view. In addition, single coated and double coated samples were tested to evaluate the impact of an additional coating layer on the breakdown voltage. Test procedure and sample conditions are described in Section 5.2.

3.3 Surface Insulation Resistance

Surface insulation resistance (SIR) is defined as the electrical resistance of an insulation between two conductors and is one of the most common test methods for evaluation of the reliability in PCBs [25]. Basically, the SIR test is performed for three different reasons including the qualification of a product, evaluation of a process, or comparing the insulation materials [58]. Current leakage or discharges might result in momentary or permanent fault in a circuit assembly as a result of SIR reduction between two conductors under a high voltage [59]. In PCBs with conformal coating, the potential risk for presence of contamination under the coating layer or formation of voids during the coating application as well as degradation of the conformal coating could affect the SIR. Based on IPC-9202 standard for "material and process characterization/qualification test protocol for assessing electrochemical performance", electrometer, picoammeter or high resistance meter can be employed for SIR measurements to quantify the impact of SIR change [60].

In 2003, Zhan *et al.* [61] tested the SIR in uncleaned PCBs exposed to temperature and humidity condition to evaluate the influence of environmental condition on SIR of coated boards. They reported a high stability level to SIR degradation for conformally-coated PCBs in the absence of contamination. Three different types of coating material were tested and they found that silicone provides much better protection than urethane and acrylic. A high rate of failure was reported for tests performed at high humidity with samples of less conductor spacing.

In [62], studies were done on PCBs with conformal coating in the presence of process-related contamination. The performance of silicone coating was evaluated on assemblies exposed to high humidity and ambient temperature. They observed that the flux residues on the coated board significantly decreased the SIR and caused a failure. It was observed that the performance of the electrical components was decreased as a result of lower SIR and the coating provided limited protection in humid environment.

3.4 Capacitance and Dielectric Loss

The quality of an insulation system in a circuit assembly provides the electrical properties of the system. In PCB with conformal coating, the quality of the insulating protective layer can be assessed by measuring the capacitance and loss factor. These electrical parameters of an insulation are frequency dependant. Therefore, measuring the capacitance and the dissipation factor (dielectric loss) of a dielectric material can evaluate the properties of the dielectric over a range of frequency. These dynamic electrical measurement are non destructive and are used to indicate the insulation aging phenomena [63]. Loss tangent is a dimensionless measure that shows the magnitude of time varying electromagnetic energy loss in a dielectric material [64]. Higher loss tangent values cause more losses in the form of heat and may cause thermal breakdown in the insulation system. Monitoring the dynamic properties of an insulation material is the mean of assessment for safety and reliability in a system. One of the main factors of dielectric loss change in a material is the aging process of an insulation over time.

In this thesis, the quality of silicone conformal coating was tested in PCBs exposed to thermal and humidity aging cycles. The evaluation of the insulation material was performed using dielectric spectrometer and insulation testing equipment. Test procedure and obtained results are presented in the next chapter. No studied has done by others on the impact of aging cycles on the electrical performance of conformally-coated PCBs.

3.5 Non-electrical Test

While electrical tests are the most important test methods for PCBs, non-electrical test methods have significant impact on the acceptance requirements of the PCB [25]. Two inspection-based non-electrical test methods are visual and automatic optical inspections. The first method is totally dependant on the operator's skill, light condition, and the acceptance level for the inspection. Visual inspection is usually applied under a source of UV light and often used for detecting greasy residues, poor coating coverage, or cracks and damage in coating surface. In the automatic optical inspection, an image is taken from board and further processed and compared with expected parameters based on system programmings. This method is commonly used for inspecting the components installation, narrowed traces due to etching process, and inner-layers prior to conformal coating. Since this method detects the unaccepted boards, it prevents coating of damaged boards and consequently, saves material and time. In [65], visual inspection is employed for the evaluation of conformal coating quality exposed to thermal shock and thermal and humidity aging. Coating damages and corrosion on test samples were compared using non-electrical test methods. In this thesis, test samples were visually tested under UV light of $395 - 410$ nm wave length to indicate any voids, uncleaned areas, or defects on the coating.

3.6 Summary

In Chapter 3, electrical and non-electrical test methods for evaluation of a PCB assembly have been presented. Both destructive and non-destructive discharges were discussed. PD activity and PDIV definition were described and a literature review of previous studies on PD in PCBs were presented. Breakdown voltage test, surface insulation resistance, and dielectric measurements are discussed and available approved test methods were noted. Besides, non-electrical tests were introduced as a mean of coated PCBs visual evaluation.

The next chapter contains the experiment setup preparation part for this thesis. Test board design and preparation consist of cleaning, coating, and coating thickness measurements that will presented in the next chapter.

Chapter 4

Sample Preparation

4.1 Board Design and Variety of Samples

Two groups of test boards were designed for experimental tests in this study. Samples were chosen, designed, and fabricated according to the dielectric withstanding voltage and moisture and insulation resistance test methods. Board sketches were designed using KiCad software for accurate layout dimension and spacing and the produced image was converted to a 2D binary file format ready for commercial fabrication. The samples substrate is 1.6 mm thick FR-4 glass-reinforced epoxy laminate with single side one ounce copper of 35 µm foil thickness. Test boards are complied with IPC organization standard for qualification and performance of electrical insulating compound for printed board assemblies [12]. All boards were fabricated commercially and kept in sealed packaging to minimize the corrosion and contamination exposure.

The first group of test boards were designed based on [16] and consisted of a “Y” shape pattern with two symmetric parallel traces capable of withstanding a voltage of 1.5 kV

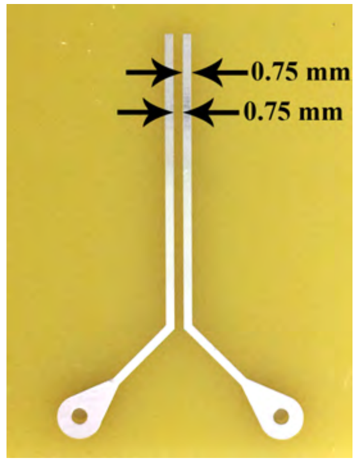

Fig. 4.1: Y shape layout test board for PD under pollution and breakdown voltage tests based on IPC-TM-650. The board size was 35 mm by 45 mm and the clearance of parallel tracks and the width of traces are both 750 μm

AC at $50 - 60$ Hz. The samples dimension were 35 mm by 45 mm and connection pins were soldered prior to cleaning and used to fed samples with a high voltage. The width of conductive paths and the clearance between traces, are both 750 μm as shown in Figure 4.1. Conductive traces were covered by hot air solder leveling (HASL) surface finish technique which is a cost effective and common protection layer for copper against oxidation.

The second group used for moisture and insulation resistance tests consist of “D” comb pattern from IPC-B-25 standard test boards. This group of samples were selected according to the IPC-TM-650 test method [18]. This pattern consists of two parallel comb layout having 41 bias traces in total. Both conductive path width and spacing between adjacent traces are 0.318 mm and traces are fed through connection pins located on one side of the board. These test samples have the dimension of 47 mm by 60 mm. Two different surface finish of HASL and electroless nickel immersion gold (ENIG) as described in Section 2.1.2 were chosen for this group of test boards. Figure 4.2 shows the “D” comb pattern test boards

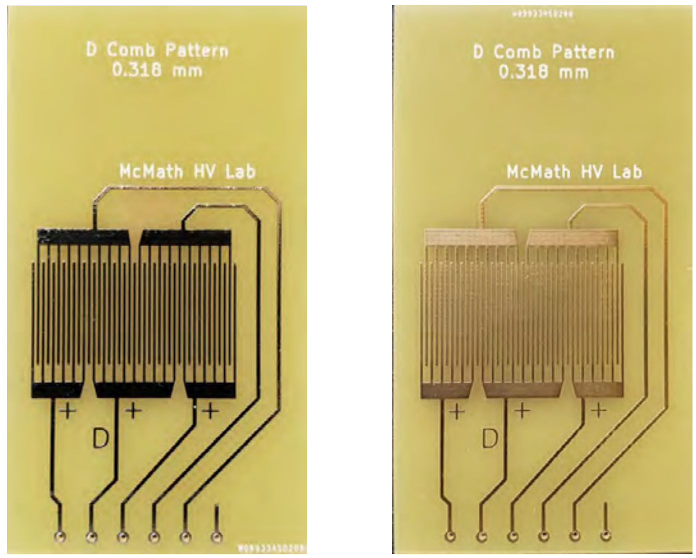

(a) **(b)**

Fig. 4.2: Standard D comb pattern test samples. Clearance between conductors and width of each trace of the comb lines are equal to 0.315 mm. a) Test board with HASL surface finish, b) Test board with ENIG surface finish.

with two surface finishes.

In order to provide better classification in assessments, a variety of test samples were prepared for each test method and unique codes were assigned to each sample. A total number of twenty samples were divided into four groups based on the surface finishing and thickness of the coating. One of five allocated samples was kept as the control and the rest were used for testing purposes. Test coupons for PD under pollution and breakdown voltage tests were divided into three different groups based on the coating layer. Twelve samples were prepared for breakdown voltage test in four conditions and three samples were prepared for PD testing. Table 4.1 shows the type of samples and assigned code for each category based on surface finishing and coating properties.

Table 4.1: Test samples variations and related test method. Samples are classified based on surface finishing and the thickness of the coating. A total number of 35 samples were prepared for this experiment.

Row	Code	Quantity	Test Method	Trace Layout	Surface Finishing	Coating Layers
1	GD	5	Moisture and Insulation Resistance	D Comb	ENIG	Double
2	GS	5				Single
3	HD	5			HASL	Double
4	HS	5				Single
5	YS	9	PD under pollution and Breakdown	Y Shape		Single
6	YD	3				Double
7	YN	3				No Coat

4.2 Cleaning

As described in Section 2.2.1 and according to [17], surface contamination is the main deterrent for adhesion of the coating material to the surface of an assembly. As discussed before, any inadequate cleaning process could leave undesired residues on the surface and may result in poor coating and reduction of the SIR. In industry, based on the flux type, soldering process, and components on the boards, different methods are employed for cleaning. Various types of solvents are available for organic contaminants, flux residues, and ionic residues [37, 17]. Test boards in this study were cleaned after the connection pins were soldered and prior to coating process in order to maximize the coating quality. The cleaning process was done in the following consecutive steps [8]:

- Boards were soaked for 5 minutes in an ultrasonic bath of 0.35 ammonia alkaline solution at 35 °C.
- Rinsed for 5 minutes with deionized water to remove alkaline solution.
- Were soaked in isopropyl alcohol for 5 minutes to remove greasy residues.
- Further rinsed with deionized water for 5 minutes.

- Finally the cleaning process was enhanced by drying the cleaned boards using a nitrogen gun for an even complete drying.

All the cleaning processes were conducted in the University of Manitoba Nano System Fabrication Lab (NSFL) clean environment. The clean area environment has 10 particles of 0.5 microns per cubic foot (Class 10) while the university engineering building has 1 million particles per each cubic foot [66]. Once the cleaning process was completed and boards were dried, specimens were put in clean sealed bags to prevent any exposure to contamination. Figures 4.3 and 4.4 show the test boards soaking in the ultra sonic bath of Ammonia solution and isopropyl alcohol respectively. In addition to sample cleaning, all the equipment was thoroughly wiped with isopropyl alcohol prior to the cleaning and coating procedure and boards were handled with clean disposable gloves the entire time.

4.3 Coating

As described in Section 2.1, a range of different polymers and associated application methods are available for conformal coating of PCBs. In this study, MG-Chemicals 422B silicone modified conformal coating was used as the coating polymer [67]. This coating material is a combination of silicone and acrylic which makes the application and rework easier and provides a faster cure time at room temperature. Silicone is selected in this study because it is widely used in high voltage applications and provides an excellent humidity and chemical resistance along with outstanding dielectric properties. Among the variety of techniques used for application of conformal coating (Section 2.2.5), the dipping method was employed in this research due to the following reasons. First, the quality of coating and the thickness of coating layer was controllable by immersion and withdrawal speed adjustments. Besides,

Fig. 4.3: Cleaned plastic clips hung from aluminum bars are holding the samples in ultra sonic bath of Ammonia solution at 35 ±1 °C.

applying an even, uniform coating layer to a number of test boards was practical in each dipping cycle. Finally, providing the required application equipment was possible in the lab. For coating application purpose, an automated programmable machine was designed and developed at McMath High Voltage Lab. The machine was equipped with an actuator mounted on an aluminum assembly for vertical movement of a tray of PCBs over the dipping tank as shown in Figure 4.5. The coating device is capable of coating about 60 pieces of boards of 5 cm width in each dipping cycle. The system is controlled using a digital micro-controller to keep the immersion and withdrawal speed of the moving actuator at 15 cm/min according to the MG-Chemicals 422B silicone modified TDS [67]. The main control unit also

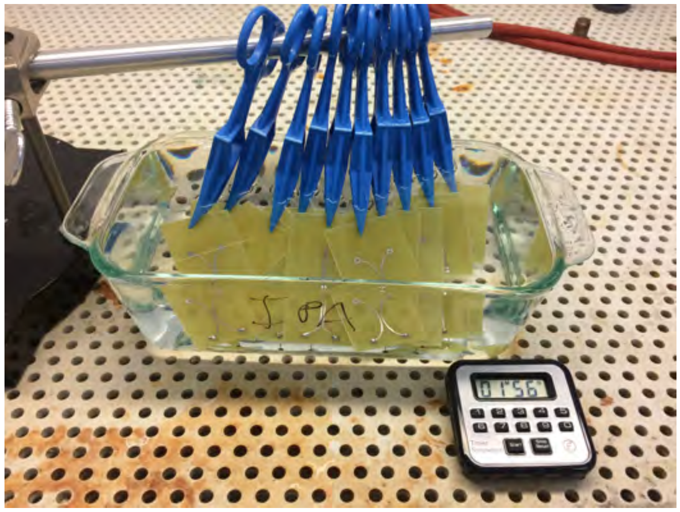

Fig. 4.4: Cleaning test boards by removing greasy materials from surface using isopropyl alcohol soaking for 5 minutes.

measures the temperature and relative humidity of the environment throughout the process to ensure the coating condition complies with coating material TDS as suggested in [12]. Test boards that were prepared for coating were mounted vertically on different trays in order to make the coating process faster by replacing trays of samples into the coating machine. Boards were held using spring clips attached to the tray.

Coating application involved the immersion of boards into a container of coating material at the controlled speed followed by withdrawal at the same rate after a dwell time of 1 minute. The dwell time in the tank is to ensure the coating material covers the entire surface and any possible bubbles formed on the surface are removed. Figure 4.6 shows the mounted test boards immersing in the dipping tank. Some of the test specimens were dipped additional times to have samples with higher coating thickness for moisture and insulation resistance and breakdown voltage tests. Samples with additional coating layers were prepared to investigate the impact of thicker coating on the outcome of the proposed

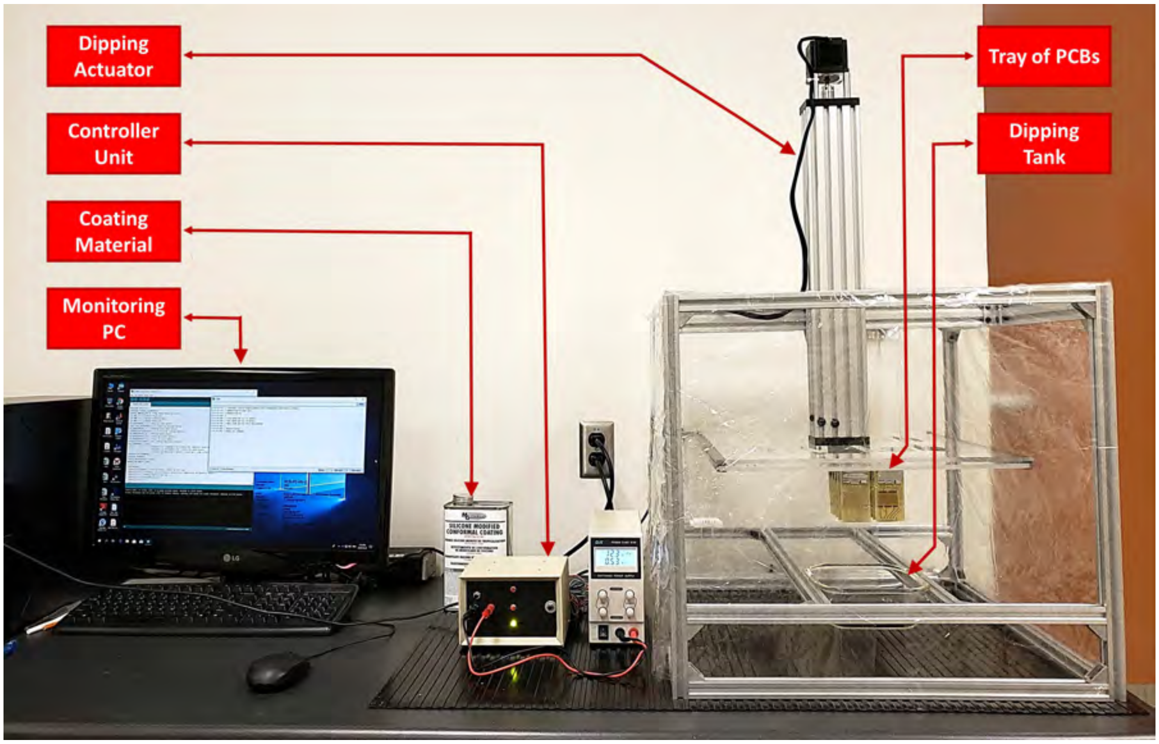

Fig. 4.5: Conformal coating application device with controlled speed that was designed and developed in McMath High Voltage Lab. The micro-controler unit adjusts the actuator speed and send the system report to PC. Boards are mounted on a tray, ready for dipping in a tank of silicone coating polymer.

tests.

Since the solvent in the coating material might dissolve previous coatings, the dwell time was reduced to 10 seconds for the additional dipping process to prevent any negative influence on the coating quality. Besides, a time of 8 to 10 minutes is allowed before additional coating application to let the previous coating partially settle. Temperature and humidity of the coating room was recorded at 22 ℃ and 25% RH respectively which are in the acceptable range based on standard requirements and the material TDS.

Once all the coating applications were completed, samples were cured for 48 hours at

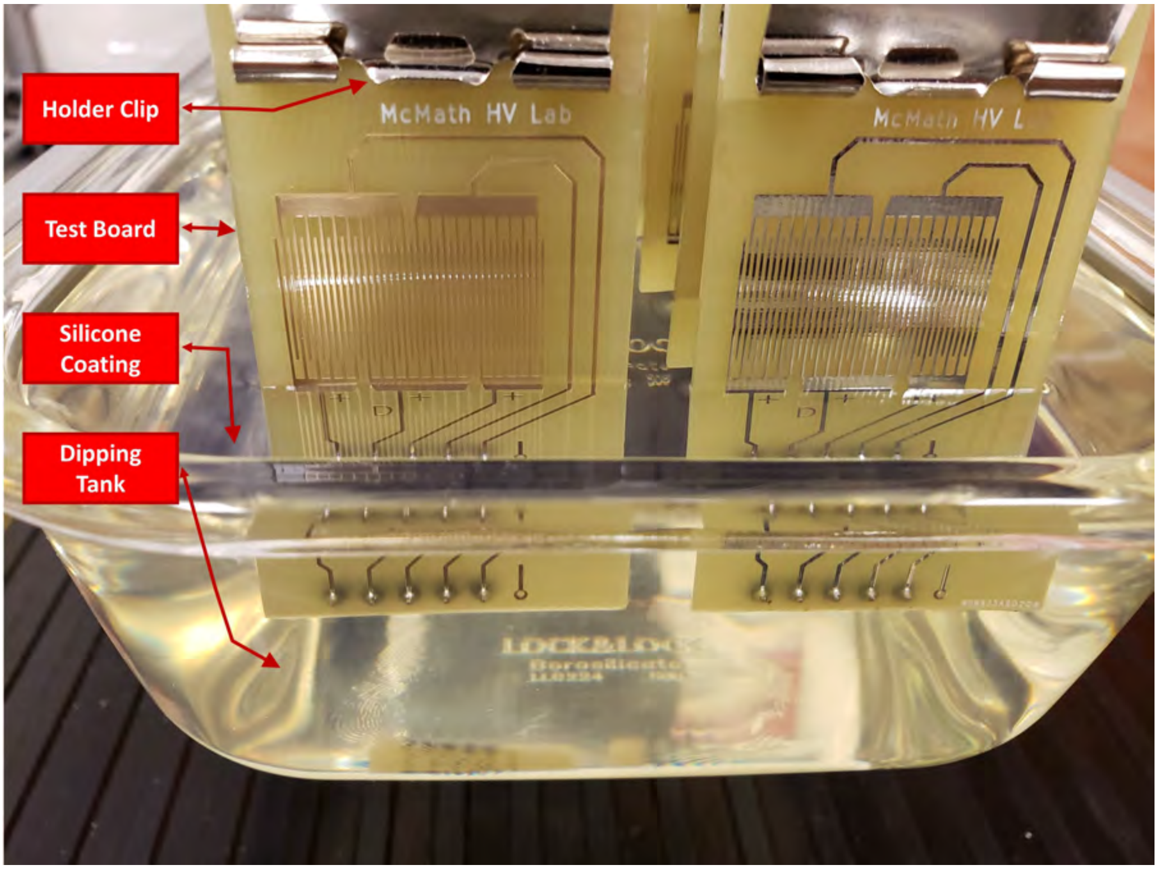

Fig. 4.6: Test boards are dipped in the tank of silicone conformal coating material. Boards are held vertically using spring clips.

room temperature of 25 ℃. During the curing time, boards were held horizontally to avoid any coating dripping and make the coating surface as even as possible.

4.4 Thickness Measurement

The final thickness of the fully cured conformal coating on the test samples was measured using a precise digital micrometer. The resolution of the micrometer was 0.0005 inch which is sufficiently lower than the measured values. The thickness of three different points on the top, middle, and bottom of the sample was measured. Since both sides of the test boards were coated in dipping method and the clamp micrometer reads the total thickness, the bare board thickness was subtracted from measured value and the result was divided by two to get the actual coating thickness. The average thickness for each sample as well as the mean thickness for each group was also calculated. A range of $25-52$ µm of cured coating thickness was measured for coated samples. Samples with additional coating layers had a thickness in range of $127-141$ µm. A small thickness difference is observed between different points on a board which was due to the uneven surface and micrometer accuracy. Table 4.2 shows the thickness measurements for each sample in the test and calculated average thickness for the groups sample.

All the measurements for samples were done using the same micrometer and the tool is calibrated before use to maximize the accuracy. Samples were kept in room temperature ($22-25$ ℃) during the thickness measurement process to avoid any thermal condition influences on coating thickness. The micrometer measuring surfaces were cleaned periodically to prevent any accumulation of coating material that may cause false readings. The bare board thickness value was measured prior to the application of coating and the average value for bare board thickness is used in the calculations.

4.5 Visual Inspection

As described in Section 2.2.7, visual inspection under UV light is a method to assess the success of coating process. Test boards in this study were visually controlled for any obvious defects based on the standard [68]. Additionally, samples were examined under UV light to control the coating coverage and possibility of presence of voids or contamination on the

Table 4.2: Coating thickness measurements of test samples. The average thickness value is presented for each group.

Sample Code	Measurements (Inches)				Bare Board Thickness (Inches)	Dual Side Coating (Inches)	Coating Layer Thickness (Inches)	Coating Layer Thickness (Microns)	Coating Thickness Average (Microns)
	Point 1	Point 2	Point 3	Average					
GD1	0.0730	0.0725	0.0725	0.0727	0.0625	0.0102	0.0051	129.1167	128.6933
GD2	0.0730	0.0720	0.0725	0.0725	0.0625	0.0100	0.0050	127.0000	
GD3	0.0735	0.0720	0.0725	0.0727	0.0625	0.0102	0.0051	129.1167	
GD4	0.0730	0.0720	0.0725	0.0725	0.0625	0.0100	0.0050	127.0000	
GD5	0.0735	0.0725	0.0725	0.0728	0.0625	0.0103	0.0052	131.2333	
HD1	0.0720	0.0735	0.0705	0.0720	0.0625	0.0095	0.0048	120.6500	135.8900
HD2	0.0735	0.0730	0.0730	0.0732	0.0625	0.0107	0.0053	135.4667	
HD3	0.0740	0.0735	0.0735	0.0737	0.0625	0.0112	0.0056	141.8167	
HD4	0.0740	0.0730	0.0735	0.0735	0.0625	0.0110	0.0055	139.7000	
HD5	0.0735	0.0740	0.0735	0.0737	0.0625	0.0112	0.0056	141.8167	
GS1	0.0655	0.0650	0.0655	0.0653	0.0625	0.0028	0.0014	35.9833	36.8300
GS2	0.0660	0.0655	0.0660	0.0658	0.0625	0.0033	0.0017	42.3333	
GS3	0.0660	0.0650	0.0650	0.0653	0.0625	0.0028	0.0014	35.9833	
GS4	0.0655	0.0650	0.0645	0.0650	0.0625	0.0025	0.0013	31.7500	
GS5	0.0660	0.0655	0.0650	0.0655	0.0625	0.0030	0.0015	38.1000	
HS1	0.0670	0.0665	0.0665	0.0667	0.0625	0.0042	0.0021	52.9167	46.8993
HS2	0.0665	0.0660	0.0660	0.0662	0.0625	0.0037	0.0018	46.5667	
HS3	0.0665	0.0660	0.0660	0.0662	0.0625	0.0037	0.0018	46.5667	
HS4	0.0670	0.0665	0.0660	0.0665	0.0625	0.0040	0.0020	50.8000	
HS5	0.0670	0.0660	0.0660	0.0663	0.0625	0.0038	0.0019	48.6833	
YS1	0.0645	0.0650	0.0650	0.0648	0.0625	0.0023	0.0012	29.6333	24.6944
YS2	0.0645	0.0645	0.0645	0.0645	0.0625	0.0020	0.0010	25.4000	
YS3	0.0645	0.0645	0.0640	0.0643	0.0625	0.0018	0.0009	23.2833	
YS4	0.0650	0.0645	0.0645	0.0647	0.0625	0.0022	0.0011	27.5167	
YS5	0.0645	0.0640	0.0640	0.0642	0.0625	0.0017	0.0008	21.1667	
YS6	0.0645	0.0645	0.0645	0.0645	0.0625	0.0020	0.0010	25.4000	
YS7	0.0645	0.0645	0.0640	0.0643	0.0625	0.0018	0.0009	23.2833	
YS8	0.0645	0.0640	0.0640	0.0642	0.0625	0.0017	0.0008	21.1667	
YS9	0.0645	0.0645	0.0645	0.0645	0.0625	0.0020	0.0010	25.4000	
YD1	0.0670	0.0665	0.0665	0.0667	0.0625	0.0042	0.0021	52.9167	54.3278
YD2	0.0675	0.0665	0.0665	0.0668	0.0625	0.0043	0.0022	55.0333	
YD3	0.0675	0.0665	0.0665	0.0668	0.0625	0.0043	0.0022	55.0333	

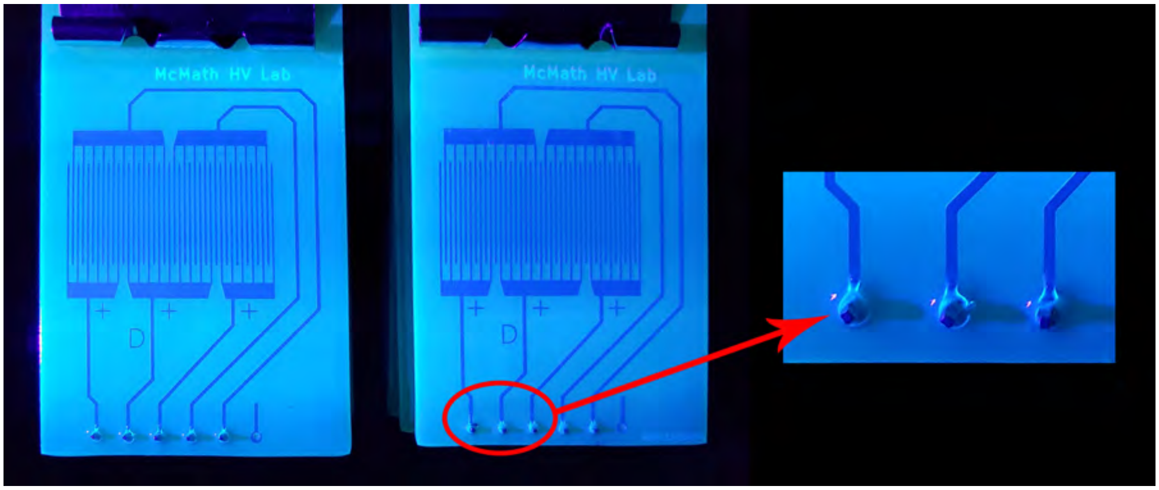

Fig. 4.7: Test boards under inspection using UV light. There is no issue observed on the cleaned, coated samples rather than a small boundary region around the connection pins.

coating. The MG Chemical 422B silicone modified has fluorescent characteristic property and has the absorption spectrum of 375 nm and the emission spectrum of 437 nm [67]. This physical property in the coating material makes the inspection of the coating easier. A UV LED with 395 – 410 nm wave length and 3 watts output power was used as the source of UV light. The light wave length falls in the inspection range for the coating material in this study.

Samples were tested in a room without any other active light sources to provide a better visual inspection. Boards were held in a distance of 10 cm away from the UV light source for optimal evaluation. Any shade, glow, or unusual diverse in blue surface might be a defect on the coating. Figure 4.7 shows two sample test coupons under UV inspection test. No evidence of delamination, cracks, or contamination on the cleaned, fully cured coated samples were observed. There is only a small boundary region around the connection pins seen in the inspection as shown in Figure 4.7. This is the product of flux residues from the soldering process of the connection pins. Since the proper cleaning for removing organic salts, oily residues, and alkaline has been performed and the observed tiny boundary region is far from the comb pattern in test boards, samples meet the qualification requirements for this study according to [37, 18].

4.6 Summary

Chapter 4 was on sample preparation for the experiments in this thesis. Selection of the test board based on the proposed tests was described. Design and specifications of prepared samples were presented. Cleaning process and the employed coating application technique were given and measurements of the coating layer in samples were done. Visual inspection of prepared sample under UV light was performed and observations were reported. Experimental setup for PD and breakdown tests are provided in the next chapter. Tests on new samples are conducted and observations are reported.

Chapter 5

Electrical Test of New Samples

5.1 PD Under Pollution

In this part of experiments, PD in coated test boards were examined in the presence of two different pollutants. As described in Chapter 4.1, samples with "Y" shape pattern were used as test vehicles in the PD test. Drops of 5 % sodium chloride solution and aluminum particles were used as two types of contamination on the coatings layer. Aluminum powder with particle size between 130 µm to 290 µm were used as conductive particles on the top of the coating. The particles size were sufficiently smaller than the trace size and the gap between traces (750 µm) to prevent any bridging between tracks. In order to evaluate the performance of a coated PCB by means of PD, a voltage could be applied to traces [56] or the coating could be exposed to corona discharges [54]. In this study, the first approach is employed as a more realistic operational situation for a PCB. Voltage applied to the traces of the sample under the test and PD is measured using a commercial PD measuring system[1]

[1]Omicron MPD 600

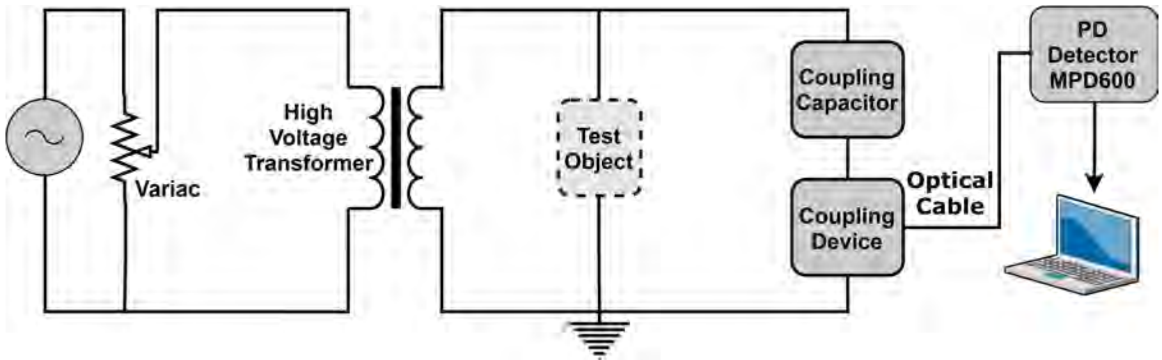

Fig. 5.1: PD test setup block diagram. Object under the test is connected to the high voltage transformer fed through the variac. Coupling device is in series with the coupling capacitor according to IEC60270 standard. The coupling device is connected to the measuring equipment via an optical link.

connected to a computer. A block diagram illustrating the test setup and connections is shown in Figure 5.1.

5.1.1 Test Procedure

Experimental test setup and PD measurement procedure were conducted in accordance with IEC60270 standard [7]. A 60 Hz transformer was used as the high voltage source with noticeably low-level background noise to provide more accurate PD measurements. The transformer input voltage was controlled using a variac. Test samples were placed in a test cell to prevent any undesired movement and the high voltage source was connected to the soldered pins on the PCB under test. Figure 5.2 shows the actual test setup with a sample test board mounted inside the test cell. For this part of the study, test boards were mounted horizontally in the test cell to avoid any movement of the salt water drop. Three different zones on a test board were selected for the drop of 5 % salt water. Point A is a spot far away from traces. Point B is on the top of only one trace and point C is in the middle of traces

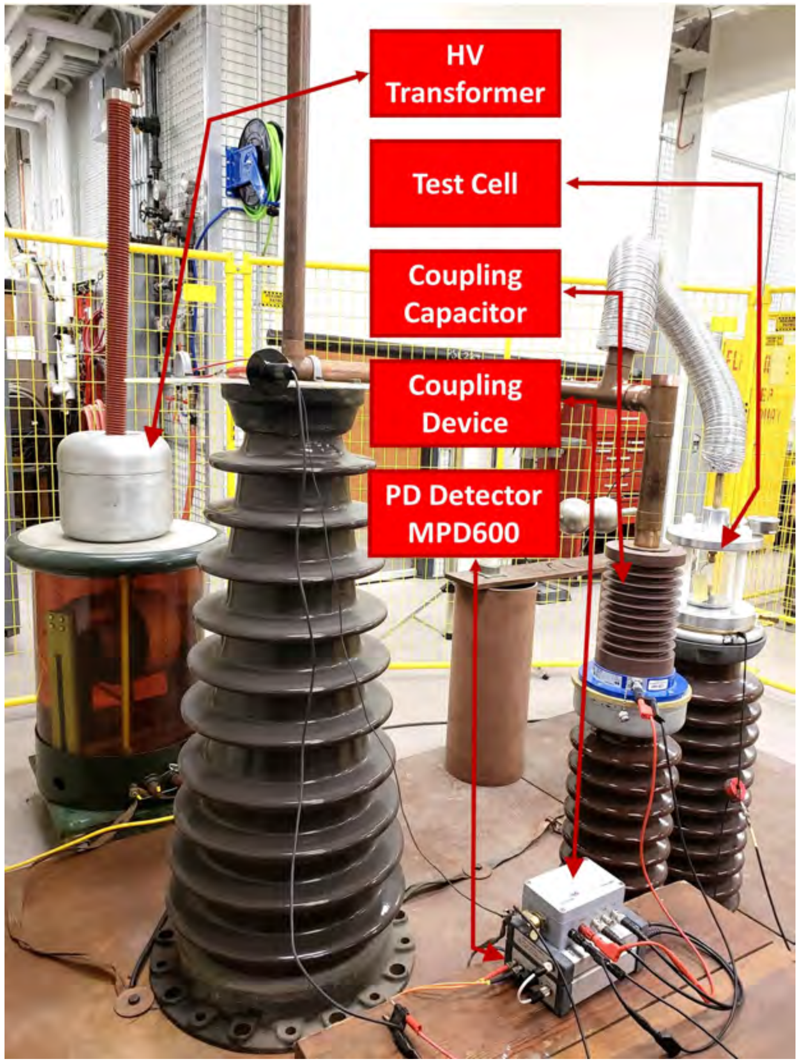

Fig. 5.2: Test setup for PD under pollution test. Test board is connected to high voltage source and mounted in the test cell.

with the drop covering both traces. Figure 5.3 illustrates the cross section of coated boards and three different dedicated locations of the drop on test boards. Once the salt water drop is placed on the top of a coated sample, the voltage was increased using the variac upon detecting a PD using the software. Patterns of PD for samples were observed and data was

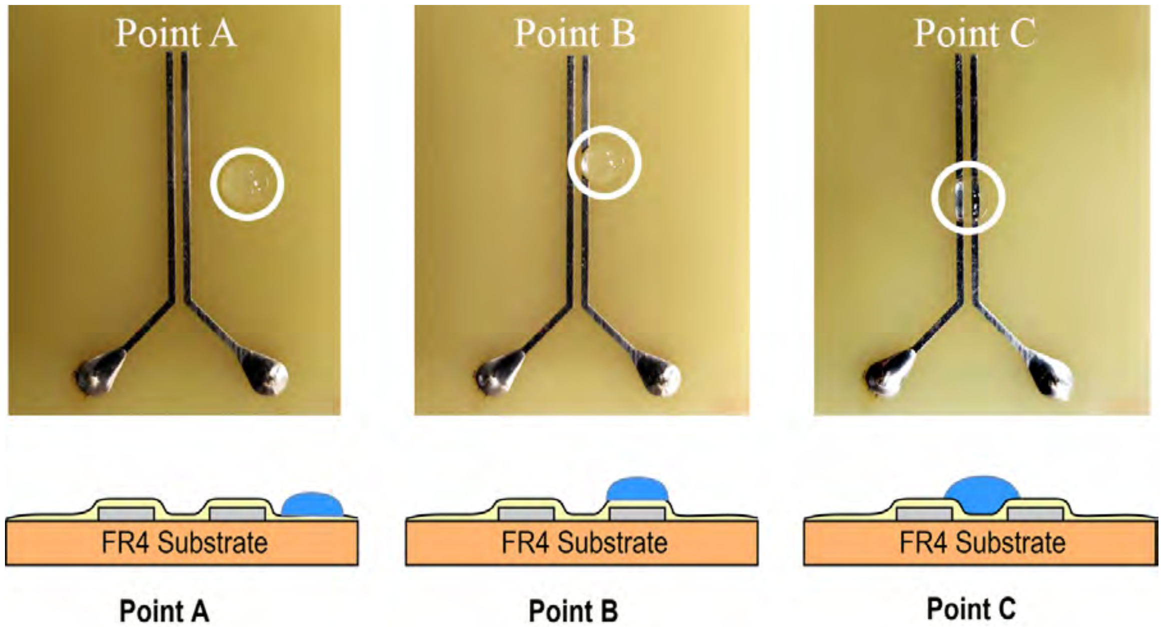

Fig. 5.3: Coated test board with saltwater drop on three different selected locations and the illustrate of cross section of the samples.

saved. After the PD test samples were removed from the test cell and the salt water drop wiped from the surface, visual inspection of specimens was performed for any damage or defect on the board or the coating.

In the second part of the PD under pollution experiments, aluminum particles were used as conductive particles on the top of coated board. The same test setup was used in this part of experiments as well. Similar to the previous part, during the test, boards were held in horizontal position to prevent any unwanted movement of the particles on the sample surface. One sample with coating and one uncoated board were examined. Samples were energized and the supplied voltage was increased using the variac till the PDs were detected or any discharges happened. Aluminum particles were poured on the coating surface and distributed as evenly as possible on the board. Figure 5.4 shows the test specimen with

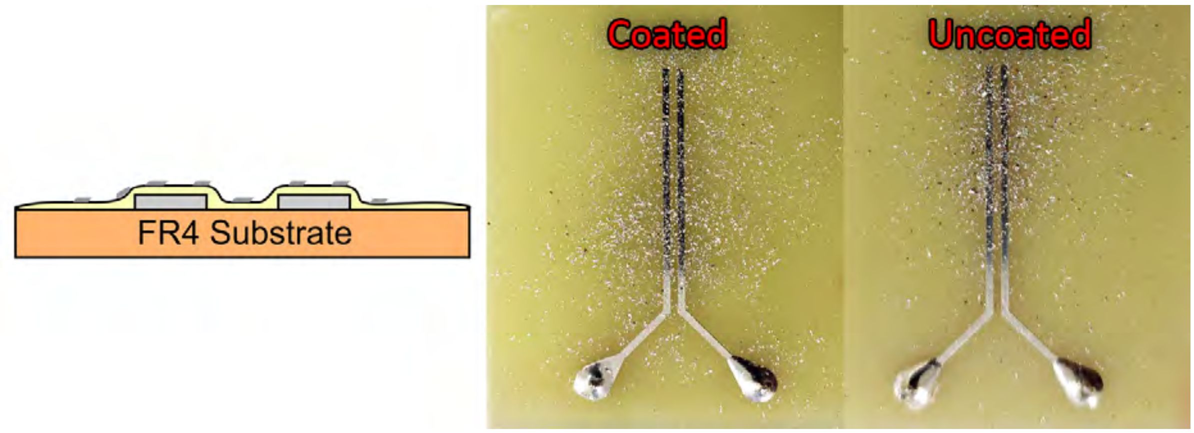

Fig. 5.4: Coated and uncoated test boards with aluminum particles distributed evenly on top.

aluminum particles on top.

5.1.2 Results and Observations

The impact of the salt water drop as a conductive solution was examined on coated samples with "Y" shape traces. According to the applicable standards [27, 16], samples are able to withstand 1.5 kV at $50 - 60$ Hz. For the sample with salt drop on point A, the voltage was raised gradually up to 1.9 kV which was 25 % over the nominal designed value and was kept at this level for duration of 5 minutes. No PD was detected with the measuring tools and no momentary discharge was observed. The sample with salt water drop on point B started producing PD with a magnitude of 20 pC at 870 V and the phase resolved PD pattern recorded by PD measurement device (Omicron MPD 600) is shown in Figure 5.5. Further increase of the supplied voltage in this part of experiment resulted in relocating of the salt water drop to the space between the traces. This movement is occurred due to the presence of high electric field in the gap and the permitivity of the salt water ($\varepsilon_r \approx 80$). After the

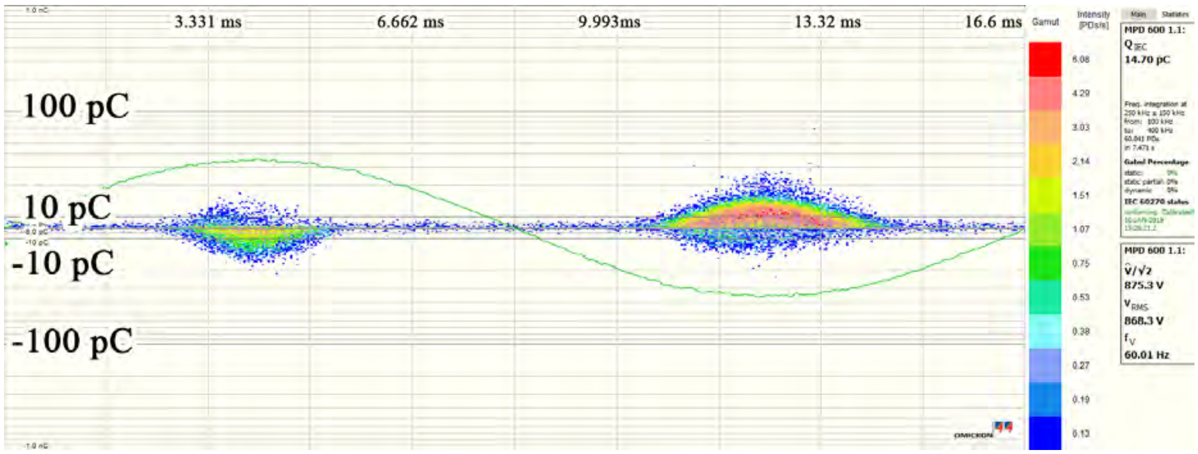

Fig. 5.5: Phase resolved PD pattern for coated test sample with saltwater drop on point B.

salt water drop was moved to the gap, momentary discharges started to happen and PD was no longer detected. In the last part of this test, the salt water drop was placed on point C where both traces and the space between were covered by the salt water drop. No PD signal was detected and similar to the previous situation (drop on point B), discharges occurred through the drop. The presence of contamination and salt water drop in this experiment, in the gap between traces, disturbed the uniformity of the electric field distribution and resulted in discharges through the contaminant. Due to the high temperature of the discharges that occurred through the drop, corrosion was observed on the traces of coated sample. Edges of the conductors experienced severe damage and the HASL surface finishing was removed in some points as shown in Figure 5.6.

The experiment for conductive particles on coated and uncoated samples were conducted using the same setup. During the voltage raise, some rare momentary discharges were observed that resulted in displacement of the aluminum particles. At a voltage of 1.63 kV, PD signals were detected for samples with conformal coating. As shown in Figure 5.7, the

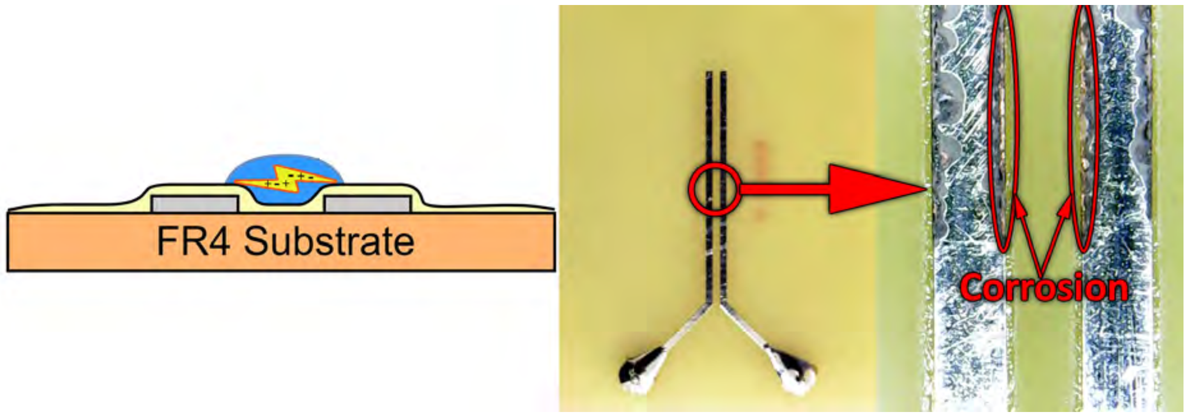

Fig. 5.6: Disruptive discharges through the contamination resulted in corrosion of the traces.

highest magnitude of detected PD signals were 50 pC. Higher voltage levels only increased the number and frequency of the momentary discharges. After the test finished, the aluminum powder was wiped from the surface and test board were visually examined for any defects. Some dark spots were found on the samples which were the product of the momentary local discharges.

Applying the conductive particles on the uncoated sample did not provide any PD. Since no dielectric was present between traces and the conductive particles, increasing the supplied voltage only resulted in discharges which started to occur at voltages 1.3 kV and higher, up to 1.5 kV. Locations with a higher density of the aluminum particles suffer from more electrical discharges. At the moment of each discharge, aluminum particles were bounced from the discharge spot and consequently the location of the discharge was changed to another location of the board.

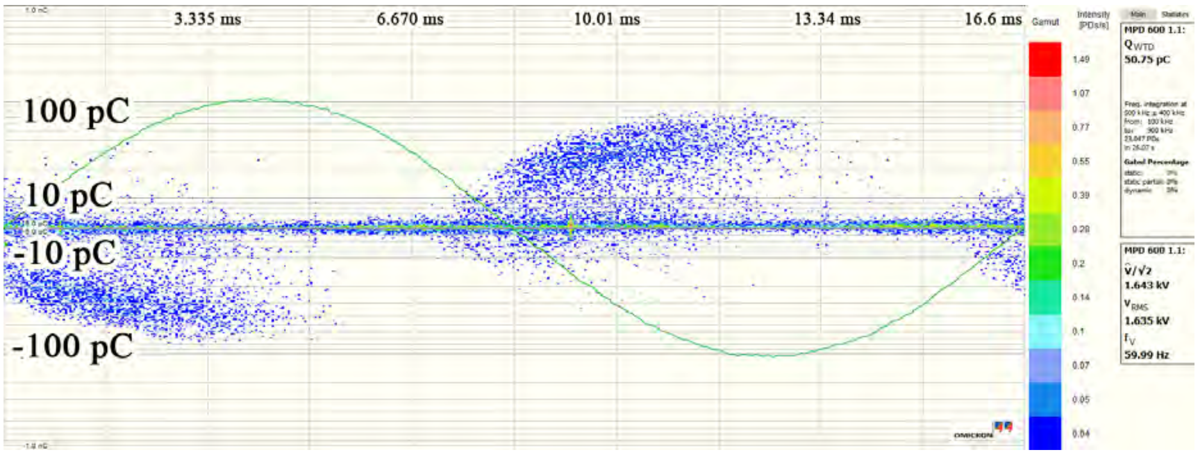

Fig. 5.7: Phase resolved PD pattern for coated PCBs with aluminum particles on top.

5.2 Breakdown Voltage

The breakdown voltage test was performed as described in Section 3.2 for coated and uncoated test samples in four different conditions. Samples with an additional coating layer as well as single coated and uncoated samples were tested to evaluate the impact of additional coating layer on the ability of a PCB to withstand high voltages. Since in low air pressure condition PD is more likely to happen [69], some of the samples were examined in low air pressure test condition. A sealed chamber was used to provide the low air pressure environment at 33 kPa (sea-level air pressure is 101 kPa). Samples were energized using the high voltage transformer and voltage was raised at a rate of $50V/s$ using a variac until breakdown happens. Test was conducted using the same experimental test setup that was used in Section 5.1.

Table 5.1: Breakdown voltage test results for samples in four different conditions.

Sample Type	Code	Breakdown RMS Voltage (kV)	Mean Breakdown Voltage (kV)
Uncoated	YN1	1.83	1.81
	YN2	1.79	
	YN3	1.8	
Coated Low air pressure	YS4	1.91	1.89
	YS5	1.87	
	YS6	1.89	
Coated	YS7	2.42	2.43
	YS8	2.39	
	YS9	2.48	
Double Coated	YD1	2.44	2.48
	YD2	2.52	
	YD3	2.49	

5.2.1 Test Procedure

In this part of experiments, three groups of coated test boards consisting of a Y trace pattern were examined in four conditions. For each test condition, three samples were examined and the breakdown voltage for each sample was recorded. Voltage was increased until the breakdown occurred in samples. The voltage at the moment of the breakdown was measured using a digital voltmeter and the PD detection setup. Before the test, measured voltage on the PD detection setup was calibrated with the digital multi-meter to provide the same measured value as the voltmeter. Once the breakdown happened in the sample, the insulating material completely failed and conductor traces were bridged. The highest recorded voltage before the significant voltage drop was recorded as the breakdown voltage for each sample. Table 5.1 shows the sample variety and related breakdown voltage that was recorded for each specimen in the test. For safety purposes of the test, a $50M\Omega$ resistor was used in series with the transformer output to limit the increased current flow at the moment of breakdown. Before the insulation breakdown point, some momentary discharges were observed in the form of spark-overs in some samples. These momentary discharges occurred randomly in voltages close to the insulation breakdown point.

5.2.2 Results and Observations

Mean insulation breakdown voltages of 2.43 and 2.48 kV were recorded for single and double coated test boards, respectively. Uncoated samples and test boards with coating in the low air pressure condition had average breakdown voltages of 1.81 and 1.89 kV, which was noticeably lower than that measured breakdown voltage for coated and double-coated test boards. While test boards are initially designed to withstand at 1.5 kV, as described in Section 4.1, the experiment has proved the advantage of coating layer by improving the breakdown voltage to make a more robust PCB assembly. Test boards with additional coating layer provide breakdown point of fairly close to the single coated board. The influence of additional coating layer can not be observed in this experiment.

5.3 Summary

In this chapter, PD test was conducted on conformally-coated test boards in the presence of pollution and conductive particles. The impact of pollution at different locations on a test boards was examined. Degradation of coated PCB as a result of PD under pollution was observed and the breakdown voltage of coated and uncoated specimens were extracted. The impact of coating layer on breakdown voltage was observed and the result was compared with low-air pressure test. The following chapter covers the assessments of thermally-aged coated samples. Dielectric properties of samples are tested after cycles of aging and assessments are followed by PD and breakdown voltage tests.

Chapter 6

Assessment of Aged Samples

6.1 Thermal Aging

A series of experiments were conducted to evaluate the impact of aging on the performance of conformal coating in PCBs. Samples with conformal coating were exposed to dedicated heat and humidity aging cycles in accordance to approved tests for moisture and insulation resistance as described in Section 2.2.7. Samples were examined at first, fourth, seventh, tenth, twentieth, and thirty sixth cycles. The evaluation assessment section of the standards test method was extended to dielectric measurements and breakdown test rather than the measurement of SIR and visual inspection. The performance of the coated samples was evaluated by measuring the capacitance and dielectric loss. Samples were tested using a dielectric spectrometer as well as performed tests for breakdown voltage. Visual inspection under UV light along with macro imaging from samples were also performed. Aging cycles were included heating and cooling periods in presence of high humidity level. Each thermal aging cycles was as follows:

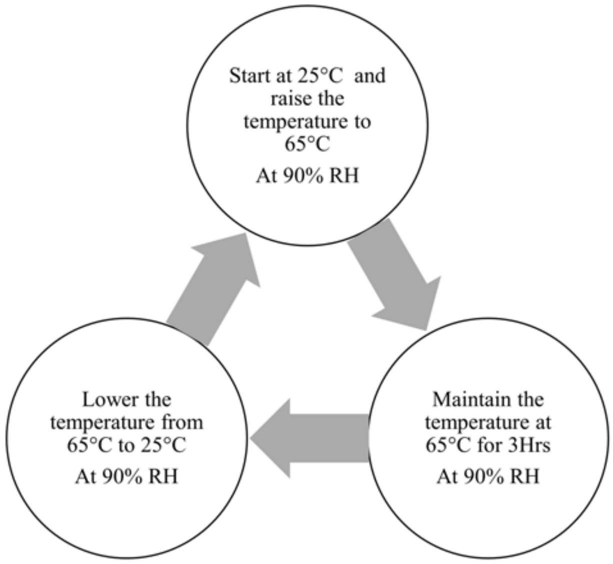

Fig. 6.1: Thermal and humidity aging cycles sequence diagram.

- **Pre-heating:** Start test at 25 ℃ and increase the temperature to 65 ±3 ℃.
- **Heating:** Maintain the chamber temperature at 65 ±3 ℃ for a duration of 3 hours.
- **Cooling:** Cool down the chamber to 25 ±3 ℃ .

Once the chamber is cooled down to 25 ±3 ℃, one cycle has finished. During all the cycles, the humidity of the chamber was maintained at 90± 5 %RH and no delays were allowed between the aging cycles. Figure 6.1 shows the thermal aging cycles diagram. A fully controlled thermal aging chamber was designed and developed in McMath High Voltage Lab as a part of experimental design in this study. A high quality double layer insulated container was used as the chamber box. Heating and cooling sources, humidifier, sensors, and a main control unit were designed and customized for the chamber. One heat source of 150 W power, heating an element mounted in a heat-sink, was the heating source and the chamber cooling source was a chiller that circulates cold water into the heat-sink. Two ultrasound atomizer mist were installed inside the chamber to provide the required humidity throughout the cycles. The air inside the chamber was circulated using two brush-less blower fans to provide a consistent temperature and humidity in every zone inside the chamber. Humidity and temperature were measured in one second intervals using a digital sensor and the read data was sent to a digital micro-controller to switch the sources. The micro-controller unit was programmed to measure values and control the sources based on the set parameters. Figure 6.2 shows inside the final chamber with installed parts that was built in house and was used for this study.

6.2 Aging Setup

The coated “D” comb pattern test broads with HASL and ENIG surface finish were aged and examined in this experiment. The samples included those with single and double layer coating variety. In total, four groups of test boards as presented in Section 4.1, were placed in the chamber for aging cycles. One control sample of each kind was kept for evaluation and comparison purposes. Coated boards were mounted vertically on a tray using spring clips and the tray was placed inside the thermal aging chamber. The plexiglas tray was used to provide a shield against the any possible condensation drips on the test boards and hold the samples at same level during the aging process. Specimens were held vertically at the same level as the humidity and temperature sensor to ensure the sensors reading are accurate for the samples zone. A partition plate was installed between the samples and cooling and heating sources to prevent direct heat or cool transfer to the samples under aging. This yields the consistent aging process for all samples in the chamber. Each test board has three positive and two negative connection pins. Test samples were connected in parallel by

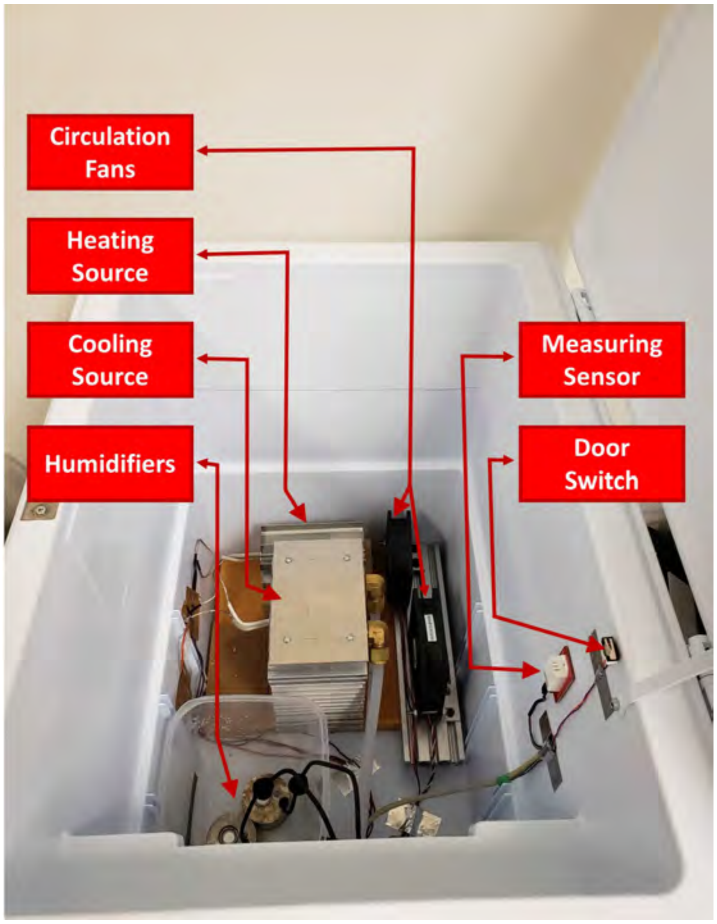

Fig. 6.2: Programmable thermal aging chamber setup that has been designed and built in McMath HV Lab controlled by a micro-controller.

connection wires and were connected to a power supply. Test samples were energized using a 50 V DC power supply through the connection pins that were soldered prior to cleaning step in Section 4.2. Energizing the boards, represent real operational condition for coated samples. One sample of each group were aged without applying voltage to investigate the impact of aging on non-energized situation. Figure 6.3 shows test broads inside the chamber and ready for aging cycle to start.

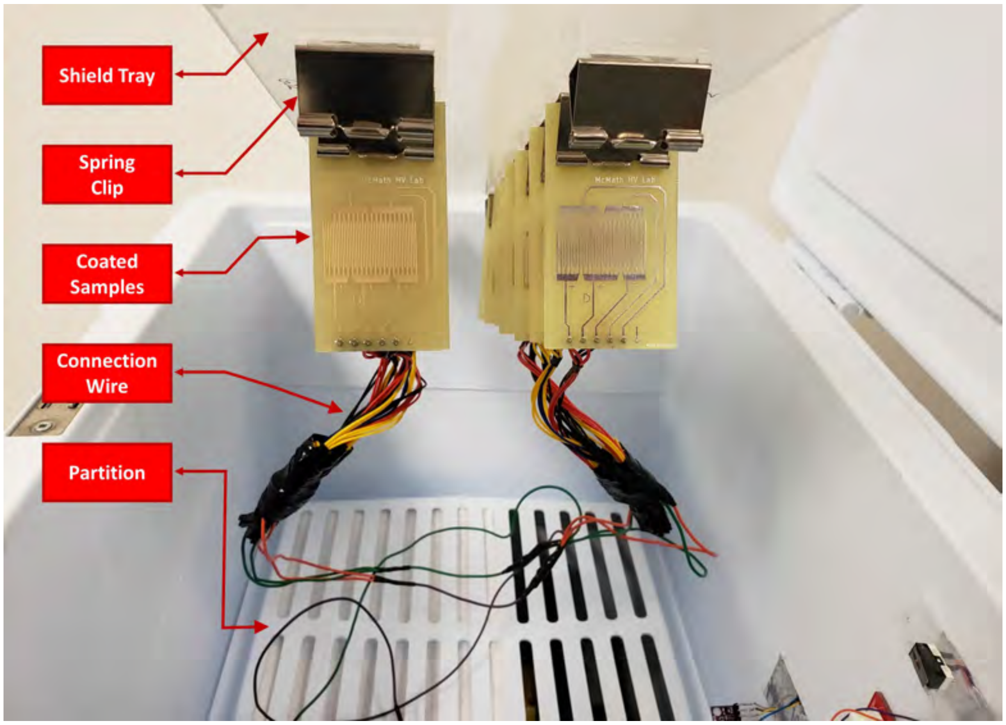

Fig. 6.3: Boards are ready for thermal aging in the chamber. Test samples are mounted vertically on the tray and power supply connection wires are connected.

Temperature and humidity were measured, controlled, and recorded by a micro-controller during cycles. The micro controller switched on the heater unit until the temperature was raised to the set point for heating cycle. Since the relative humidity (RH) is temperature dependant, two humidifiers were consistently switched on and off to maintain the humidity at 90± 5 %RH. Humidifiers were fed from clean reverse osmosis water from a reservoir outside of the chamber. Required water for humidifiers was pumped using a small water pump and a piping line. During the 3 hours of heating cycle, the heater was switched on and off to maintain the temperature at desired value. Once the heating cycle finished, the micro-controller opened a valve to let the cold water circulate inside the cooler heat-sink. The cold water of 0 ℃ was provided from a chiller which was the main cooling source for the chamber.

Upon starting the pre-cooling cycle, a significant amount of humidity was condensed on the surface of the cooling heat-sink in form of water drops. This resulted in fluctuation in level of humidity inside the chamber. After the temperature was lowered to 25 ±3 ℃ the system delayed for one minute and then started the next pre-heating cycle. Figure 6.4 shows graphs of recorded temperature and humidity over three aging cycles in the chamber. Elapsed time from the start of three aging cycles is shown on the graphs.

6.3 Visual Inspection

Test samples were visually examined under UV light to observe level of degradation in coating and traces of specimens. The same equipment and procedure as described in Section 4.5 was employed for this part of inspections and samples were observed after dedicated cycles. No evidence of visual damage was observed in samples up to 10^{th} cycle. Some blurred areas on boundary region around conductors were seen and levels of corrosion on traces were appeared in the form of dark points on the edge of traces after 10 cycles of aging. Exposure to heat and humidity provided a harsh environment for samples and higher level of degradation in samples was observed after 20 and 36 cycles. The corrosion of the traces became more severe and more dark points was formed around patterns as well as dark spots around connection pins. A slight peeling of the coating layer was seen on the area around pins and edges of some specimens. These dark point damages are evidences of penetration of moisture in the coating layer which resulted in the oxidation of traces. Besides, due to difference in coefficient of thermal expansion (CTE) between substrate, conductor traces, and the coating layer, the adhesion of the coating layer was decreased and, consequently, more moisture was entrapped. Figure 6.5 shows four test samples from new to 36 cycles of aging under UV light inspection.

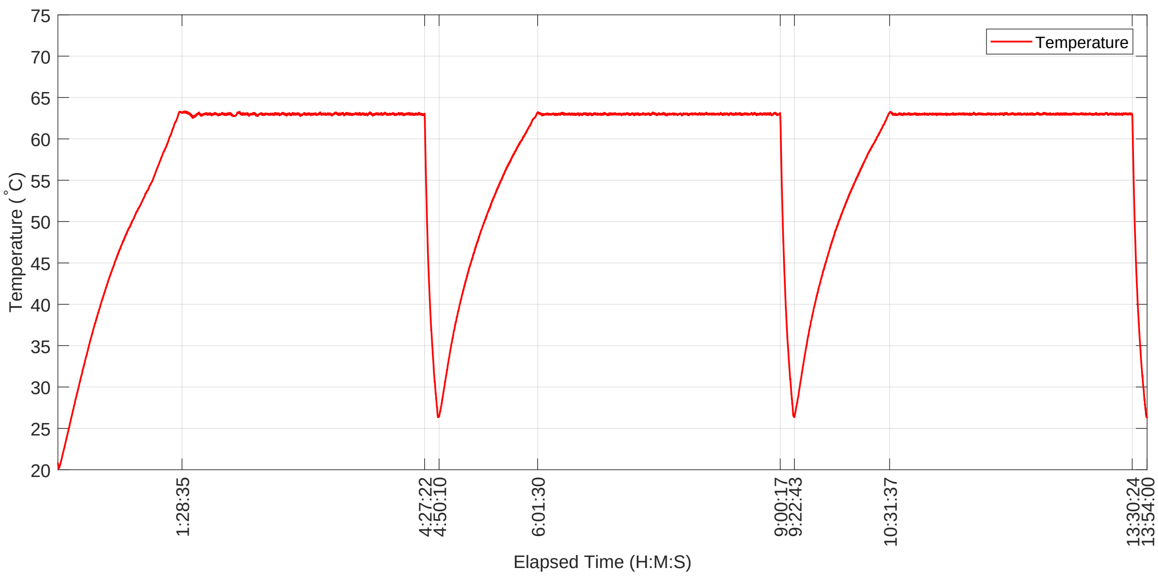

(a)

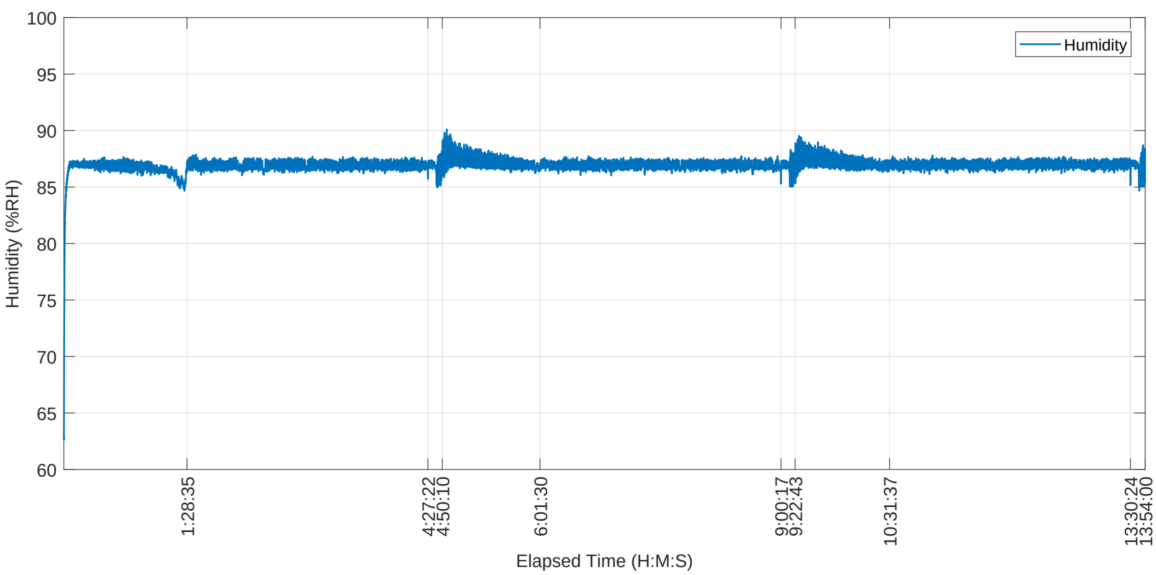

(b)

Fig. 6.4: Graphs of recorded temperature and humidity over three aging cycles. a) Temperature change graph in three cycles of thermal and humidity aging recorded by the chamber micro-controller unit, b) Humidity change graph in three cycles of thermal and humidity aging recorded by the chamber micro-controller unit.

There is noticeable aging observed after 10 cycles. Sample which experience 36 aging cycles have clear damages on coating layer especially around the edges of conductor traces.

In addition to UV inspection, test samples were visually inspected using macro imaging technique from surface of specimens. A level of 360 X magnification was selected for enlarged images. This zoom level covered two adjacent traces in a sample. Figure 6.6 shows the images from test board with HASL surface finish exposed to 36 cycles of thermal and humidity aging. A sample point between traces of “D” comb pattern were selected for macro imaging. Both the coating layer and conductor traces degradation can be seen in presented images. Clear transparent coating layer on the new sample has no evidence of bubble, crack, or oxidation (Figure 6.6a). Figure 6.6b shows a sample after 1 cycle. A light boundary region on sides of traces was formed in this step. After 4 cycles, degradation of traces was started and some small points were observed on the traces as shown in Figure 6.6c. By the end of 7^{th} aging cycle, obvious dark points appeared on the traces and formation of bubbles started. Degradation was seen on traces boundary regions and, on the surface of coating (Figure 6.6d). The macro image of 10 and 20 cycles aged sample show clear symptoms of coating degradation that was appeared in the form of bubbles and uneven coating surface along with oxidation of traces (Figures 6.6e and 6.6f). The most severe damage was observed in sample after 36 cycles of aging in the form of some dark regions as evidences of electrical discharge that has occurred between adjacent traces. The coating layer of this sample was suffered from peelings, cracks, and failure at the point of discharge (Figure 6.6g).

Similar macro imaging were performed for test samples with ENIG surface finish. Images from samples are shown in Figure 6.7. The same trend of aging was observed in the form of development of a boundary region around traces and formation of an uneven surface on the coating from cycle one to cycle ten. Oxidation of the conductor traces was observed as green

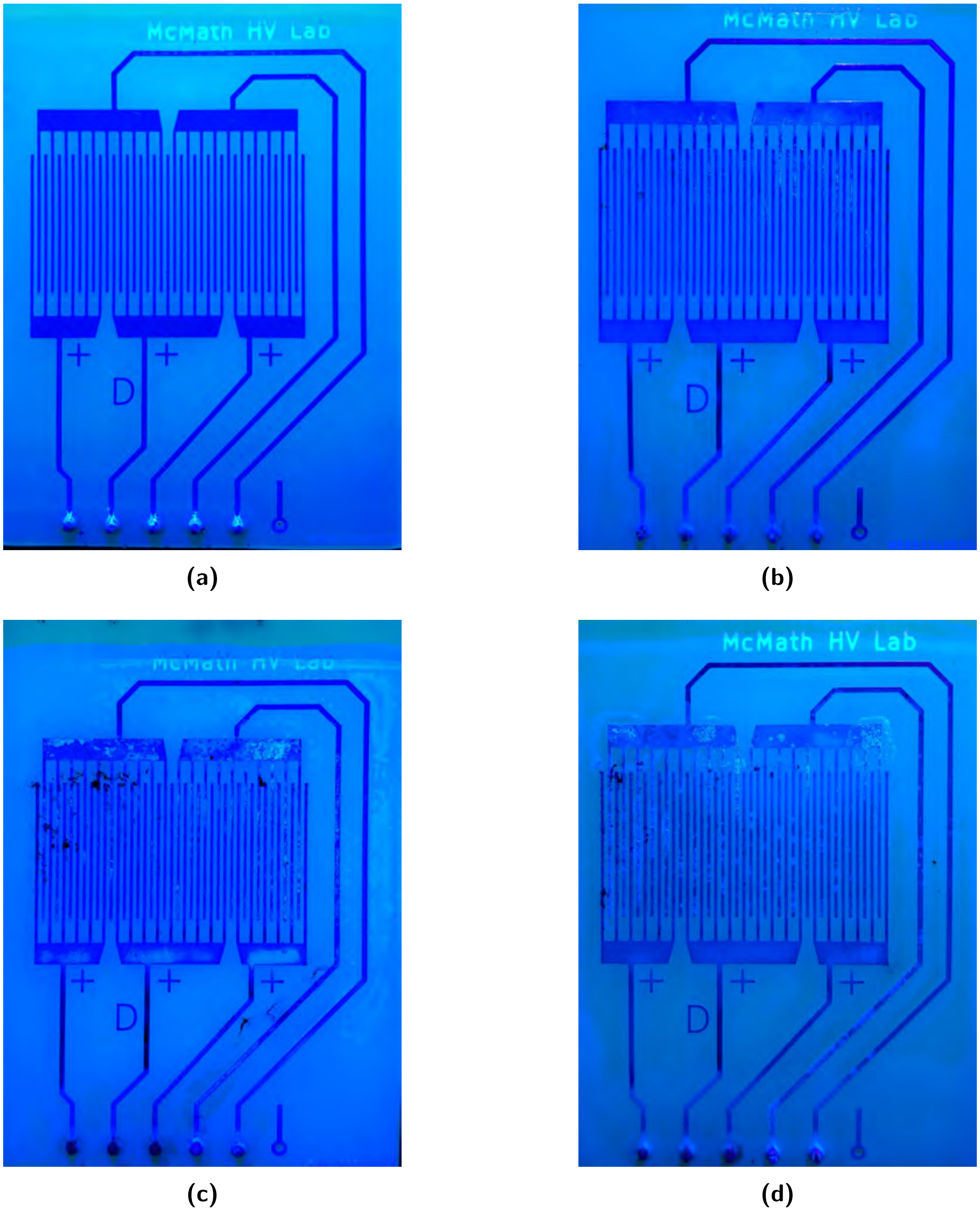

(a) (b) (c) (d)

Fig. 6.5: Test boards under UV inspection after 36 cycles of thermal and humidity aging. Coating degradation and corrosion in traces is observed due to high humidity condition. Some blurred areas are seen on samples that show delamination of the coating layer: a) new coated sample, b) after 10 cycles aged sample, c) after 20 cycles aged sample, d) after 36 cycles aged sample.

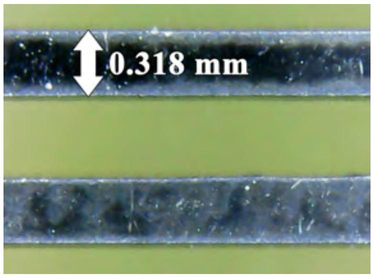

(a)

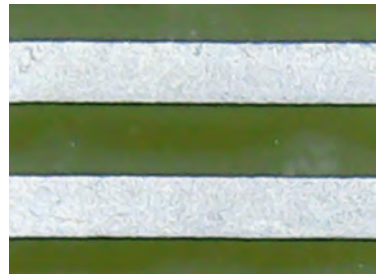

(b)

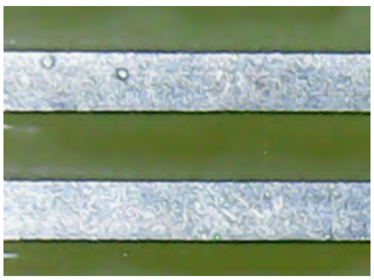

(c)

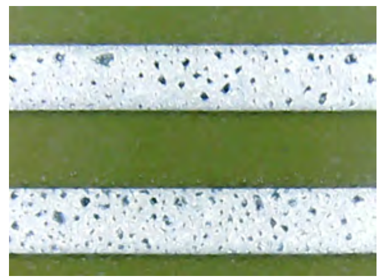

(d)

(e)

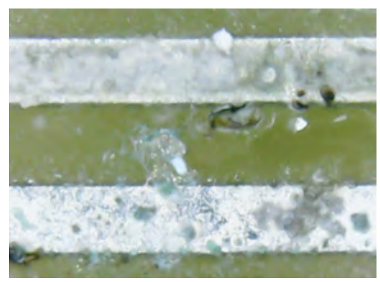

(f)

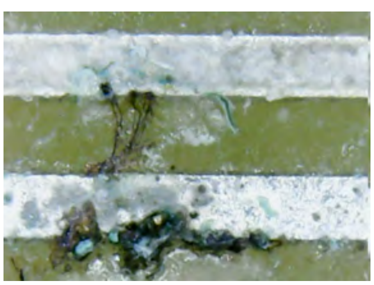

(g)

Fig. 6.6: Macro imaging with 360 X magnification from traces of test boards with HASL finish which have degraded during 36 cycles of thermal and humidity aging under energized condition: a) new sample, b) 1 cycle aged, c) 4 cycles aged, d) 7 cycles age, e) 10 cycles aged, f) 20 cycles aged, g) 36 cycles aged.

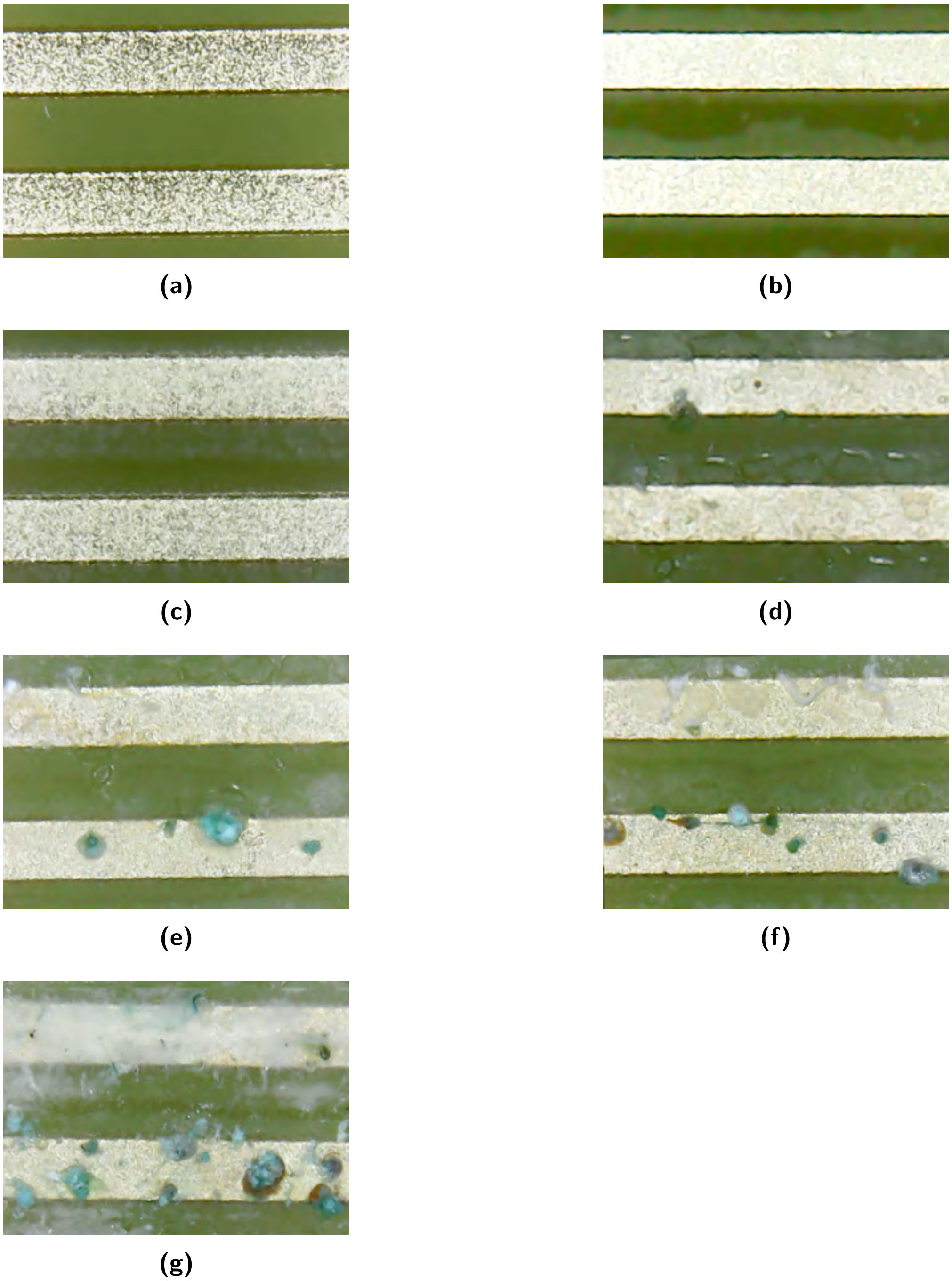

Fig. 6.7: Macro imaging with 360 X magnification from traces of test boards with ENIG finish which have degraded during 36 cycles of thermal and humidity aging under energized condition: a) new sample, b) 1 cycle aged, c) 4 cycles aged, d) 7 cycles age, e) 10 cycles aged, f) 20 cycles aged, g) 36 cycles aged.

spots on conductors which represents the oxidation of nickel which is used in ENIG surface finish. Test boards with ENIG surface finish were degraded less than those of with HASL surface finish after 20 cycles. Conformal coating delamination was observed in sample with ENIG surface finish after 36 cycles of aging. It was seen that a significant amount of moisture was absorbed by the coating and most of the areas on traces were covered by oxidation spots as sown in Figure 6.6g.

6.4 Dielectric Measurements

Evaluation of the test boards from dielectric properties point of view were conducted. ModuLab XM MTS materials test system capable of accurate impedance measurements over a wide range of frequencies was the equipment that was used in this experiment. The system was also equipped with a high voltage module which was able to measure the impedance of the sample under the test in high voltage and measure the capacitance and loss tangent. The dielectric spectrometer was calibrated prior the test, using the manufacturer provided dummy test cell. A calibration test with known parameters and expected results indicated that the system is working properly and provides right results. A voltage controlled impedance with constant level of 70 V RMS was set on the system. Samples were examined using the dielectric spectrometer and measurements of capacitance and dielectric loss were conducted over a frequency range from 10 Hz to 100 kHz. Samples were connected to the dielectric spectrometer through BNC coaxial cable connections as shown in Figure 6.8. Four group of test boards, with five samples in each group, were tested in this part of experiment as described in Chapter 4. All five new samples of the same group were examined prior to the aging process. Measurements of capacitance and loss tangent for samples of a same group

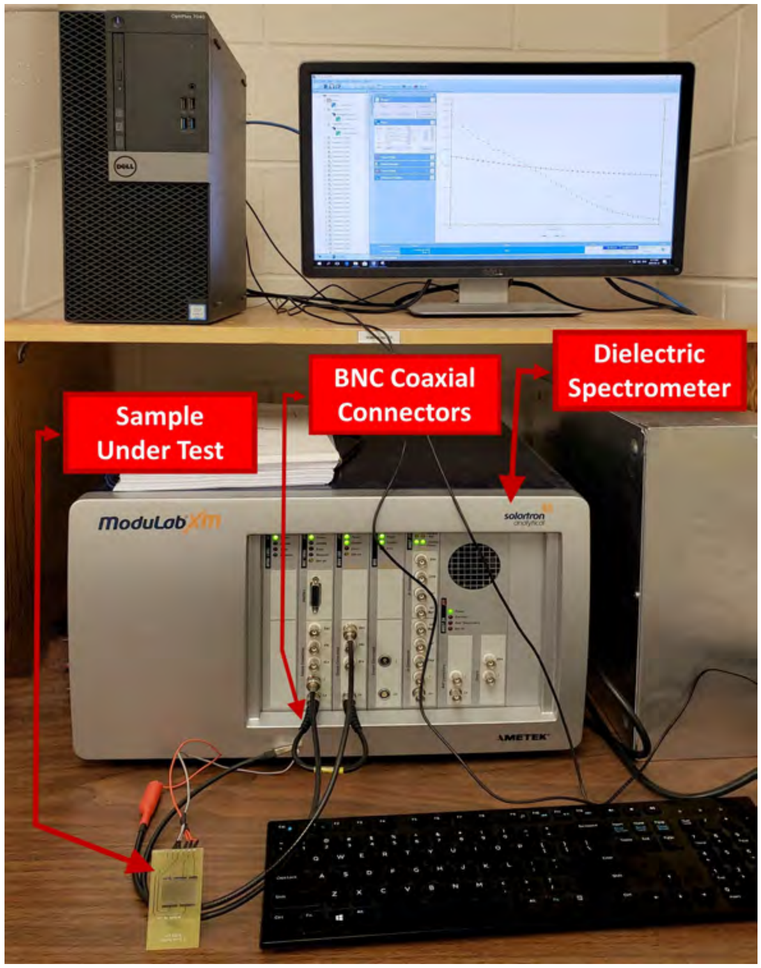

Fig. 6.8: Test samples connected to the dielectric spectrometer for measurements of capacitance and dielectric loss. Sample is connected to the device via BNC coaxial cables.

were compared with each other. Standard error of the mean value for measurements of the frequency range was calculated and the final results were plotted using error bars. Figure 6.9 show the mean capacitance and loss tangent of the new single coated test boards with ENIG surface finish.

The standard deviation from the mean values of measurements are presented as error bars. The plot of capacitance shows the values in pico-Farad unit for easier understanding.

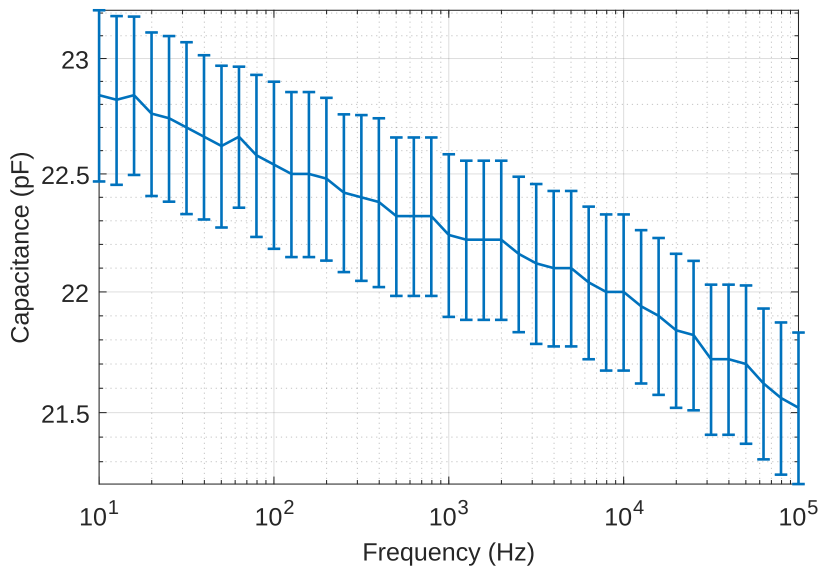

(a) Mean value of the capacitance is plotted and error bars show the standard error of the mean capacitance values.

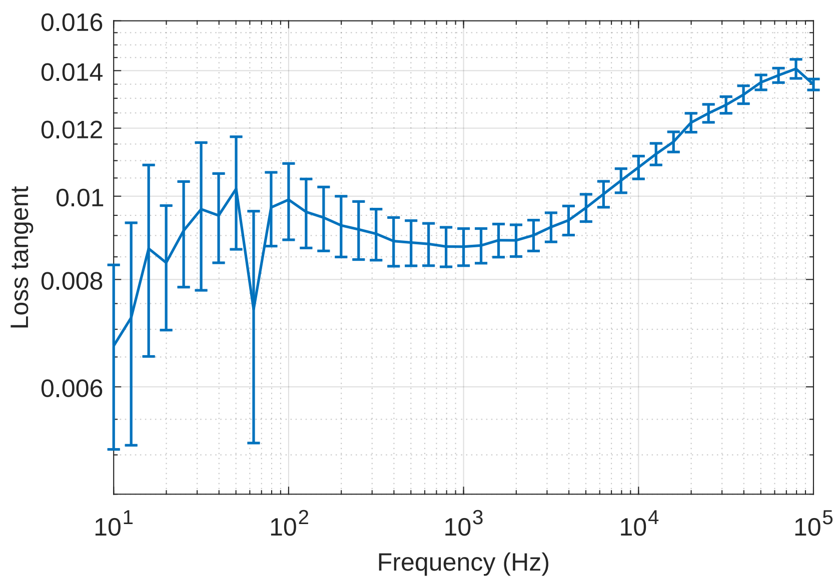

(b) Mean value of the loss tangent is plotted and error bars show the standard error of the mean loss tangents values.

Fig. 6.9: Plots of mean capacitance and loss tangent of the new single coated test boards with ENIG surface finish from 10 Hz to 100 kHz.

At 60 Hz, a significant variation in measurements of loss tangent is observed. This is due to the influence of noises from surrounding devices and power systems in the lab that has impacted this measurements. Other than the error in measurement at 60 Hz, the results of this comparison showed that samples of a same group have relatively same capacitance and loss tangent values over the frequency range of 10 Hz to 100 kHz. The capacitance of the samples has decreased by raising the frequency and have a value of 22.5 to 23.5 pF at 10 Hz which has declined to 21 to 22 pF at 100 kHz. The plot for dielectric loss shows an increasing trend of loss tangent in samples by raising the frequency. The mean value of loss tangent has started at 0.007 at 10 Hz and has increased to about 0.014 at 100 kHz. As shown in Figure 6.9, the measurements of loss tangent have smaller error range and are more accurate in higher frequencies.

The same measurements were performed for new coated samples with HASL surface finish. Figure 6.10 shows the capacitance and loss tangent data of single coated HASL samples that are reported in the form of plots with error bars.

A similar trend of decrease was observed for capacitance of HASL samples, started at just above 23 pF at 10 Hz followed by a fall to about 22 pF at 100 kHz. The plot for dielectric loss of HASL samples illustrates a raise trend in loss tangent from around 0.006 at 10 Hz to just above 0.013 at 100 kHz. Fairy similar capacitance and dissipation factor values over the measured frequency have obtained from samples with different surface finish. Plots of capacitance and loss tangent measurements for samples of a same group showed that test results are relatively the same. Therefore, for ease of plotting and reading, the mean capacitance and loss tangent values was plotted in onward figures. All the measurements are plotted over the frequency of 10 Hz to 100 kHz.

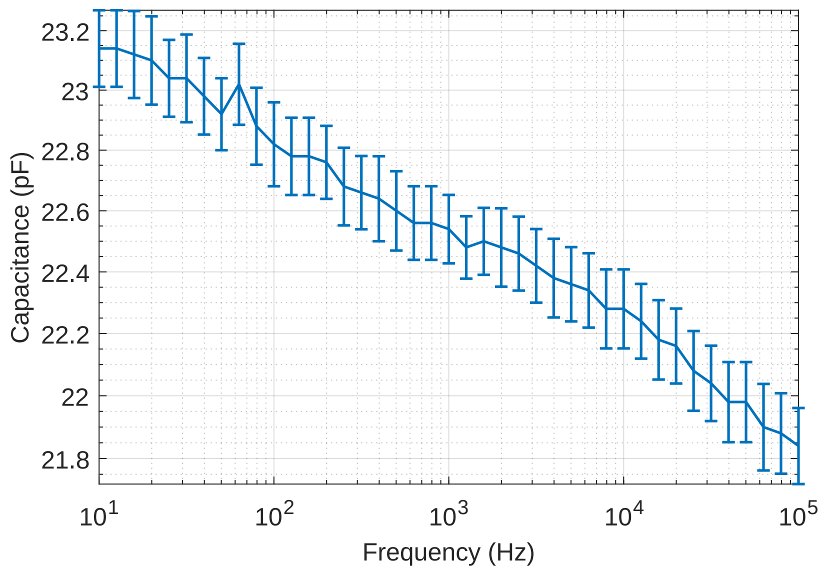

(a) Mean value of the capacitance is plotted and error bars show the standard error of the mean capacitance values.

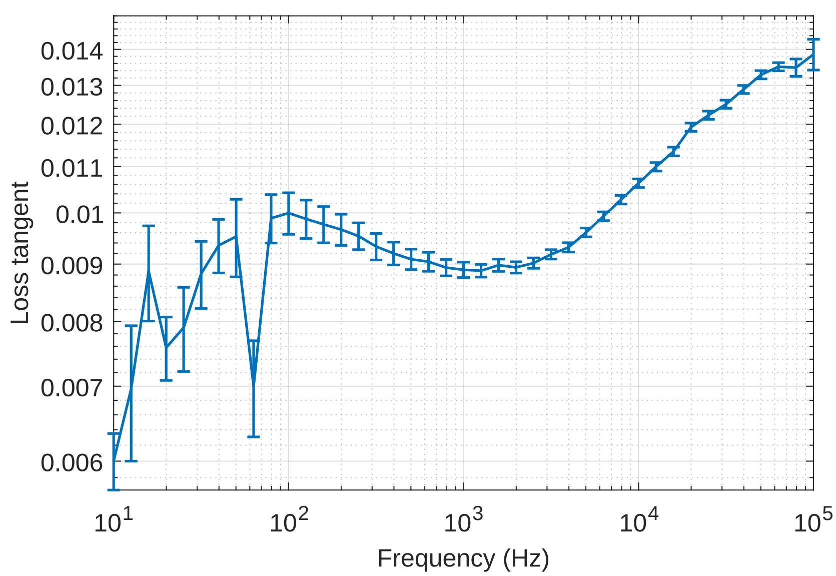

(b) Mean value of the loss tangent is plotted and error bars show the standard error of the mean loss tangents values.

Fig. 6.10: Measurements of capacitance and loss tangent in five new coated samples with HASL finish from 10 Hz to 100 kHz.

6.4.1 Aging of Energized Samples

In this study, specimens were tested after dedicated cycles of aging, using the same dielectric spectrometer and setup. Test boards of this part of experiment were energized by 50 VDC during the aging process. The results obtained from samples were plotted and compared over the same frequency range. Measurements of capacitance and dielectric loss for double coated sample with ENIG surface finish from new to 20 cycles aged are presented in Figure 6.11. A decreasing trend of capacitance by raising the frequency was seen over all levels of agings. It was observed that the sample capacitance has increased as a product of thermal and humidity aging cycles. While the new sample had a capacitance of 26 pF at 10 Hz, it raised to well over 31 pF after 20 cycles. This was due to absorption of water by the coating layer and, since the permitivity of the water is much higher than that of the conformal coating, the capacitance has increased. At higher frequencies, the capacitance has increased as well. However, the amount of change in capacitance at higher frequencies was smaller from about 24 to 25 pF. The plot of dielectric loss shows a declining trend from 10 Hz to 10kHz followed by an almost stable value up to 100 kHz in all aging measurements. It can be seen that the dielectric has become more lossy as the sample has aged. The most significant change in loss tangent was observed after first cycle of aging especially at low frequencies. The amount of change in dielectric loss value at high frequencies was small and it was almost constant from cycle 4 to 20.

Plots of capacitance and loss tangent for a double coated sample with HASL finish and energized condition are shown in Figure 6.12. Similarly, a capacitance decrease by raising the frequency was observed over all aging cycles. The capacitance at 10 Hz had a value around 26 pF which was fairly close to double coat ENIG sample. However, after 20 cycles of aging, the capacitance has increased to just above 45 pF at 10 Hz which is a significant change in

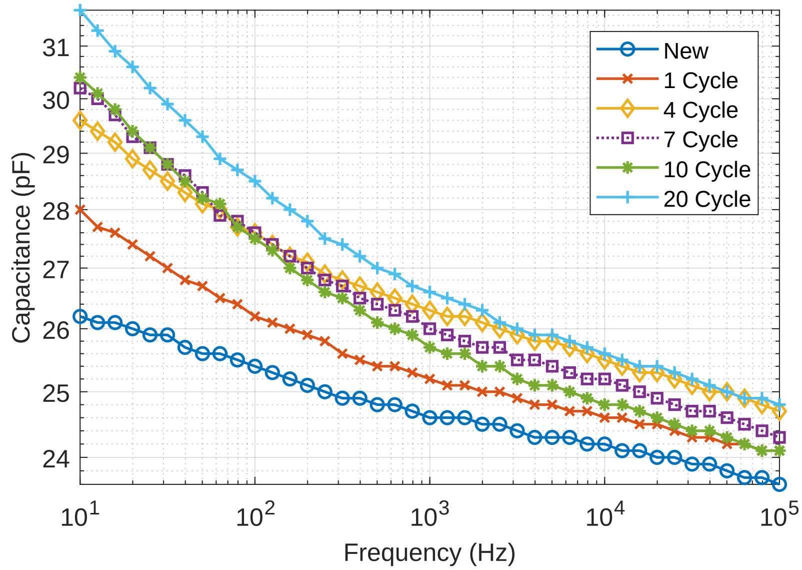

(a) Plot of capacitance measurements over 20 cycles of aging.

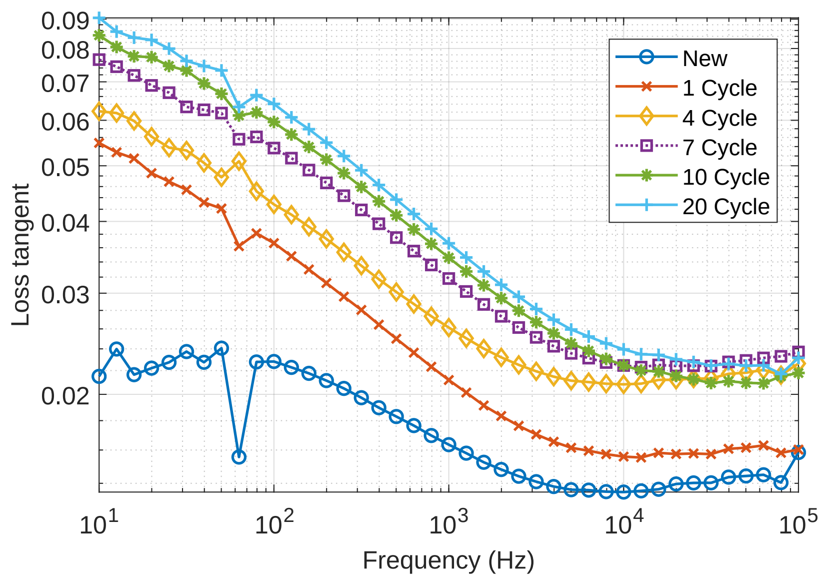

(b) Plot of loss tangent measurements over 20 cycles of aging.

Fig. 6.11: Comparison of capacitance and loss tangent measurements for double coated sample with ENIG finishing from 10 Hz to 100 kHz frequency over 20 cycles of aging. Samples were energized by 50 VDC during the aging process.

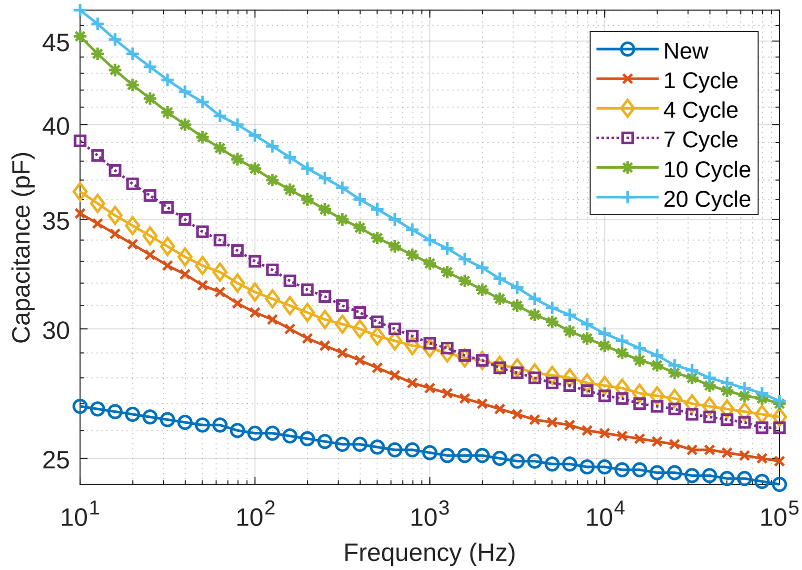

(a) Plot of capacitance measurements over 20 cycles of aging.

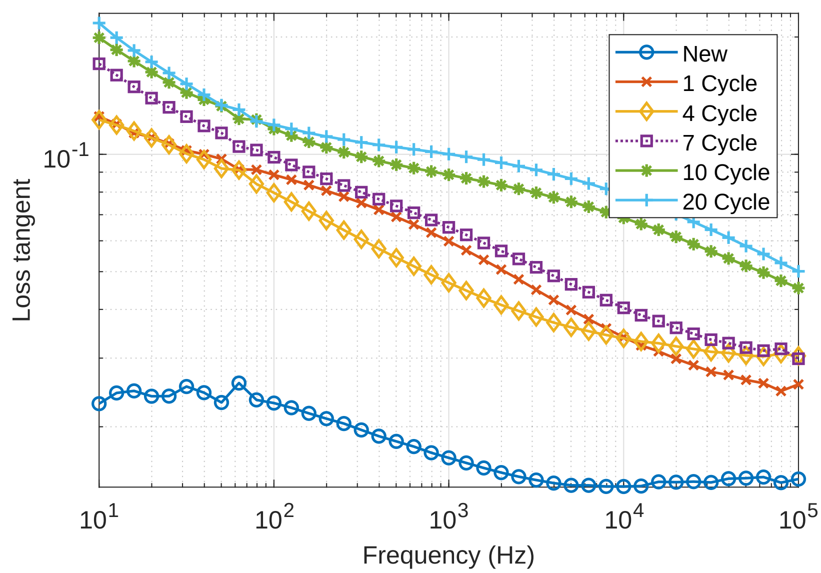

(b) Plot of loss tangent measurements over 20 cycles of aging.

Fig. 6.12: Comparison of capacitance and loss tangent measurements for double coated sample with HASL finishing from 10 Hz to 100 kHz frequency over 20 cycles of aging. Samples were energized by 50 VDC during the aging process.

comparison with new coated board or even double coated board with ENIG finish. There is a slight change in capacitance observed between 10^{th} and 20^{th} cycles. The plot of loss tangent for double coated sample with HASL surface finish also shows a remarkable change in dielectric loss value. The loss tangent has jumped by ten times from 0.02 to about 0.2 at 10 Hz frequency. These changes are evidences of humidity absorption and shows the negative influence of thermal and humidity aging on coated sample with HASL surface finish. While the overview of a double coated sample with ENIG finish and HASL finish are similar, the latter one had more evidences of degradation with significant changes in parameters.

Measurements for single coated sample with ENIG surface finish are provided below. Figure 6.13 shows the capacitance and dielectric loss change after aging cycles over the range of frequency. A decreasing trend of capacitance by increasing the frequency was seen for this sample. The most outstanding observation for this sample was that the capacitance value has increased extremely after 20 cycles of aging. Initial capacitance of the new coated board was 23 pF and the value increased to 32 pF after 10 cycles. After 20 cycles of aging, the capacitance reached 2.7 nF. The negative impact of humidity penetration was highly destructive after 10 cycles due to a thinner protective coating layer in this sample. The same rapid increase was noted for loss tangent plot after 20 cycles of aging. This loss tangent value shows the coating between traces has significantly degraded and lost its dielectric properties and became lossy especially at frequencies lower than 10 kHz.

Plots for a single coated sample with HASL surface finish are presented in Figure 6.14. The capacitance plot with a declining trend in value is observed. The level of change for this sample as a result of aging is not as bad as single coated sample with ENIG finish. At low frequency, the capacitance has increased from to 23 pF to about 81 pF. At 100 kHz, the capacitance has experienced a level of change from 22 pF to 24 pF. The measurements

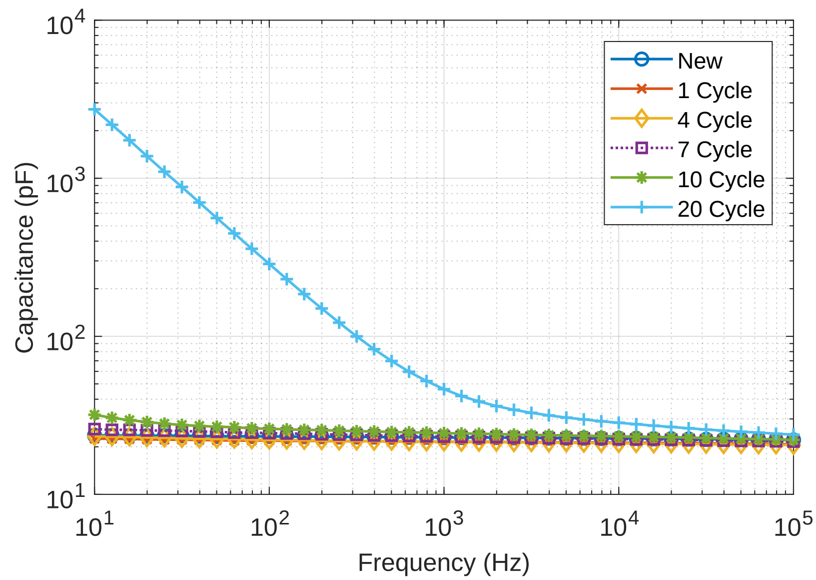

(a) Plot of capacitance measurements over 20 cycles of aging.

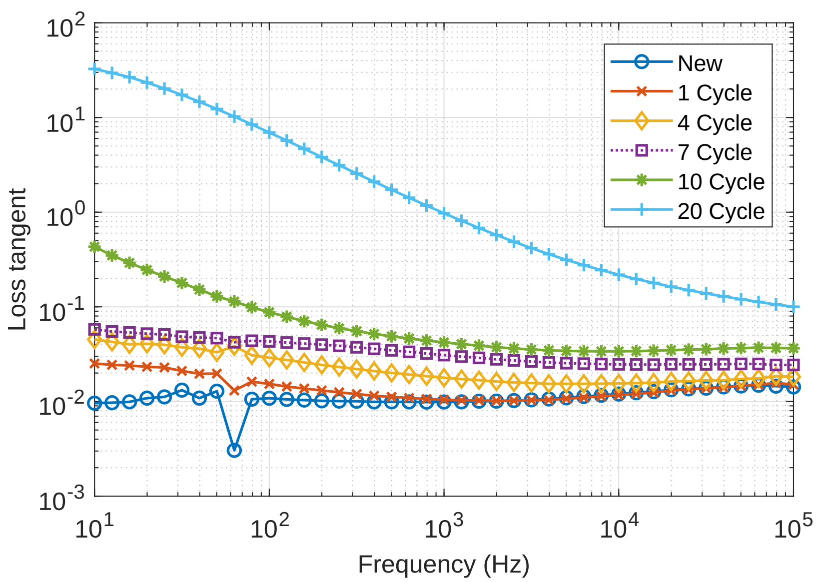

(b) Plot of loss tangent measurements over 20 cycles of aging.

Fig. 6.13: Comparison of capacitance and loss tangent measurements for single coated sample with ENIG finishing from 10 Hz to 100 kHz frequency over 20 cycles of aging. Samples were energized by 50 VDC during the aging process.

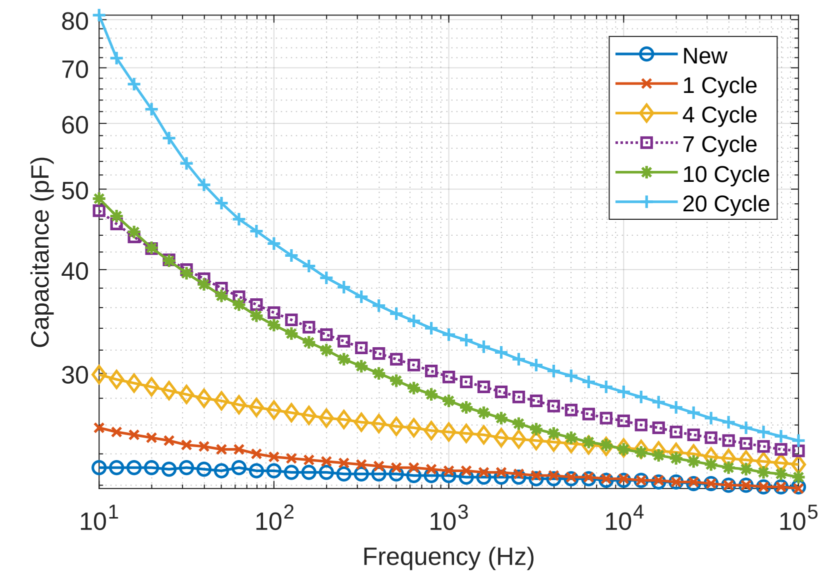

(a) Plot of capacitance measurements over 20 cycles of aging.

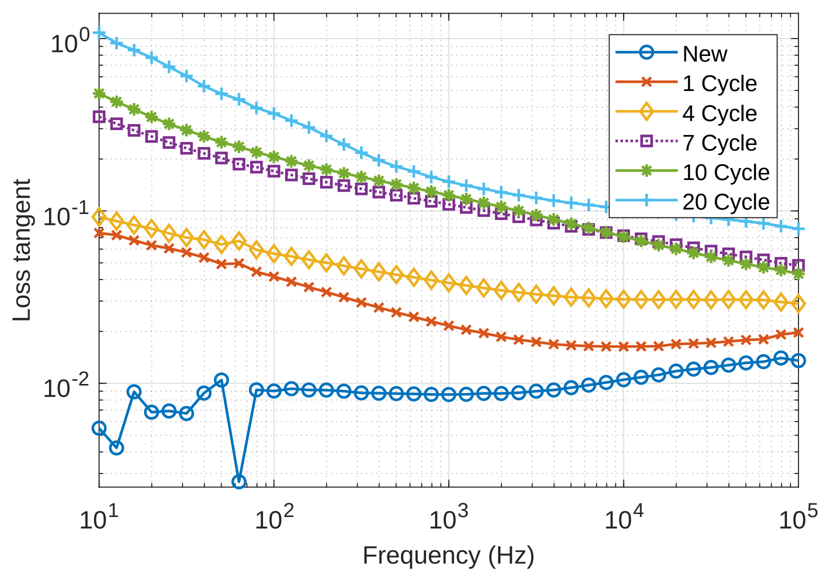

(b) Plot of loss tangent measurements over 20 cycles of aging.

Fig. 6.14: Comparison of capacitance and loss tangent measurements for single coated sample with HASL finishing from 10 Hz to 100 kHz frequency over 20 cycles of aging. Samples were energized by 50 VDC during the aging process.

of capacitance after cycles 7 and 10 have quite same values. The 20^{th} cycle of aging had a noticeable impact on the sample. Both capacitance and loss tangent have suffered even from one aging cycle which shows the susceptibility of thin coating film. The dielectric loss is doubled from first to last cycle of aging. Both samples with thinner coating layer have experienced a higher level of dielectric loss as a result of high humidity and thermal aging. Single coating layer in these samples provided a lower level of protection against thermal and humidity aging.

In samples with additional applied coating, the one with ENIG plating performed marginally better than the sample with HASL finish. Under energized condition, the level of increase in dielectric loss as a product of aging was lower for double coated ENIG finish sample. Once the humidity penetrated in the coating layer, the oxidation of ENIG plating significantly increased the dielectric loss especially at lower frequencies up to 10 kHz.

6.4.2 Aging of Non-Energized Samples

During the aging process, one sample of each group was placed inside the chamber without the supplied power. This experiment was conducted to investigate how the energized condition will impact on the aging process. The same aging cycles were implemented for these samples and same measurements were performed following the aging process. Figure 6.15 shows macro imaging from single coated test boards with ENIG surface finish which has aged under the non-energized condition. It can be seen that the level of degradation is significantly lower than that of energized samples. A few development of bubbles was observed after 7^{th} cycle of exposure to temperature and humidity aging. After 20^{th} cycle, only degradation of the coating layer was observed and no evidence of oxidation on traces was noticed. Plots of capacitance and loss tangent measurements over the frequency of 10 Hz to

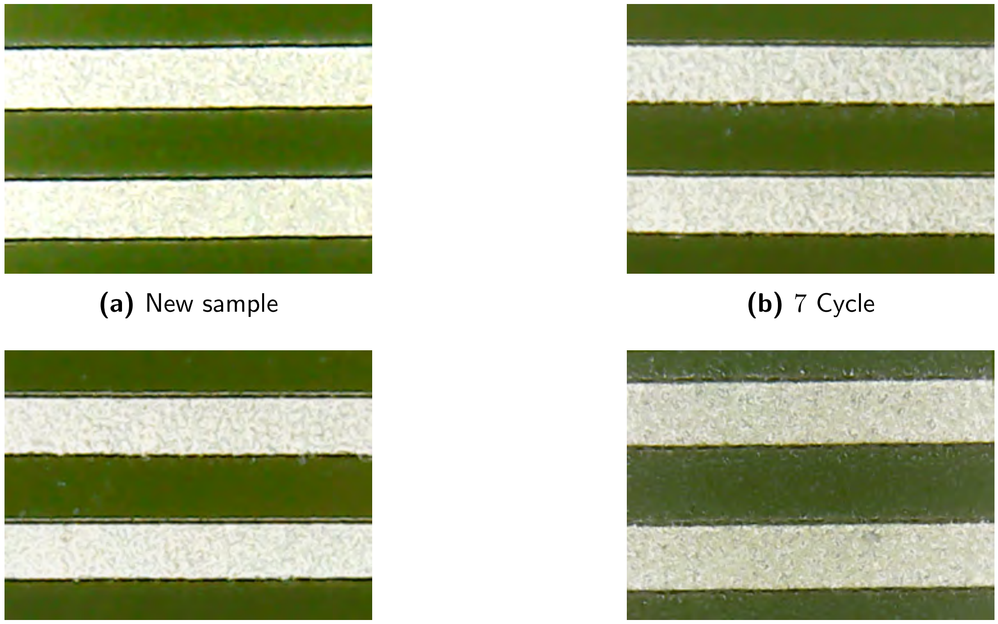

(a) New sample (b) 7 Cycle

(c) 10 Cycles (d) 20 Cycles

Fig. 6.15: Macro imaging from traces of single coated test boards with ENIG finish which have degraded during 20 cycles of thermal and humidity aging under non-energized condition.

100 kHz for single coated ENIG sample after dedicated cycles are presented in Figure 6.16. The plots show that both capacitance and loss tangent have increased as a result of aging process. After 20 cycles, the capacitance at 10 Hz has increased from about 23 pF to 25 pF and the capacitance value has raised just by 0.5 pF at 100 kHz. Besides, the same small change of dielectric loss was seen after 20 cycles in this sample. At a low frequency of 10 Hz, the loss tangent has experienced a small growth of 0.05 after 20 cycles and the amount of change for this parameter was only 0.003 at 100 kHz. It can be seen that the non-energized sample has degraded less than the energized one. Same measurements from a sample with additional coating layer under same condition was performed. Figure 6.17 shows the data for non-energized ENIG sample with additional coating layer. Small changes in the parameters

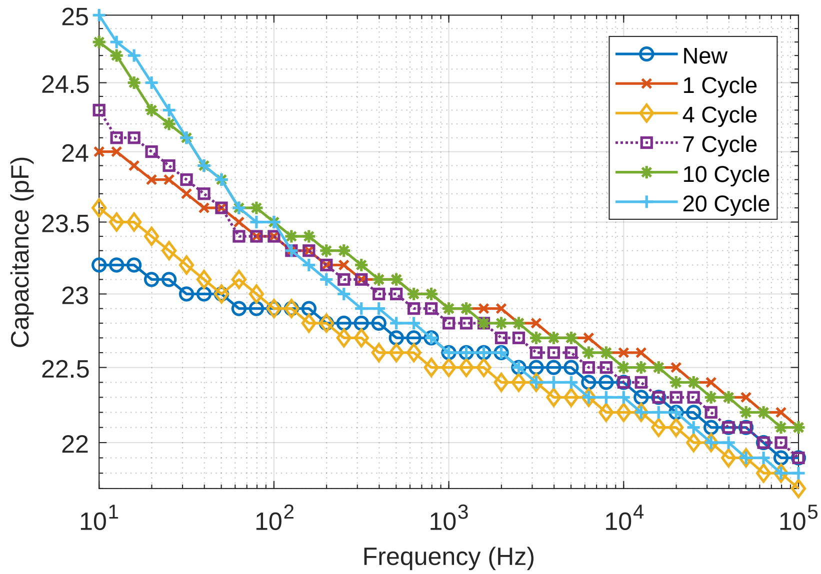

(a) Plot of capacitance measurements over 20 cycles of aging.

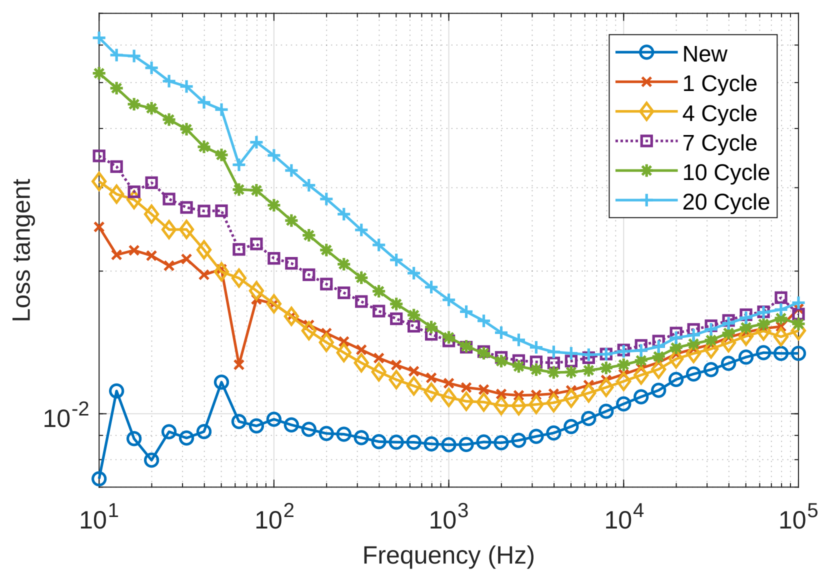

(b) Plot of loss tangent measurements over 20 cycles of aging.

Fig. 6.16: Comparison of loss tangent measurements for single coated sample with ENIG finishing from 10 Hz to 100 kHz frequency over 20 cycles of aging. Samples were not energized during the aging process.

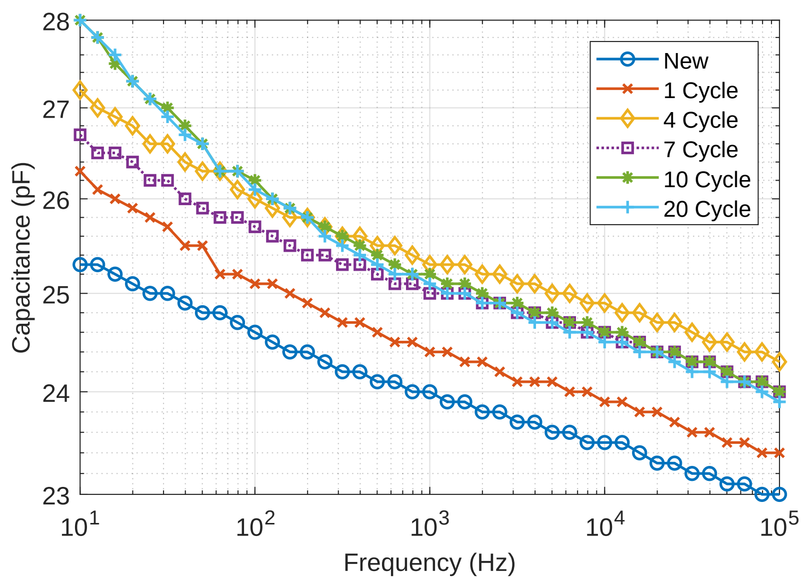

(a) Plot of capacitance measurements over 20 cycles of aging.

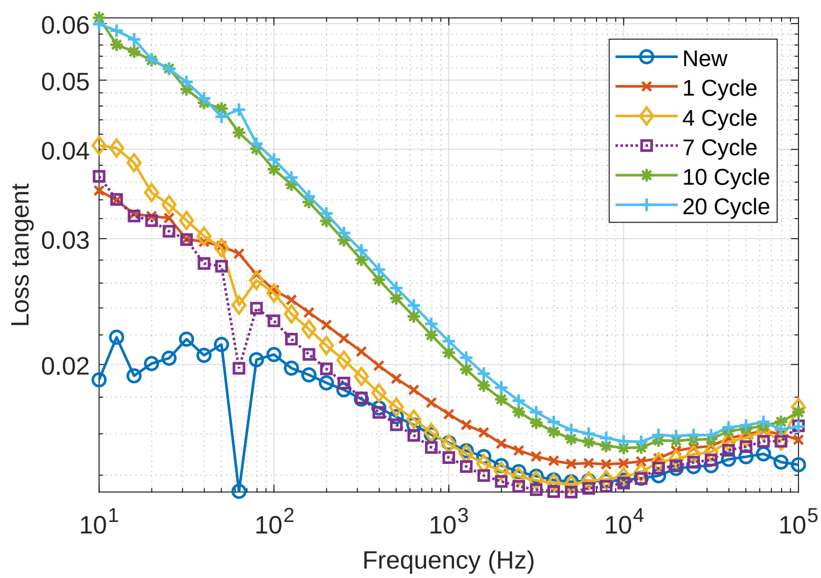

(b) Plot of loss tangent measurements over 20 cycles of aging.

Fig. 6.17: Comparison of loss tangent measurements for double coated sample with ENIG finishing from 10 Hz to 100 kHz frequency over 20 cycles of aging. Samples were not energized during the aging process.

of the double coated sample was noticed as well. Double coated sample changes were even less than those of single coated test board. Although the aging cycles have impacted these samples, no evidence of extreme change was observed. Aging cycles for single and double coated specimens with HASL surface plating was conducted in the same manner. Figure 6.18 shows the capacitance and loss tangent measurements for non-energized sample with HASL finish and single coating layer. At 10 Hz frequency, changes of capacitance and loss tangent were 2.5 pF and 0.05 respectively. Smaller changes in parameters were observed at 100 kHz. Results of double coated sample with HASL surface plating were fairy similar to single coated one. Significantly smaller changes in parameters of non-energized sample were observed in comparison with energized specimens. Plots of parameters measurements for HASL sample with additional coating are presented in Figure 6.19. It was seen that these samples have degraded less than energized samples with the same condition. The amount of change in capacitance and loss tangent was noticeably lower than those of energized samples. Figure 6.20 shows the macro images from single coated sample with HASL finishing after cycles of aging. Some dark points as evidences of the moisture on traces of the sample were observed after 20 cycles of aging. Rather than dark points, a small shrinkage was observed for the coating layer around traces which appeared after the 7th cycle.

In comparison with energized samples with the same aging cycles, non-energized boards were degraded slightly. The great influence of applied voltage on the level of degradation was observed. Energized board absorbed more humidity from the humid environment inside the chamber. This could be due to the presence of electric field between traces as a result of applied voltage. Since the permitivity of the water vapour is higher than that of the coating material, the humidity was absorbed by the energized traces. This phenomena also happened during the experiments of PD under pollution for coated boards and described in

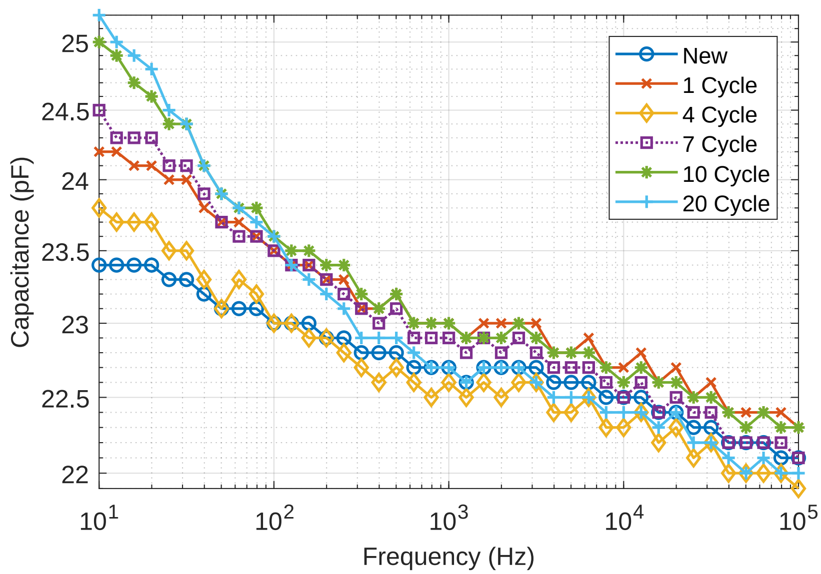

(a) Plot of capacitance measurements over 20 cycles of aging.

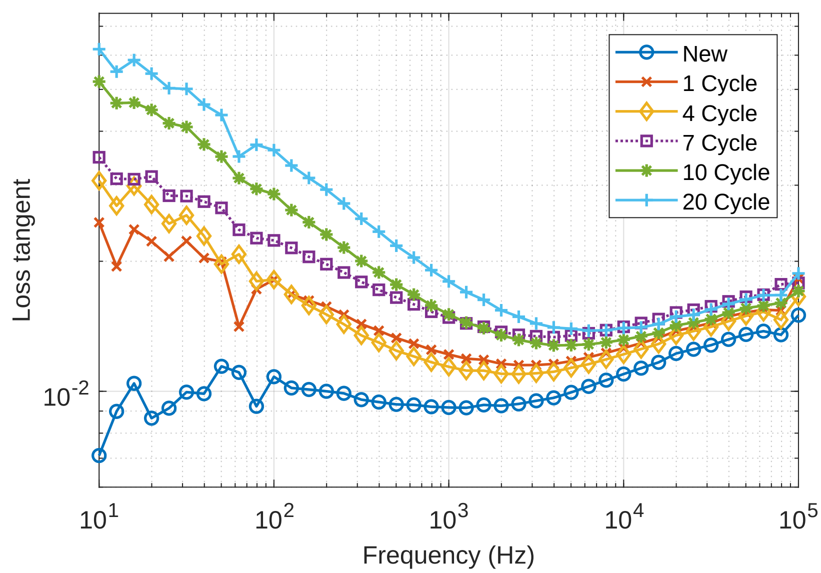

(b) Plot of loss tangent measurements over 20 cycles of aging.

Fig. 6.18: Comparison of loss tangent measurements for single coated sample with HASL finishing from 10 Hz to 100 kHz frequency over 20 cycles of aging. Samples were not energized during the aging process.

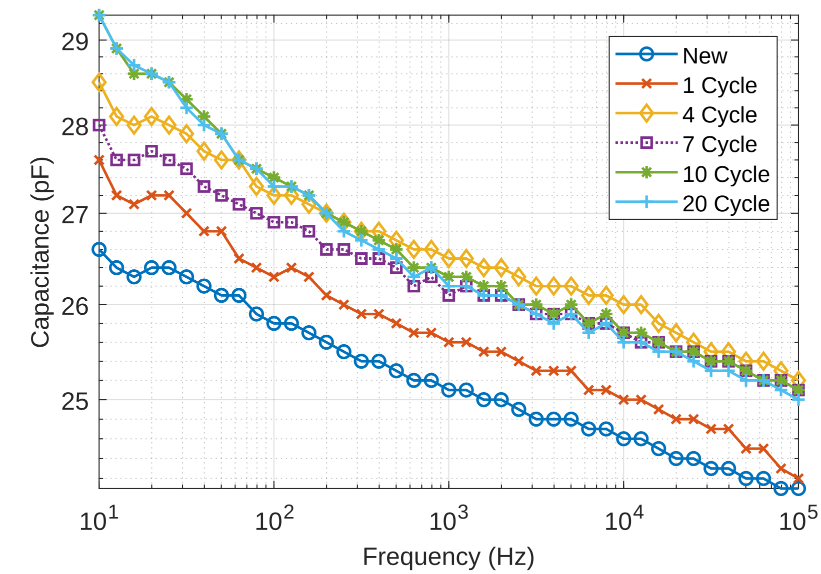

(a) Plot of capacitance measurements over 20 cycles of aging.

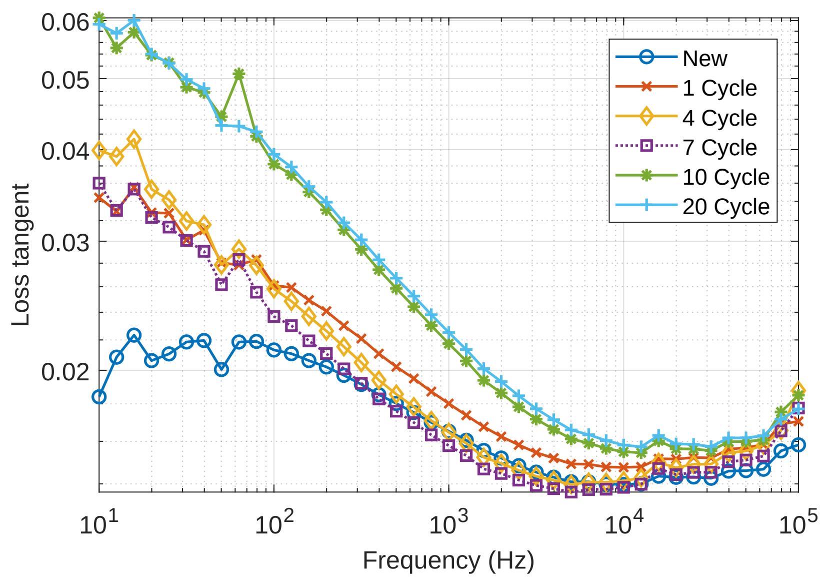

(b) Plot of loss tangent measurements over 20 cycles of aging.

Fig. 6.19: Comparison of loss tangent measurements for double coated sample with HASL finishing from 10 Hz to 100 kHz frequency over 20 cycles of aging. Samples were not energized during the aging process.

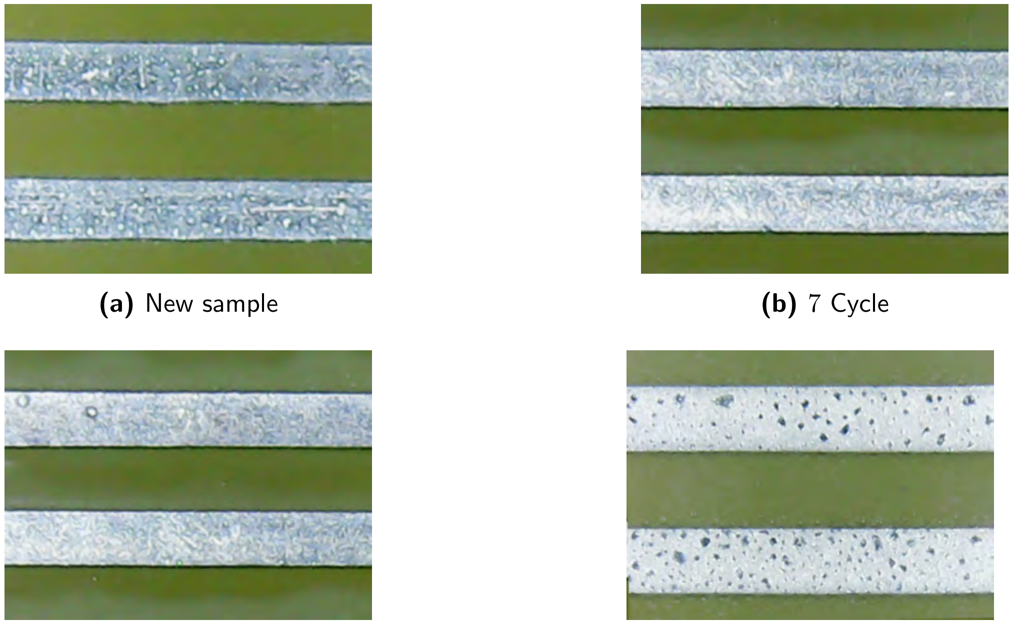

(a) New sample

(b) 7 Cycle

(c) 10 Cycles

(d) 20 Cycles

Fig. 6.20: Macro imaging from traces of single coated test boards with HASL finish which have degraded during 20 cycles of thermal and humidity aging under non-energized condition.

Section 5.1. It was also noticed that the higher penetration of moisture trough the coating layer resulted in oxidation of the traces and, consequently, advanced level of degradation on a coated PCB occurred. The advantage of additional coating layer was observed as the double coated boards had even smaller changes in their capacitance and loss tangent parameters.

6.4.3 Additional Aging of Energized Sample

After the 20 cycles of aging were finished, we extended the process of aging for some of the test samples. The designed aging chamber was run for 16 more cycles with energized samples inside. Samples were tested and results of capacitance and loss tangent were extracted same as previous experiment. Figure 6.21 shows the plots of capacitance and dielectric loss for samples with ENIG surface finish after 36 cycles of aging.

A noticeable increase was observed in both parameters after the 36th cycle of aging. The capacitance of the sample increased to 180 pF at 10 Hz and about 27 pF at 100 kHz. The loss tangent for this sample has increased significantly after additional aging cycles. Based on the measured parameters, the sample was far from its initial values which means the high level of degradation in this sample.

Dual coated test sample with HASL surface plating were also tested. Measurements are presented in Figure 6.22. Increasing the capacitance and loss tangent happened in this test board as well. However, it was noticed that the amount of change in parameters are not as extreme as those of the same sample with EING finish. The capacitance at 10 Hz increased from 47 pF to 60 pF between cycle 20 and 36 and the value changed slightly at high frequencies. The loss tangent plot also shows an increase of 0.4 at and a fairly slight change between 20th and 36th cycles for frequencies of 10 Hz and 100 kHz, respectively.

The additional aging was performed for single coated test board with ENIG and HASL surface plating as well. The result of capacitance and loss tangent change are presented in Figure 6.23 for the ENIG plated, and in Figure 6.24 for the HASL plated test sample. It was observed that the level of degradation for single coated samples were more severe in comparison with double coated specimens. Both single coated test boards experienced a significant change in parameters. The level of change in loss tangent for the sample with ENIG plating was higher than that of for HASL sample between cycle 20 and 36. Since the capacitance of both samples increased notably, it can be noted that an excessive amount of moisture was absorbed by the conformal coating layer.

The above observations showed a good level of performance for single coated sample with ENIG surface finish only up to a level of degradation. It was seen that once degradation of

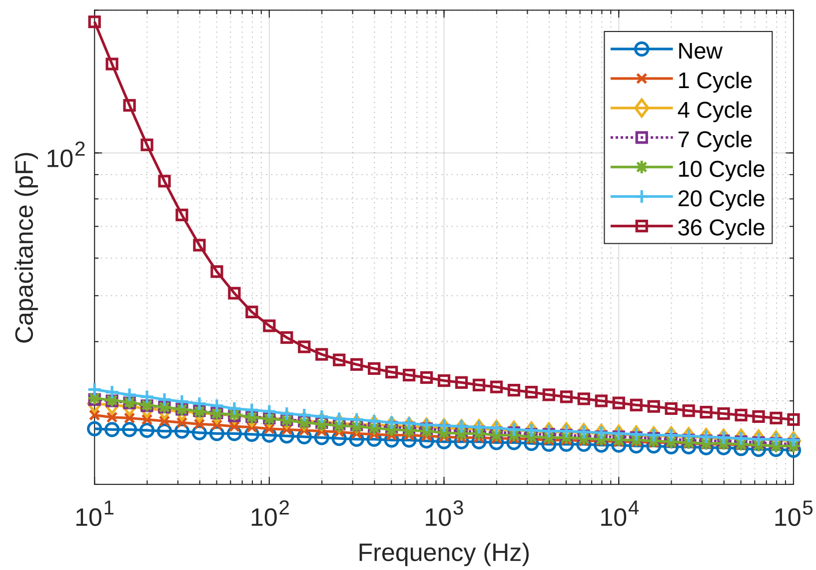

(a) Plot of capacitance measurements over 36 cycles of aging.

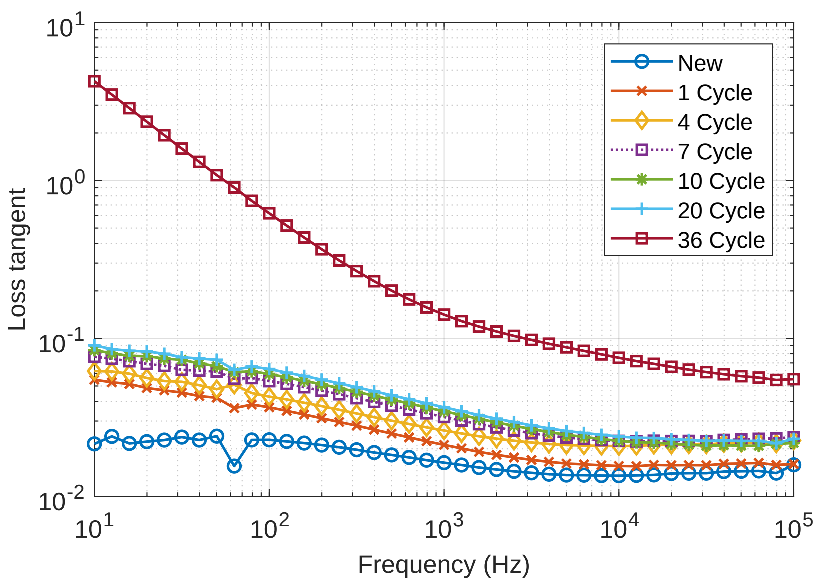

(b) Plot of loss tangent measurements over 36 cycles of aging.

Fig. 6.21: Comparison of loss tangent measurements for double coated sample with ENIG finishing from 10 Hz to 100 kHz frequency over 36 cycles of aging. Samples were energized by 50 V DC during the aging process.

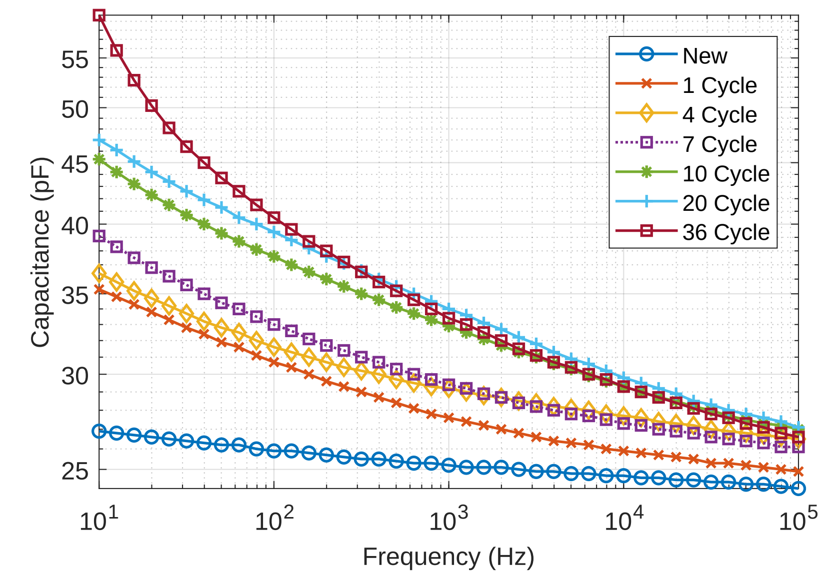

(a) Plot of capacitance measurements over 36 cycles of aging.

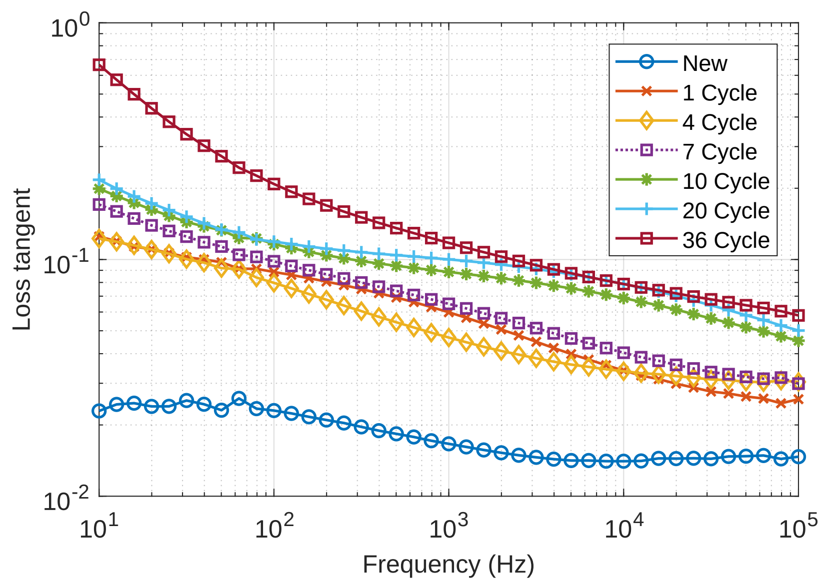

(b) Plot of loss tangent measurements over 36 cycles of aging.

Fig. 6.22: Comparison of loss tangent measurements for double coated sample with HASL finishing from 10 Hz to 100 kHz frequency over 36 cycles of aging. Samples were energized by 50 V DC during the aging process.

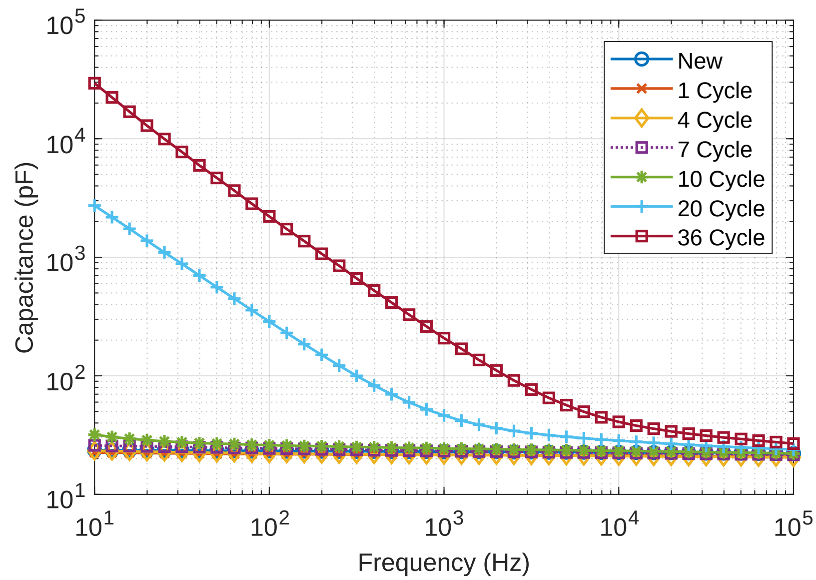

(a) Plot of capacitance measurements over 36 cycles of aging.

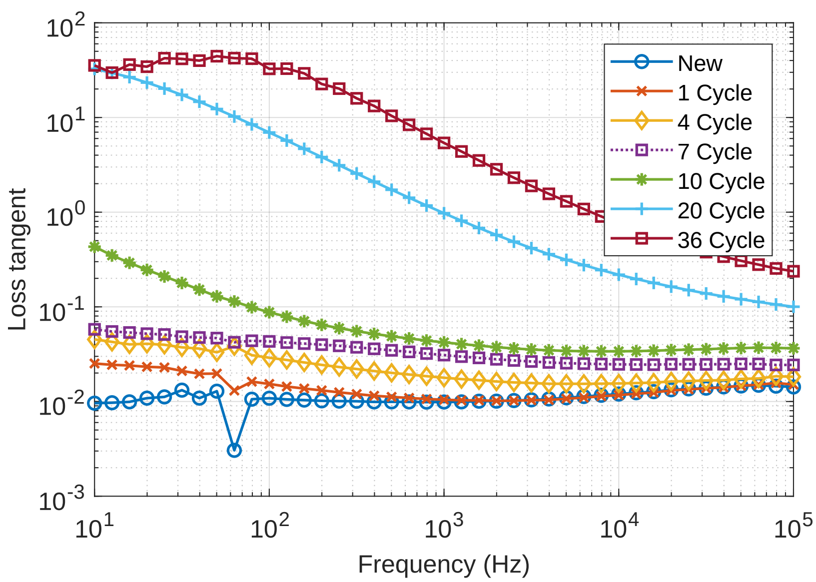

(b) Plot of loss tangent measurements over 36 cycles of aging.

Fig. 6.23: Comparison of loss tangent measurements for single coated sample with ENIG finishing from 10 Hz to 100 kHz frequency over 36 cycles of aging. Samples were energized by 50 V DC during the aging process.

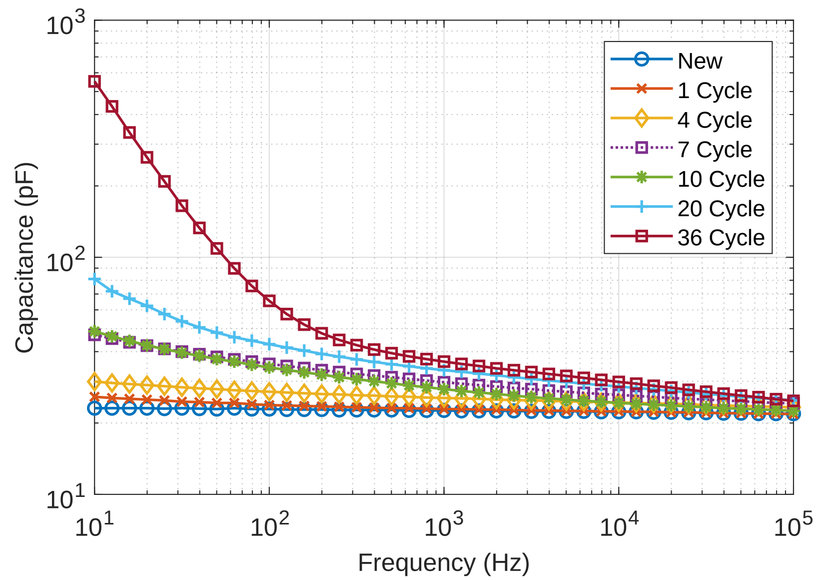

(a) Plot of capacitance measurements over 36 cycles of aging.

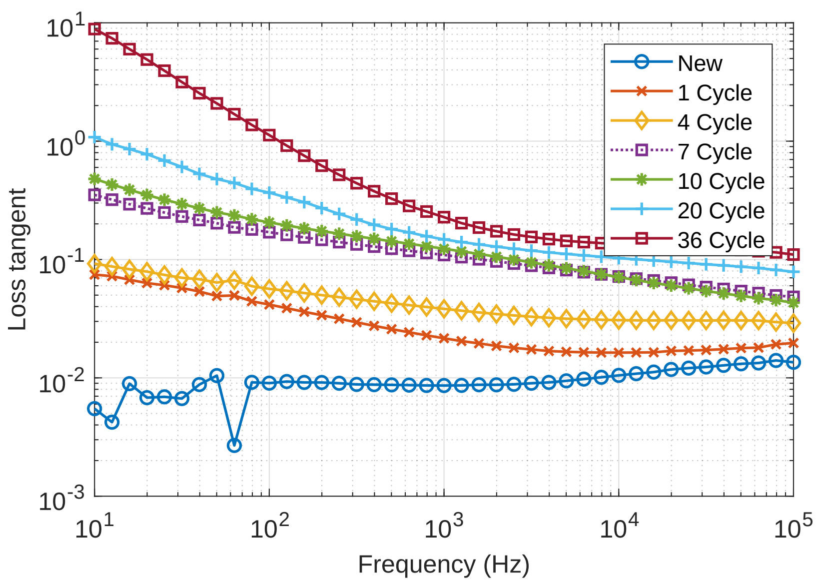

(b) Plot of loss tangent measurements over 36 cycles of aging.

Fig. 6.24: Comparison of loss tangent measurements for single coated sample with HASL finishing from 10 Hz to 100 kHz frequency over 36 cycles of aging. Samples were energized by 50 V DC during the aging process.

ENIG sample developed more, both loss tangent and capacitance have increased extremely. This is noted as a result of oxidation of the surface plating. The sample with HASL finish, experienced a gradual level of degradation after aging cycles.

6.5 Measurements of PD

In this part of the experiments, PD in silicone conformally-coated aged test samples with "D" comb pattern were tested. Two types of HASL and ENIG surface plated specimens with single and double coating layer were examined after 20 and 36 cycles of aging. Electrical properties of the new and aged samples were evaluated using PD measurement technique. Measurements of PD were conducted in atmospheric air pressure and all reported voltages are RMS values. Test setup for PD measurements described in Section 5.1.1 was enhanced by replacing the variac with a digital adjustable power source as shown in Figure 6.25[1]. The new test setup was capable of fime controlling of the output voltage. This yielded a better voltage steps and more accurate PD measurements. Test boards were mounted in test cell and were fed through the soldered pins on the PCB under test as shown in Figure 6.26.

Frequency of the applied voltage was fixed at 60 Hz and the AC applied voltage was increased by a rate of about 35 volts per minute upon detection of PD signal. A 5 pC in magnitude was set on the measuring software as the minimum limit for PD detection. Any PDs lower than 5 pC magnitude were considered as noise and filtered by the Omicron software. Once the PD signals were detected, RMS value of the applied voltage was recorded as PDIV and the phase resolved PD plot was saved. In some samples, further increase in voltage resulted in detection of more PDs with higher magnitudes. Some of the coated test boards including new samples, provided a good electrical performance and no PD was

[1]The digital variac was not available during the early measurements.

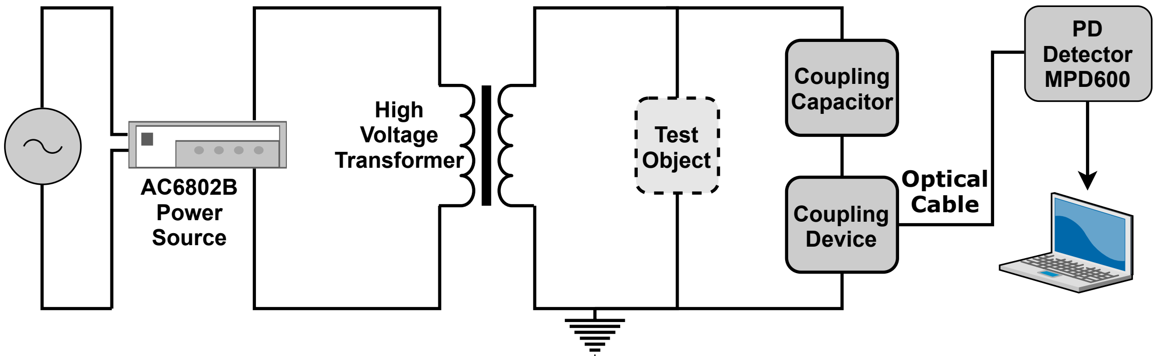

Fig. 6.25: PD test setup block diagram. Sample under the test is connected to a high voltage transformer which is fed through a digital adjustable power supply.

detected even by increasing the applied voltage up to 3 kV. Test boards of ENIG and HASL group without coating layer were also tested. No PD signal was detected from bare test boards and only momentary discharges were occurred between traces.

The test sample with double coating with ENIG surface finish and 20 cycles of aging was examined. The applied voltage was increased until the first PD was detected at 1.57 kV with a magnitude of 9 pC. Increasing the voltage in this sample resulted in PDs of higher magnitude. Figure 6.27 shows the phase resolved PD pattern for this sample at 1.69 kV with PDs magnitude of 50 pC.

Measurements of PD in the sample with HASL surface finish and double layer of coating after 20 cycles of aging were performed. First PD signal was detected at 1.69 kV with a magnitude of 7 pC. Figure 6.28 shows the pattern for PDs of 10 pC magnitude in this sample at 1.85 kV. Both number and magnitude of detected PDs were increased at higher voltages.

The single coated test sample with ENIG surface finish was tested after 20 cycles of aging. Applied voltage was increased upon detection of PD signal. The first PD signal was detected

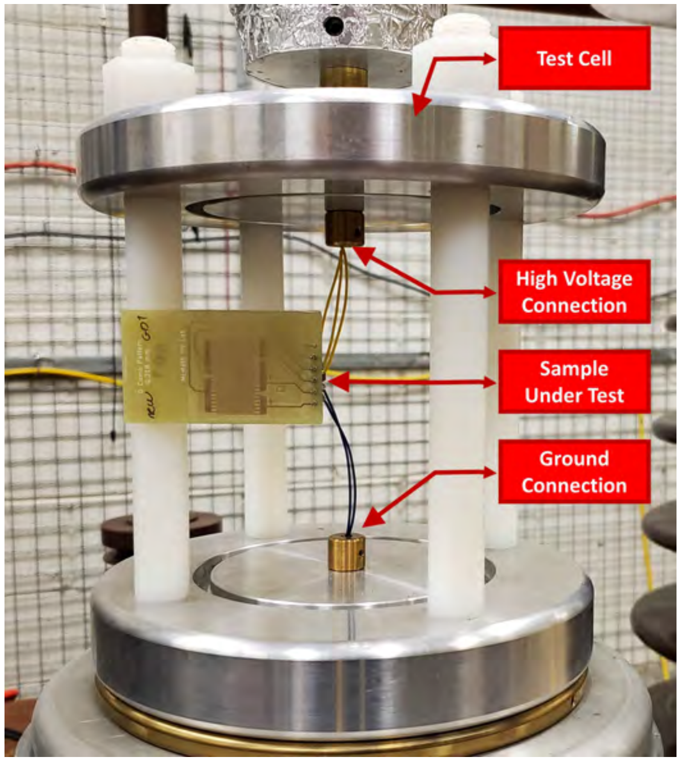

Fig. 6.26: Test sample mounted in the test cell and connected to high voltage source for PD testing.

at 653 V with a magnitude of 7 pC. Increasing the voltage to 692 V was resulted in PDs with magnitude of 21 pC as shown in Figure 6.29. As was observed in the previous chapter, the level of degradation was severe in single coated specimens in comparison with double coated ones of the same surface plating. Measurements of PD proved the lower electrical performance of this sample as a significantly lower PDIV was recorded for this sample.

The first PD signal for a 20 cycle aged, single coated sample with HASL surface finish was detected at 768 V with a magnitude of 12 pC.The applied voltage to the sample was increased, and more PDs were detected with a magnitude of 35 pC after raising the voltage up to 846 V. Figure 6.30 shows the phase resolved PD pattern for single coated sample with

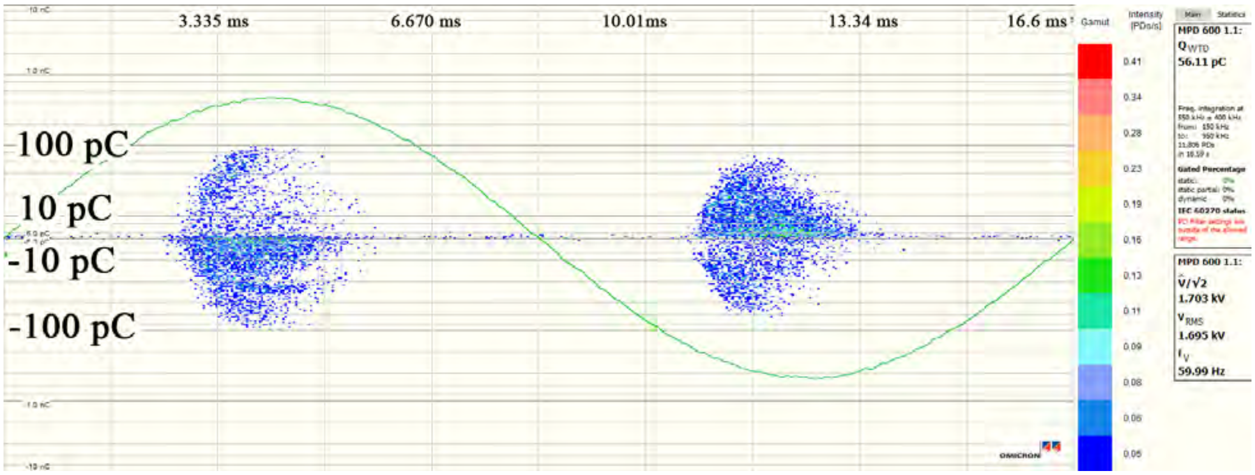

Fig. 6.27: Phase resolved PD pattern for a 20 cycle aged double coated test board with ENIG surface finish.

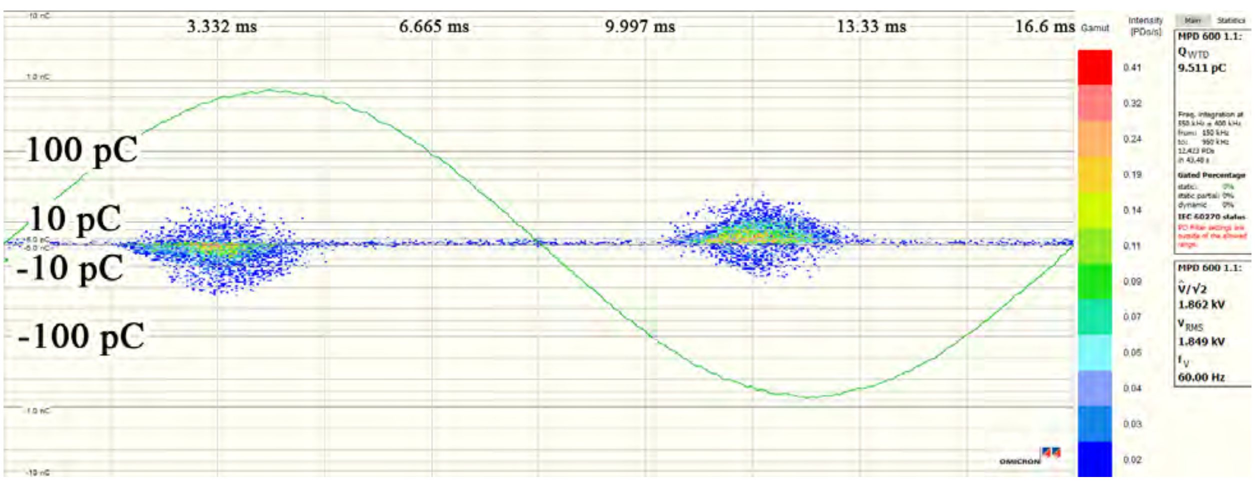

Fig. 6.28: Phase resolved PD pattern for a 20 cycle aged double coated test board with HASL surface finish.

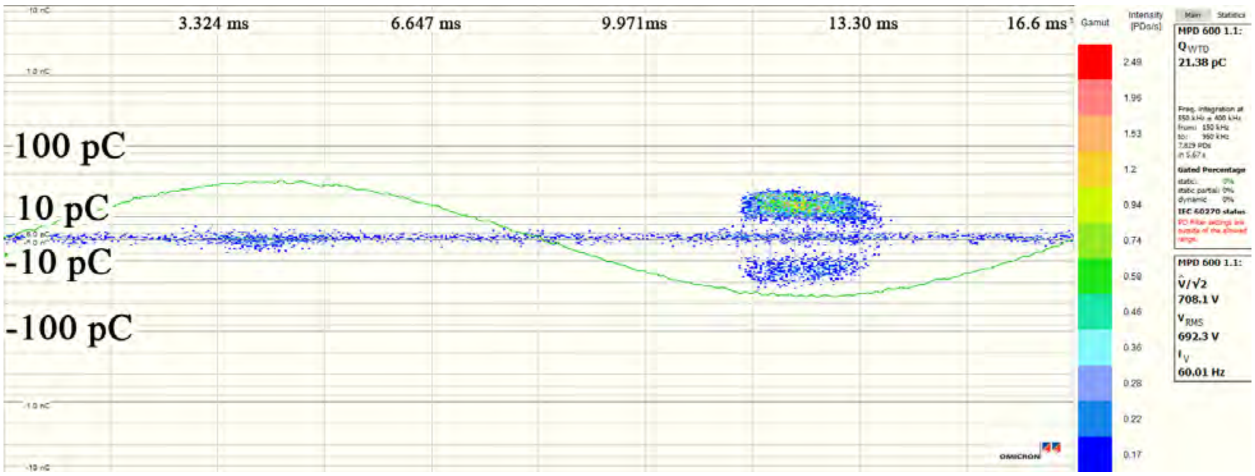

Fig. 6.29: Phase resolved PD pattern for a 20 cycle aged single coated test board with ENIG surface finish.

HASL finish. It was observed that this sample has a noticeably lower PDIV in comparison with double coated board with the same plating. Compared to the test board with ENIG surface finish, the sample with HASL surface plating provided a higher inception voltage after 20 cycles of aging.

PD experiments were conducted for samples of 36 cycles aged. The test sample with single coating and ENIG surface finish was examined. First PD was detected at 457 V with a magnitude of 9 pC. Figure 6.31 shows the PD pattern for this sample at voltage 496 V with PDs of 15 pC in magnitude. The PDIV of this sample was even lower than that of 20 cycle aged. The negative impact of thermal and humidity aging on the PDIV of this sample was observed.

The sample with HASL surface finish and single coating layer was tested too. PD was detected at 590 V with a magnitude of 10 pC. Increasing the voltage up to 654 V resulted in PDs with magnitude of 20 pC as shown in Figure 6.32. It was observed that this sample

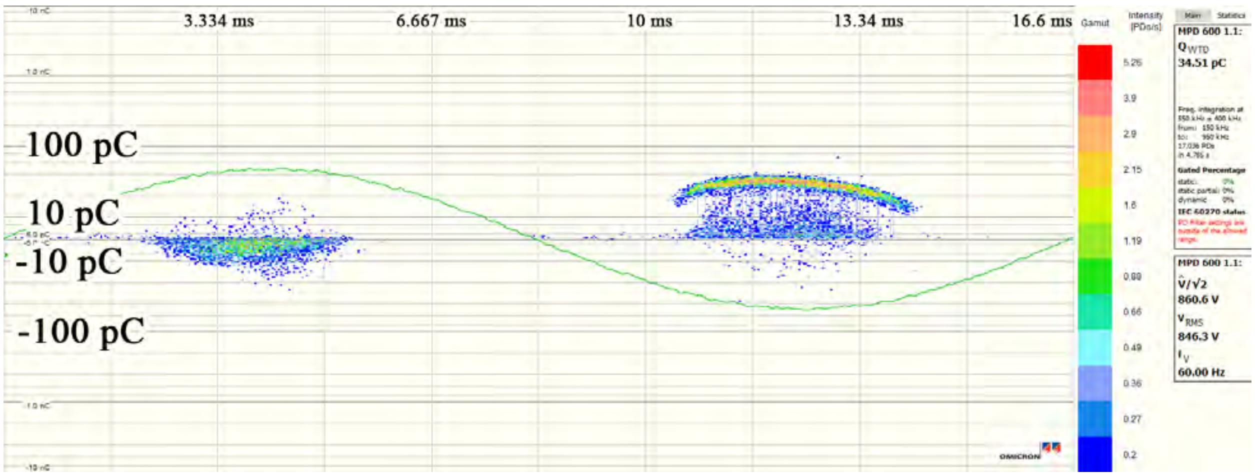

Fig. 6.30: Phase resolved PD pattern for a 20 cycle aged single coated test board with HASL surface finish.

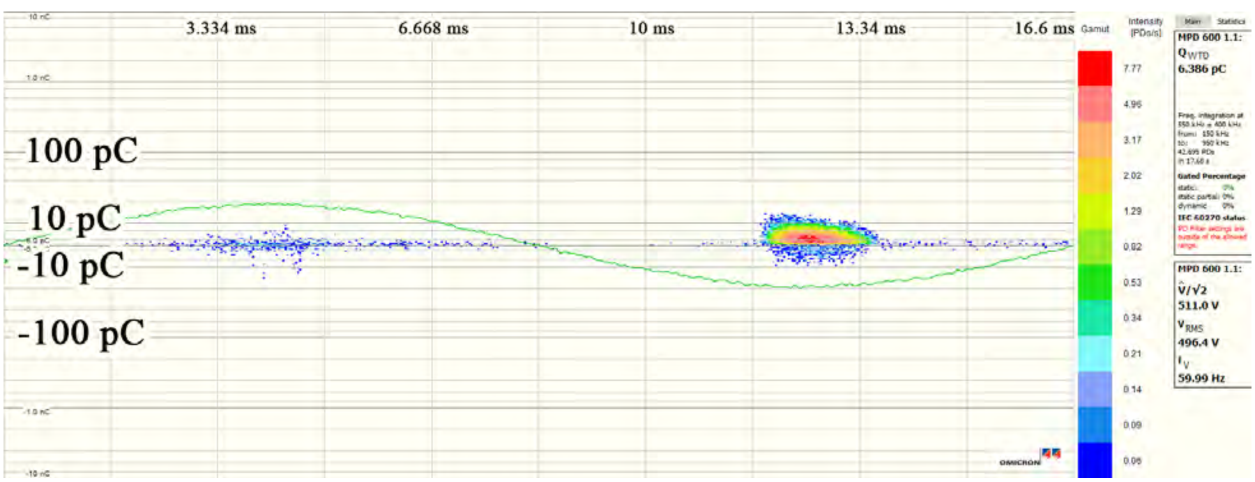

Fig. 6.31: Phase resolved PD pattern for a 36 cycle aged single coated test board with ENIG surface finish.

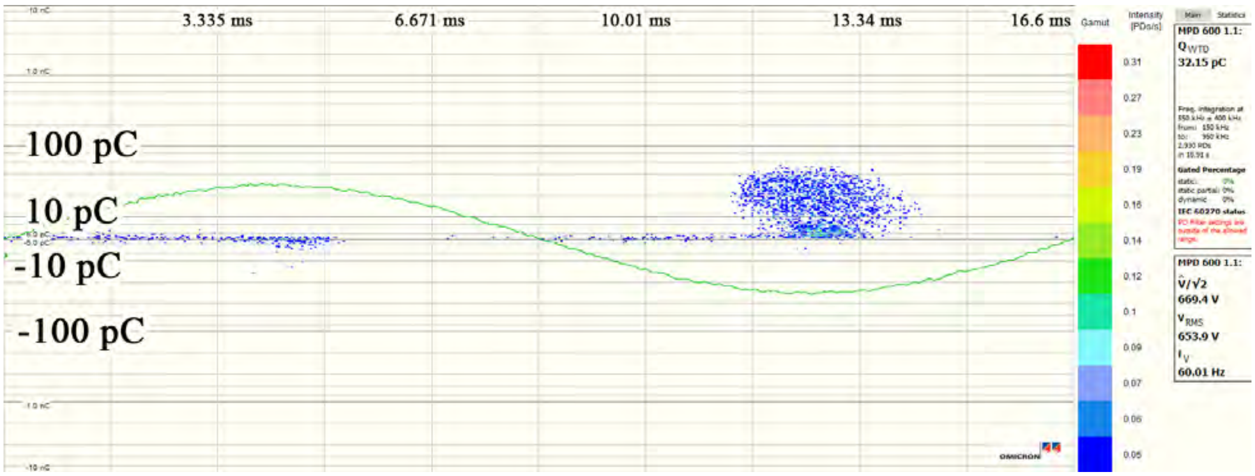

Fig. 6.32: Phase resolved PD pattern for a 36 cycle aged single coated test board with HASL surface finish.

has a lower PDIV in comparison with a sample of same condition with lower aging cycles.

Test specimens with double coating layer after 36 cycles of aging did not provided any PD. Increasing the applied voltage to these samples only resulted in momentary discharges between connection pins. This happened because the coating layer on the comb pattern provided a fair dielectric between traces on the sample. However, the weak point of these specimens was the tips of connection pins due to severely pealed and damaged coating layer around that area.

6.6 Breakdown Voltage

In the last part of these experiments, breakdown voltage of conformally-coated samples with “D” comb pattern was examined. The spacing between traces of the comb pattern on test boards was 0.318 mm. Based on the IPC 2221 standard which defines the minimum electrical conductor spacing for PCBs as a function of voltage, this clearance is recommended for operating voltages of higher than 500 V at sea level to 3050 m for a bare board. Measurements of breakdown in this part were conducted in atmospheric air pressure and reported voltages are RMS values. The breakdown voltage test, as described in Section 3.2, defines the potential difference at which the insulating material failure occurs. Since this test is destructive and sample will burn after the test, it was performed as the last part of assessments in this study. The same setup as used for PD measurements in Section 6.5 was employed. The voltage was increased at a rate of 35 V/min using the digital power supply upon detection of breakdown in sample. The breakdown voltage of samples was recorded as the highest measured voltage before the sample failure. Before the sample breakdown point, some momentary discharges were occurred in a number of samples. Once the breakdown was occurred, the supplied voltage was disconnected from the sample. Increasing the voltage up to 3 kV did not resulted in breakdown in some of the samples due to the good dielectric performance provided by the coating layer. Recorded breakdown voltage of each sample are provided in Table 6.1. In order to provide a better comparison between samples, the measured PDIV from previous experiment is also presented.

From the above provided breakdown voltages, the positive impact of conformal coating layer was observed. While the bare samples have a breakdown voltage of 1.2 kV, new coated samples of all kind provided a better electrical performance and did not resulted in breakdown up to 3 kV. No momentary discharge or PD was recorded for both single and double coated specimens with HASL and ENIG surface finish. This confirms the advantageous influence of the applied coating layer in samples with conformal coating. The adverse impact of thermal and humidity aging on breakdown voltage and PDIV was observed in all aged specimens. Breakdown voltage of samples with single coating layer were declined significantly as the product of 20 and 36 cycles of aging. As discussed in Section 6.4, samples with

Table 6.1: Breakdown voltage and PDIV of new and aged test samples with and without confromal coating.

Surface Finishing	Coating Layer	Aged Cycle	PDIV (RMS)	Momentary Discharge (RMS)	Breakdown Voltage (RMS)
ENIG	Double	36	No PD	1.69 kV (Between Connection Pins)	1.84 kV
		20	1.57 kV	No discharge	1.92 kV
		New	No PD	No discharge	>3 kV
	Single	36	460 V	570 V	695 V
		20	653 V	690 V	715 V
		New	No PD	No discharge	>3 kV
	No Coat	New	No PD	970 V	1.2 kV
HASL	Double	36	No PD	1.85 kV (Between Connection Pins)	1.92 kV
		20	1.69 kV	No discharge	1.89 kV
		New	No PD	No discharge	>3kV
	Single	36	590 V	770 V	815 V
		20	768 V	846 V	980 V
		New	No PD	No discharge	>3 kV
	No Coat	New	No PD	945 V	1.2 kV

ENIG surface plating were degraded more than those of HASL finish after aging process. While breakdown voltages of about 700 V was recorded for aged samples with ENIG surface plating, specimens with HASL surface finish had breakdown voltages of greater than 800 V. Comparison between double coated samples with other coated specimens yielded the positive influence of additional coating layer by increasing the breakdown voltage even after 36 cycles of aging. Double coated samples after 36 cycles of aging provided a better withstand voltage than a bare PCB.

6.7 Summary

In this chapter, temperature and humidity aging process was described and tests of aged samples were performed. A programmable, controllable chamber capable of providing heating and cooling cycles in the presence of humidity was designed and developed. Four groups of specimens, each containing five samples were subjected to cycles of thermal aging. Capacitance and loss tangent of specimens were measured after a number of cycles and results were compared based on coating thickness and surface plating of the test boards. PD measurements were conducted and PDIV of samples were recorded. Finally, breakdown voltage test was conducted for samples and results from different samples with various conditions were reported and compared. The advantage of coating layer and impact of thermal aging were discussed.

Chapter 7

Concluding Remarks

7.1 Conclusions

In this thesis, the electrical performance of conformally-coated PCBs was tested in a series of experiments. Standard test methods were employed and implemented for the purpose of testing. Test boards with different trace layouts and surface finishings were designed and fabricated. A conformal coating dipping application machine was designed, built, and used for applying the coating layer on the surface of prepared samples. Pre-coating preparations including connection pins soldering and cleaning the samples were performed. MG-Chemicals 422B Silicone modified conformal coating was used as the coating material for this study. Coating with different thicknesses was applied on samples to evaluate the impact of coating layer thickness on the performance of the boards. An automated programmable chamber was also designed and setup for thermal and humidity aging test. Qualification inspections were performed on prepared samples prior the experiments. Test samples were coded based on the trace layout, surface plating, and coating thickness for distinguishing the final results. Measurements of new specimens were extracted and obtained data from samples were recorded for comparison.

In the first part of experiments, the impact of pollution and conductive particles on coated samples was examined. Additionally, breakdown voltage test was performed for coated samples with different configurations to investigate the influence of coating layer on electrical breakdown voltage. Experiments confirmed that the pollution location play an important role on PD activity and the occurrence of momentary discharges on a coated PCB. Pollution located away from energized traced did not influence the coated sample. Presence of the pollution on top of the traces resulted in PD and decreased the PDIV. The electrical field between traces displaced the pollution which had a higher permittivity than the coating material. Momentary discharges occurred through the pollution on the top of coating layer and between energized traces. Discharges adversely impacted the coated board and resulted in severe corrosion of the traces. Experiments for conductive particles on top of coated sample showed that PDs are more likely to happen in the presence of conductive particles. Momentary discharges and increased number of PDs due to the presence of conductive particles resulted in coating degradation and, therefore, decrease the life time of a coated PCB assembly.

Experiments on the assessment of aging of conformally coated samples were conducted in this thesis. Test samples with a “D” comb pattern including HASL and ENIG surface finishing were designed, prepared, and coated for this part of tests. Samples were classified in four groups based on surface plating and the thickness of the applied coating film. Test boards were exposed to cycles of temperature variation in the presence of humidity inside the designed chamber. A group of samples were energized at 50 V DC during the aging cycles and some of the samples were aged un-energized. Measurements of capacitance and loss tangent over a range of frequency from 10 Hz to 100 kHz were performed for new and aged samples. The capacitance and loss tangent of all samples increased as a result of aging. The reason for this change in the capacitance and loss tangent was the absorption of the moisture by the coating layer due to presence of electric field between the traces. It was observed that samples with an additional coating layer provided a better performance since the level of change in the capacitance and loss tangent was lower than those of single coated ones even after 36 cycles of aging. Samples with single coating layer suffered from significantly higher increase in capacitance and loss tangent values after 20 cycles. This confirms the higher vulnerability of single coated PCBs due to humidity and temperature. It was also observed that samples with ENIG surface finish performed marginally better than those with HASL surface plating only up to a certain degradation level. Once the oxidation of ENIG surface finish started, significant changes in the capacitance and loss tangent of samples were noticed. The adverse influence of surface finish degradation was also confirmed by extending the aging process to 36 cycles.

Measurements of capacitance and loss tangent in non-energized samples showed a noticeable smaller change in the capacitance and loss tangent. Besides, lower level of degradation of conductor traces was observed in non-energized samples. This confirms the less amount of absorbed moisture by the coating layer due to the lack of electric field between traces.

7.2 Future Work

In this thesis, the reliability of conformally-coated printed circuit boards was assessed in a series of experiments. Test samples of various condition were coated and examined according to the standard test methods. Experimental study on coated samples can be extended and more experiments can be conducted to improve the assessments on the reliability of PCBs under different operational conditions.

In this section, further studies and possible extended experiments are suggested. Proposed tests can be enhanced and might be combined to obtain more accurate results.

- Partial discharge measurements under pollution can be conducted under low air pressure to investigate the impact of air pressure on PD activity. Different types of pollutant can be tested on coated samples with different coating thickness.
- Different types of conformal coating material with various properties and final thickness can be examined for experiments and a classification of conformal coating material based on operational condition can be reported.
- Accelerated aging process of test specimens can be extended to higher temperature difference and could be performed under various humidity levels.
- Since the aging process of the samples was conducted in a chamber, the real operational condition should be estimated based on the number of applied cycles to map the cycles into aging process under operational conditions.
- Since the frequency of the applied voltage has an impact on the PD activity, measurements of breakdown voltage and PD can be performed at high frequencies up to 400 Hz (the frequency of voltage in an aircraft, for example).
- Test samples of various layouts and topologies can be tested. Other types of surface plating can be tested and test boards with more track clearance should be examined.
- Thermal shock test can be performed for samples with conformal coating and the impact of fast temperature change on the performance of samples can be examined.

- Reliability and performance of coated samples can be evaluated under salt spray exposure and thermal cycling.

References

[1] M. Howse, "All electric aircraft," *Power Engineer*, vol. 17, no. 4, pp. 35–37, Aug 2003.

[2] A. Emadi and M. Ehsani, "Aircraft power systems: technology, state of the art, and future trends," *IEEE Aerospace and Electronic Systems Magazine*, vol. 15, no. 1, pp. 28–32, Jan 2000.

[3] I. Cotton, A. Nelms, and M. Husband, "Higher voltage aircraft power systems," *IEEE Aerospace and Electronic Systems Magazine*, vol. 23, no. 2, pp. 25–32, Feb 2008.

[4] *Boeing Commercial Airplanes*, AERO magazine, 2007, Issue 28.

[5] W. G. Dunbar, "Designing and building high voltage power supplies," *AFWAL-TR-88-4143*, vol. 1, Aug. 1988.

[6] B. Dobbs, W. G. Dunbar, and C. Tarvin, "High voltage design guide summary," in *Proceedings of the 24th Intersociety Energy Conversion Engineering Conference*, Aug 1989, pp. 423–428 vol.1.

[7] *IEC 60270 High-voltage test techniques-Partial discharge measurements*, International Electrotechnical Commission Std., 2001.

[8] C. Emersic, R. Lowndes, I. Cotton, S. Rowland, and R. Freer, "Degradation of conformal coatings on printed circuit boards due to partial discharge," *IEEE Transactions on Dielectrics and Electrical Insulation*, vol. 23, no. 4, pp. 2232–2240, August 2016.

[9] R. Tarzwell and K. Bahl, "High voltage printed circuit design and manufacturing notebook," Sierra Proto express, Nov. 2004.

[10] F. Oldervoll, "High electric stress and insulation challenges in integrated microelectronic circuits," *IEEE Electrical Insulation Magazine*, vol. 18, no. 1, pp. 16–20, Jan 2002.

[11] What is a conformal coating? By: HumiSeal. [Online]. Available: https://chasecorp.com/humiseal/conformal-coating/

[12] *IPC-CC-830 Qualification and Performance of Electrical Insulating Compound for Printed Wiring Assemblies*, IPC Std., Aug. 2002.

[13] F. Paschen, "Ueber die zum funkenbergang in luft, wasserstoff und kohlensure bei verschiedenen drucken erforderliche potentialdifferenz," *Annalen der Physik*, vol. 273, no. 5, pp. 69–96, 1889. [Online]. Available: https://onlinelibrary.wiley.com/doi/abs/10.1002/andp.18892730505

[14] C. Emersic, R. Lowndes, I. Cotton, S. Rowland, and R. Freer, "The effects of pressure and temperature on partial discharge degradation of silicone conformai coatings," *IEEE Transactions on Dielectrics and Electrical Insulation*, vol. 24, no. 5, pp. 2986–2994, Oct 2017.

[15] W. Pfeiffer, "Partial-discharge testing of components for low-voltage equipment," *IEEE Transactions on Electrical Insulation*, vol. 26, no. 2, pp. 247–257, April 1991.

[16] *IPC-TM-650 Dielectric Withstanding Voltage - Polymeric Conformal Coating*, IPC Association Connecting Electronics Industries Std. 2.5.7.1, Jul 2000, IPC-TM-650 Test Method.

[17] *IPC-HDBK-830 Guidelines for Design, Selection and Application of Conformal Coatings*, IPC Association Connecting Electronics Industries Std. IPC-HDBK-830, Oct 2002.

[18] *IPC-TM-650 Moisture and Insulation Resistance - Polymeric Conformal Coating*, IPC Association Connecting Electronics Industries Std. 2.6.3.4, Jul 2003, IPC-TM-650 Test Method.

[19] E. Zeynali, R. Bridges, and B. Kordi, "Investigation of partial discharge in aircraft conformally-coated printed circuit boards," in *2019 IEEE Electrical Insulation Conference*, Calgary, AB, Canada, Jun. 2019.

[20] J. Ladou, "Printed circuit board industry," *International journal of hygiene and environmental health*, vol. 209, pp. 211–9, 06 2006.

[21] K. Gilleo, "The circuit centennial," *Circuit Tree*, 2003.

[22] A. Hanson, British Patent 4681, 1903.

[23] "History of IPC's Name." [Online]. Available: http://www.ipc.org/ContentPage.aspx?pageid=IPCs-Name

[24] G. Milad, "Surface finishes in a leadfree world," *Circuit World*, vol. 34, no. 4, pp. 4–7, 2008.

[25] C. F. Coombs and H. T. Holden, *Printed circuits handbook*. McGraw-Hill New York, 2001, vol. 1.

[26] *IPC-4101A Specification for Base Materials for Rigid and Multilayer Printed Boards*, IPC Association Connecting Electronics Industries, IPC Std., Dec. 2001.

[27] *IPC-2221A Generic Standard on Printed Board Design*, IPC Association Connecting Electronics Industries Std., May 2003.

[28] *IPC-4562A Metal Foil for Printed Board Applications*, IPC Association Connecting Electronics Industries, IPC Std., May 2000.

[29] *Generic Requirements for the Physical Design and Manufacture of Telecommunications Products and Equipment*, Telcordia Std. 02, Sep. 2007.

[30] *IPC-A-610 Acceptability of Electronic Assemblies*, IPC Association Connecting Electronics Industries Std., Nov. 2004.

[31] P. Wilson, "Chapter 2 - printed circuits," in *The Circuit Designer's Companion (Fourth Edition)*, 4th ed., P. Wilson, Ed. Newnes, 2012, pp. 49 – 91. [Online]. Available: http://www.sciencedirect.com/science/article/pii/B9780081017647000025

[32] P. Taylor, "Comparison of conformal coating technologies for military devices with non-traditional conformal coatings," Master's thesis, University of Massachusetts Lowell, 2008.

[33] M. Suppa and C. Schauer, "Thick film coating materials and fast conformal coating processes - a contradiction?" in *2nd International IEEE Conference on Polymers and Adhesives in Microelectronics and Photonics. POLYTRONIC 2002. Conference Proceedings (Cat. No.02EX599)*, June 2002, pp. 165–171.

[34] "How to select a conformal coating material," Technical Bulletin. [Online]. Available: http://www.conformalcoating.co.uk/wp-content/uploads/2016/09/Technical-Bulletin-How-To-Select-A-Conformal-Coating-Material.pdf

[35] T. Charlton, "Conformal coating made easy," *Circuit Assembly*, Oct 2003.

[36] Conformal coating comparison guide. [Online]. Available: http://www.electroniccoating.com/resources/conformal-coating-comparison-guide/

[37] *IPC-CH-65 Guidelines for Cleaning of Printed Boards and Assemblies*, IPC Association Connecting Electronics Industries Std., Jul. 2011.

[38] "Conformal coating masking," Technical Bulletin. [Online]. Available: http://www.conformalcoating.co.uk/wp-content/uploads/2016/09/Technical-Bulletin-Conformal-coating-masking.pdf

[39] The essential guide to conformal coating. [Online]. Available: https://www.techspray.com/the-essential-guide-to-conformal-coating#methods

[40] "Conformal coating dipping," Technical Bulletin. [Online]. Available: http://www.conformalcoating.co.uk/wp-content/uploads/2016/09/Technical-Bulletin-Conformal-Coating-Dipping.pdf

[41] Selective conformal coating machines - simplecoat. [Online]. Available: http://www.gpd-global.com/co_website/conformal-simplecoat.php

[42] *MIL-I-46058 Insulating Compound, Electrical (For Coating Printed Circuit Assemblies)*, United States Military Standard Std., Dec 1966.

[43] *IPC-TM-650 Flexibility - Conformal Coating*, IPC Association Connecting Electronics Industries Std. 2.4.5.1, Jul 2000, IPC-TM-650 Test Method.

[44] *IPC-TM-650 Abrasion (Taber Method) Solder Mask and Conformal Coating*, IPC Association Connecting Electronics Industries Std. 2.4.27.1, Jan 1995, IPC-TM-650 Test Method.

[45] *IPC-TM-650 Fungus Resistance Conformal Coating*, IPC Association Connecting Electronics Industries Std. 2.6.1.1, Jul 2000, IPC-TM-650 Test Method.

[46] *IPC-TM-650 Thermal Shock - Conformal Coating*, IPC Association Connecting Electronics Industries Std. 2.6.7.1, Jul 2000, IPC-TM-650 Test Method.

[47] *IPC-TM-650 Hydrolytic Stability - Conformal Coating*, IPC Association Connecting Electronics Industries Std. 2.6.11.1, Jul 2000, IPC-TM-650 Test Method.

[48] *IPC-TM-650 Test Methods Manual*, IPC Association Connecting Electronics Industries Std., Jan 2003.

[49] I. Christou, "Optimisation of high voltage electrical systems for aerospace applications," Ph.D. dissertation, University of Manchester, 2001.

[50] A. Trentin, P. Zanchetta, P. Wheeler, and J. Clare, "Power conversion for a novel ac/dc aircraft electrical distribution system," *IET Electrical Systems in Transportation*, vol. 4, no. 2, pp. 29–37, June 2014.

[51] H. Koch, W. Pfeiffer, and H. Reinhard, "Performance testing of coated printed circuit boards by means of partial discharge measurements," *Proceedings of the 19th Electrical Electronics Insulation Conference,*, pp. 274–278, Sep. 1989.

[52] H. Koch, W. Pfeiffer, H. Reinhard, and H. Safran, "Partial discharge. vi: Pd testing of printed circuit boards," *IEEE Electrical Insulation Magazine*, vol. 7, no. 3, pp. 9–15, May 1991.

[53] H. Buchalla, R. Hund, H. Koch, and W. Pfeiffer, "Long time exposure influence of partial discharge (pd) to coated printed circuit boards," in *Conference Record of the 1992 IEEE International Symposium on Electrical Insulation*, June 1992, pp. 407–410.

[54] Y. Zhu, K. Haji, M. Otsubo, and C. Honda, "Surface degradation of silicone rubber exposed to corona discharge," *IEEE Transactions on Plasma Science*, vol. 34, no. 4, pp. 1094–1098, Aug 2006.

[55] C. Emersic, Chao Zhang, I. Cotton, R. Lowndes, S. Rowland, and R. Freer, "Degradation of printed circuit board coatings due to partial discharge," in *2015 IEEE Electrical Insulation Conference (EIC)*, June 2015, pp. 420–423.

[56] C. Emersic, R. Lowndes, I. Cotton, S. Rowland, and R. Freer, "Observations of breakdown through printed circuit board polymer coatings via a surface pollution layer," *IEEE Transactions on Dielectrics and Electrical Insulation*, vol. 24, no. 4, pp. 2570–2578, 2017.

[57] *Standard Test Method for Dielectric Breakdown Voltage and Dielectric Strength of Solid Electrical Insulating Materials at Commercial Power Frequencies*, ASTM International, American Society for Testing and Materials Std., 2004.

[58] R. Michalkiewicz, J. Green, and S. Opperhauser, "Surface insulation resistance testing of soldering pastes and fluxes," in *Proceedings of the Pan Pacific Microelectronics Symposium Kauai, Hawaii*, 2001.

[59] E. M. Bumiller, D. A. Douthit, and J. Pecht, *Contamination of electronic assemblies.* CRC Press, 2002.

[60] *IPC-9202 Material and Process Characterization/Qualification Test Protocol for Assessing Electrochemical Performance*, IPC Association Connecting Electronics Industries Std., Oct. 2011.

[61] S. Zhan, M. H. Azarian, and M. G. Pecht, "Surface insulation resistance of conformally coated printed circuit boards processed with no-clean flux," *IEEE transactions on electronics packaging manufacturing*, vol. 29, no. 3, pp. 217–223, 2006.

[62] U. Rathinavelu, M. S. Jellesen, and R. Ambat, "Effect of solder flux residue on the performance of silicone conformal coatings on printed circuit board assemblies," *Corrosion Engineering, Science and Technology*, vol. 48, no. 6, pp. 436–444, 2013. [Online]. Available: https://doi.org/10.1179/1743278213Y.0000000096

[63] J. K. E. Kuffel, W.S. Zaengl, *High Voltage Engineering Fundamentals*, 2nd ed. Newnes, 2000.

[64] P. Bandyopadhyay, C. Henoch, J. Hrubes, B. Semenov, A. Amirov, V. Kulik, A. Malyuga, K.-S. Choi, and M. Escudier, "Experiments on the effects of aging on compliant coating drag reduction," *Physics of Fluids*, vol. 17, no. 8, p. 085104, 2005.

[65] C. Taylor and P. Kinner, "IPC-CC-830B vs. the Real World," *Circuit Assembly Online Magazine*, April 2015.

[66] L. Lester, "The nano-systems fabrication laboratory cleanroom users manual," university of Manitoba.

[67] M. Chemicals, "Silicone modified conformal coating 422b technichal data sheet," Technichal Data Sheet, Jun. 2017.

[68] *IPC-A-600 Acceptability of Printed Boards*, IPC Std., Nov. 1999.

[69] A. N. Esfahani, S. Shahabi, G. Stone, and B. Kordi, "Investigation of corona partial discharge characteristics under variable frequency and air pressure," in *2018 IEEE Electrical Insulation Conference (EIC)*, San Antonio, TX, USA, June 2018, pp. 31–34.

Appendix A

Conformal Coating Application System

A programmable and controllable coating application machine was designed, developed, and built in house for the purpose of this study. A 3D model of the machine was designed using a CAD software as shown in Figure A.1. Table A.1 shows technical specification of the designed machine. A micro-controller was used as the main control unit. The system was programmed for controlling the speed and position of the vertical actuator in the dipping machine. Table A.2 shows the parts list of the coating machine.

1. Vertical movement linear actuator.
2. Stepper motor.
3. System chassis.
4. Dipping tank.

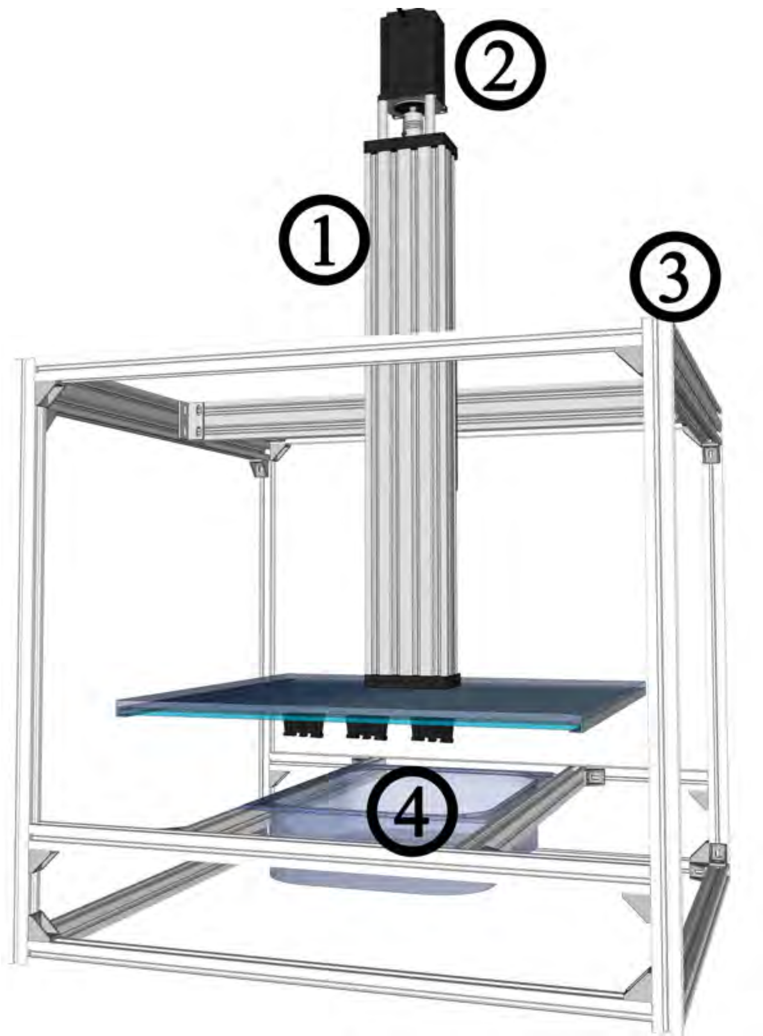

Fig. A.1: 3D sketch of the designed dipping machine.

Table A.1: Dipping machine technical specification

Technical Specifications	
Dimensions	500 mm X 500 mm X 500 mm
Actuator Type	Lead Screw
Actuator Length	500 mm
Travel Distance	400mm
Accuracy	0.05 mm ∼0.1 mm
Max Force	115 N
Max Speed	8000 mm/min
Operation Voltage	12 - 24 V DC
Peak Current (Max Load)	2.8 A

Table A.2: Parts list of dipping machine.

Part Lists				
Item	Part Name	Specification	Qty	Detail
1	Linear Actuator	C-Beam Linear Actuator Rail	1	
		Low Profile Screws M5	4	25mm
		Low Profile Screws M5	10	20mm
		Low Profile Screws M5	2	55mm
		Aluminum Spacers	2	6mm
		Aluminum Spacers	2	40mm
		Flexible Coupling	1	1/4” x 8mm
		Aluminum Spacers	2	3mm
		Eccentric Spacer	2	6mm
		Ball Bearing 688Z	2	8x16x5
		Shim	2	8mm
		Lock Collar	2	8mm
2	Motor	NEMA 23 Stepper Motor	1	Shaft Size: 1/4”
				Torque: 175 oz*in
				Step Angle: 1.8
				Peak Current is 2.8A/phase
				4 Wire Bi-Polar
				12-48VDC (Recommended)
				RoHS Compliant
3	Chasis Parts List	Cast Corner Bracket	36	
		L Bracket	7	Single
		L Bracket	7	Double
		L Bracket	5	Triple
		V-Slot Linear Rail 20x20	16	500mm
		V-Slot Linear Rail 20x40	3	500mm
		Low Profile Screws M5	7	8mm
		Tee Nuts	7	5mm
		C-Beam Gantry Plate - Double Wide	1	
4	Stepper Motor Driver	TB6600 Stepper Motor Driver	1	
5	Micro Controller	ARDUINO UNO REV3	1	